THE NON-IMPULSIVE STRETCH-RECEPTOR COMPLEX OF THE CRAB: A STUDY OF DEPOLARIZATION–RELEASE COUPLING AT A TONIC SENSORIMOTOR SYNAPSE

By A. R. Blight and R. Llinás
Department of Physiology and Biophysics, New York University Medical Centre,
550 *First Avenue, New York*, N.Y. 10016, *U.S.A.*

(*Communicated by D. C. Smith, F.R.S. – Received* 5 *June* 1979 – *Revised* 19 *November* 1979)

[Plates 1–4]

CONTENTS

A new preparation for the study of synaptic transmission is described from the thoracic ganglion of the crab *Callinectes sapidus*. The central anatomy of the non-impulsive stretch-receptor neurons of the thoracic–coxal joint and that of the promotor motoneurons with which they form synaptic junctions was studied with intracellular cobalt staining and light and electron microscopy. Attention was centred on the interaction of the stretch-receptor T-fibre and the four large motoneurons supplying the promotor muscle which have their cell-bodies on the dorsal surface of the ganglion. The presynaptic terminal region of the T-fibre appeared to be a simple cylinder in form with a diameter of 40–60 μm and containing large stores of synaptic vesicles at its periphery, opposite the complex of motoneuron dendrites.

The transmission characteristics of the junctions between receptor cell and motoneurons were studied by transmembrane current injection into the isolated T-fibre by means of a sucrose gap and simultaneous intracellular recording with microelectrodes from the presynaptic terminal and the somata of postsynaptic cells. It was shown that depolarization–release coupling in the T-fibre has similar properties to those that have been demonstrated in the squid giant synapse, with the same values for 'threshold', peak release and 'suppression potential'. The crab synapses differ from that of the squid in that they normally transmit prolonged, graded depolarizations (i.e. receptor potentials) which are decrementally conducted from the periphery. Consistent with this role, the junctions were found to be capable of continuous tonic transmission over many seconds without the strong depletion seen in more phasic synapses.

In a study of the relation between the synaptic properties and the stretch reflex it was shown that some of the time- and amplitude-dependent behaviour of the overall reflex can be encoded at the level of the synaptic transmission, largely through the parameter of transmitter availability. Conduction of electrical signals in the proximal and presynaptic part of the sensory fibre was also investigated. Transient responses to step depolarizing currents in the fibre indicate the existence of a mechanism for the partial compensation of capacitative distortion in the decrementally conducted receptor potential.

This is the first example of intracellular recording from presynaptic terminals of non-impulsive neurons with simultaneous monitoring of postsynaptic potential changes, allowing for a direct analysis of depolarization–release coupling characteristics. The use of the preparation for further study of synaptic physiology and sensorimotor systems is discussed.

1. Introduction

Much of our knowledge of the properties of transmitter release at the chemical synapse has been derived from the investigation of two types of preparation: the giant synapse of the stellate ganglion of the squid (Young 1939) and the vertebrate neuromuscular junction (recently reviewed by Martin (1977) and by Takeuchi (1977) respectively). The conceptual model of calcium-mediated depolarization–release coupling that has evolved in the last decade has relied almost exclusively on these (reviewed by Llinás (1977) and by Llinás & Heuser (1978)) and there are still few preparations in which it is possible to record intracellular potentials from presynaptic terminals while monitoring postsynaptic response. Those that are known are rather specialized, with very small transmitter stores (Auerbach & Bennett 1969) or combined electrotonic communication (Martin & Ringham 1975). It is therefore important that we extend our comparative knowledge of synaptic release systems which are more directly comparable with that of the squid, to check the general applicability of concepts which will continue to be developed from that most accessible of all synapses.

Our lack of comparative data has become a more pressing problem in recent years as it has become clearer that many central nervous system synapses may be concerned with the transmission of tonic, graded depolarizations rather than all-or-none action potentials (see reviews by Schmitt *et al.* (1976); Pearson (1976) and Shepherd (1979)). We need to know if the properties of transmitter release in such cases differ significantly from those of phasic synapses, in adaptation to the distinct type of signal that is transmitted. Initial information from receptor-cell synapses indicates that there may be considerable modification of synaptic behaviour (see, for example, Bennett 1968) whereas study of tonic inhibitory interactions in the lobster stomatogastric ganglion (Maynard & Walton 1975; Graubard 1978; Graubard & Calvin 1979; Raper 1979) and graded interactions between locust central neurons (Burrows & Siegler 1976, 1978; Burrows 1979) suggests a closer similarity of release characteristics to those established for the phasic synapse. Unfortunately, measurement of the precise presynaptic potential has not been possible in these preparations.

The large stretch-receptor fibres that innervate the receptor strand in the leg promotor muscles of decapod Crustacea were described anatomically by Alexandrowicz & Whitear (1957) and by Whitear (1965). Their unusual physiology was demonstrated by Ripley *et al.* (1964), who showed that receptor potentials are conducted decrementally from the receptor endings near the base of the leg into the thoracic ganglion, a distance that may be more than 10 mm in large crabs, without the development of regenerative action potentials. The receptor properties of these cells and their role in generating stretch reflexes have since been described by Bush and his colleagues (Bush & Roberts 1968, 1971; Roberts & Bush 1971; Bush & Cannone 1973, 1974; Bush & Godden 1974; Bush *et al.* 1975; Bush 1976, 1977). They found that the decrementally conducted receptor potential in a single axon (the so-called 'T-fibre') was sufficient to generate the reflex activation of the promotor neurons that innervate the muscle in which the receptor lies and also the muscle fibres within the receptor strand itself. It was therefore clear that some kind of synaptic interaction existed between the non-spiking receptor and the motoneurons. By analogy with other motor systems, this was likely to include a monosynaptic component.

These crab stretch-receptor to motoneuron synapses attracted investigation on several grounds. The ability of the fibres to conduct their signals over such distances relies on their large electrotonic length, partially derived from their large cross-sectional area. It would seem only

reasonable if the calibre of the fibres were to be maintained as far as the synapses made within the thoracic ganglion. It was therefore likely that the presynaptic terminal would be wide enough to be penetrated with microelectrodes, and, even if the synapse were difficult to locate accurately, the known length constant was sufficiently large for small errors of electrode location to have little effect on recorded potentials.

Two further advantages were intrinsic to the crab preparation. First, the presynaptic fibre does not generate action potentials and shows little delayed rectification (Roberts & Bush 1971); so the effect of prolonged and graded depolarization could be tested without the need to inject tetraethyl-ammonium (TEA) ions into the fibre, as is necessary in the squid to overcome the voltage-dependent potassium conductance of the spike mechanism (see, for example, Katz & Miledi 1967*b*). Secondly, the stretch receptor is tonic in its effect on the motoneurons and so can provide for the first time an insight into the properties of transmitter release at an excitatory tonic synapse mediating graded signals.

The present work gives an account of a preliminary investigation of the promotor complex of the crab thoracic ganglion, with the aim of establishing a new preparation for the study of synaptic transmission that is complementary to and comparable with the established preparations. At the same time it supplies further confirmation of the more general applicability of the concept of depolarization–release coupling that has been derived from such phasic synapses. An abstract of this work has appeared previously (Blight & Llinás 1978).

2. Materials and methods

(*a*) *Animals*

Most research on the crab stretch receptor has been carried out in *Carcinus maenas* (Bush 1977), but for this study it was found convenient to use the larger 'blue claw' crab *Callinectes sapidus*. All work was done on the receptor of the fifth pereiopod (the fourth 'walking leg'), which in this animal is modified for swimming. It is broad and flattened (figure 1) and is used in a rapid rowing motion in escape responses. Adults were obtained from dealers in Florida (usually supplying males) during the winter months, and in New York City (usually supplying females) during the summer. The animals were kept in recycled artificial seawater at 15–18 °C, and when necessary were fed on live mussels. Specimens with carapace widths (point to point) from 12 to 18 cm were used, the majority being about 15 cm.

(*b*) *Preparation*

The thoracic ganglion and promotor muscles were isolated from the crab for all anatomical and physiological investigation. At first it was found difficult to obtain isolated preparations that maintained reflex responsiveness. By monitoring the promotor stretch reflex continually through the process of dissection, it was found necessary to maintain a relatively high level of oxygen supply to the ganglion at all times during the isolation to obtain a viable preparation. All the legs and the chelipeds were severed at the coxal level and the animal was submerged in oxygenated saline for 10–15 min, during which time a certain amount of the blood was exchanged for saline by the normal open return circulation of the animal. The blood of the crab tends to clot during the process of dissection and this preliminary bleeding seemed to improve the subsequent perfusion, as judged by the health of the reflex responses.

The dorsal carapace was then cut away and the digestive gland and gonads were removed,

with forceps, under running saline. The sternal artery was severed below the heart and cannulated with a polyethylene tube for direct perfusion with oxygenated saline. Initial perfusion rates were 12–15 ml/min and only after the preparation was isolated and showed strong reflex responses was this rate reduced to 4–6 ml/min. Lower rates generally resulted in rapid, irreversible loss of responsiveness. The contents of the cephalic segment, the gills and the upper parts of the pleurites were removed and the muscles of the fourth legs, other than the promotor muscles on each side, were carefully cut away. The thoracic ganglion and the promotor muscles were left exposed, as shown in the right side of figure 1.

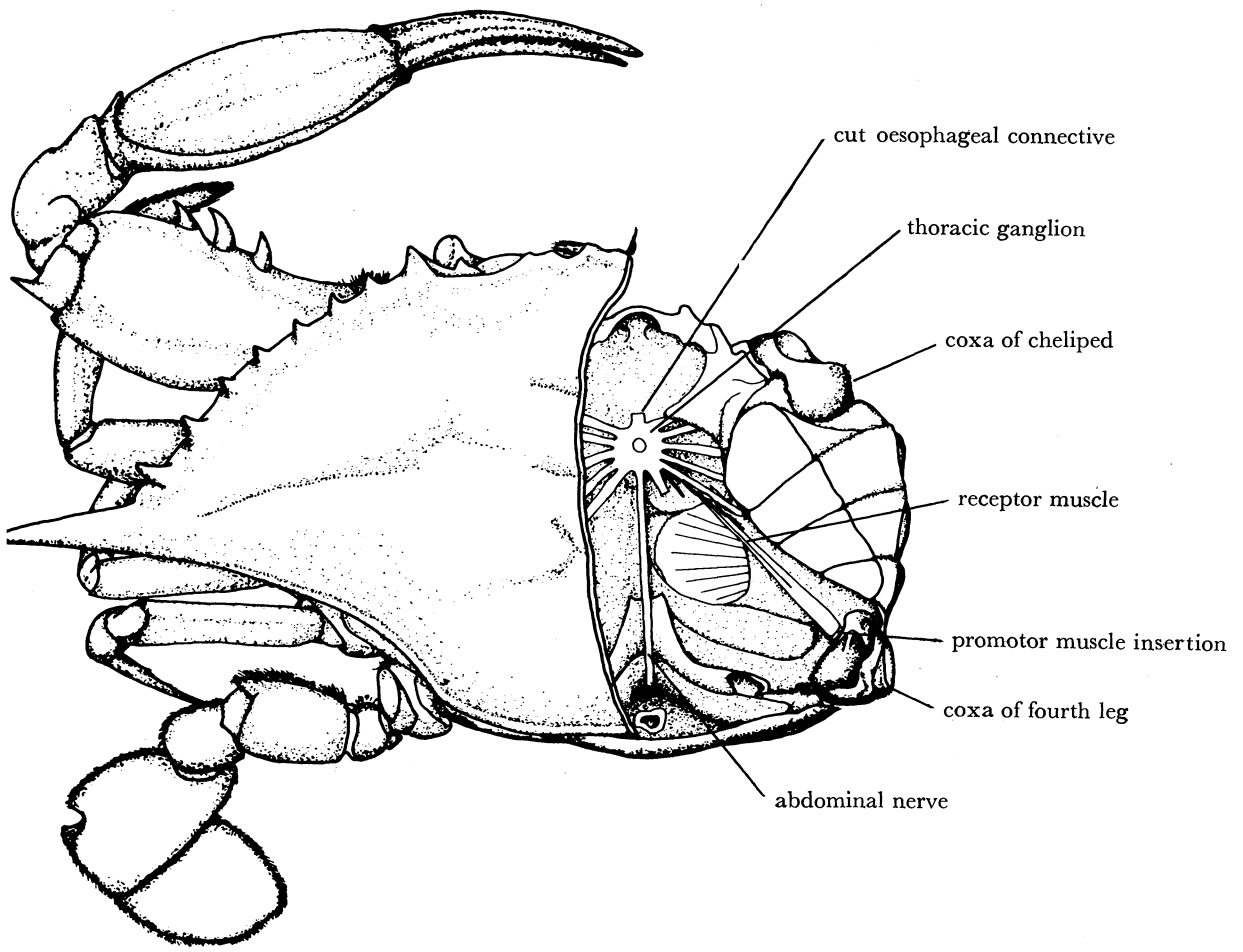

FIGURE 1. A dorsal view of *Callinectes*, with the right side shown dissected, ready for the isolation of the thoracic ganglion and stretch receptor.

The medial, white portion of the promotor muscle (see figure 4) was usually cut away, together with the dorsolateral part of the main mass, to facilitate removal of ganglion and receptors with minimal damage. All nerves other than those to the fourth legs were cut through with scissors close to the ganglion. The promotor muscle was freed from its attachment by cutting the apodeme at the coxa and cutting out the 'receptor rod' from the edge of the endosternite (as can be seen in figure 5). With the severing of remaining connective tissue attachments, the ganglion and the left and right promotor muscles could then be removed to the recording chamber for further dissection.

(*c*) *Saline*

The formula for crab saline finally adopted was derived by slight modification from those published for use with *Callinectes* by Hays *et al.* (1968) and Reingold (1975): 435 mM NaCl, 8 mM KCl, 40 mM $MgCl_3$, 10 mM $CaCl_3$, 30 mM $NaHCO_3$, 0.1 mM K_2HPO_4 in distilled water, bubbled constantly with 95% O_2 plus 5% CO_2. The concentration of bicarbonate was increased to buffer the 5% CO_2 (giving a pH of about 7.4). The phosphate was added, as suggested by Burton (1975), to reduce the tendency for precipitation of calcium carbonate. The magnesium concentration was gradually increased from the more typical 10 or 20 mM as it was found that this gave more stable membrane properties and less spontaneous activity in the motoneurons, though, together with the reduction to 10 mM calcium, this would reduce the amplitude of synaptic responses. The final level of divalent cations was approximately that of seawater. For cation substitutions a modified formula was used: 465 mM NaCl, 8 mM KCl, 40 mM $MgCl_2$, 10 mM $CaCl_2$, 10 mM Tris buffer, pH 7.4, in distilled water, bubbled with O_2. This formula was avoided for more general use because of the known and unknown biological side-effects of the synthetic buffer (Davidoff & Sears 1975).

(*d*) *Histology*

The search for a fixation technique that would give good preservation at the electron microscope level met with little success. The best results were obtained by means of the second technique quoted by Sherman & Atwood (1972), based on that of Fahrenbach (1968). The partially desheathed ganglion was fixed by submersion, generally leaving the receptor cells intact to avoid depletion of vesicles at the synapse, which would result from damage to and depolarization of the peripheral fibres.

Sensory and motor cells were stained by back-filling with cobalt chloride through their peripheral axons by the technique described in Kater & Nicholson (1973). The fibres to be filled were dissected under the microscope and the cut ends isolated by a Vaseline gap in a pool of slightly hypotonic cobalt chloride solution. It was possible to tease out single motor axons and backfill them in this manner. The ganglia were kept at 4 °C for about 24 h to obtain sufficient filling within the ganglion without the application of current. Alternatively, it was possible to obtain reasonable filling within 7–9 h with the application of a loading current at 20 °C. Motoneuron activity was monitored during the application of current to check that it produced only physiological rates of firing. This was done simply by recording differentially between the pool of cobalt chloride and the saline bath. Cobalt-treated ganglia were fixed for about 15 min and then immersed in a solution of 1–3% (by mass) ammonium sulphide in saline. The precipitation of cobalt sulphide was watched under the microscope and the ganglion was washed in saline before too much background staining could occur. It was then fixed for a further 12 h, dehydrated and embedded in Epon, to be examined as a whole mount under mineral oil and later sectioned on an ultramicrotome.

Plastic sections 1–2 μm thick were mounted on glass slides by heating and then intensified with the method of Tyrer & Bell (1974). It was found useful to introduce a further step into this technique, presoaking the slides in the developer solution for an hour or more before the addition of silver nitrate, according to the method of Bacon & Altman (1977) for cobalt whole mounts.

The problems encountered with the cobalt technique were, first, that cobalt itself tended to damage the cells. Intense vacuolization was always seen in the cytoplasm of filled cells under the electron microscope. A particular problem with the sensory fibres was that cobalt was often released from the synaptic zone and diffused into the surrounding neuropil, obscuring the anatomy in whole mounts. Secondly, the ammonium sulphide development tends to produce general ultrastructural damage. Cobalt staining was therefore replaced with the technically superior horseradish peroxide (HRP) method, but the enzyme migrated very slowly within these crustacean cells, both with back-filling and with microelectrophoresis into the soma. Cobalt was mostly used, therefore, as it gave a clearer picture of the anatomy at the light microscope level. Modifications of the cobalt technique, such as those suggested by Székely & Gallyas (1975) and Gallyas *et al.* (1978) for use in the amphibian, might have produced some improvement in ultrastructural preservation.

(e) Physiology

With the ganglion and promotor muscles isolated in the recording chamber, the promotor nerve was freed from the muscle and the peripheral end was cut at about the level of the receptor ending (see §3 for anatomy), and then drawn into a polyethylene suction electrode to monitor motoneuron activity during the rest of the dissection. The dorsal surface of the ganglion was then desheathed. In the process, the sternal artery was cut near to the ganglion so that the closed perfusion was changed to open superfusion. The receptor sensory nerve was freed of all surrounding fibres, which were trimmed close to the ganglion with fine scissors. The three large fibres of the sensory nerve, the so-called S-, T-, and D-fibres (Alexandrowicz & Whitear 1957; Whitear 1965) could then be separated and identified on the basis of their diameter ($T > S > D$), their relation to the receptor strand (which, because of obscuring connective tissue, was usually difficult to see without time-consuming dissection) and, in addition, by evoked reflex activity in the promotor nerve when they were stimulated with prolonged extracellular current pulses from a bipolar wire electrode. The D-fibre has no effect and the S-fibre has a weaker effect than the T-fibre.

With the T-fibre identified, the S- and D-fibres were cut as close to the ganglion as possible without damage to the T-fibre or motor nerve. This procedure gave the most positive identification of the fibres. The cut D-fibre has no effect on promotor activation, the S-fibre gives a strong activation that declines to little or nothing within a few seconds, whereas cutting the T-fibre of a healthy preparation gives a powerful activation of the motoneurons that declines only over the course of minutes.

All the promotor muscle and receptor rod except that immediately surrounding the receptor ending was cut away and the T-fibre was then gently stretched across the sucrose gap and sealed with Vaseline, and the ganglion was pinned out in its final position on the Sylgard (Dow-Corning) floor of the recording chamber, as seen in figure 2.

By stimulating the peripheral promotor nerve with a bipolar wire electrode, as shown in figures 2 and 3, it was possible to identify the somata of promotor motoneurons impaled with microelectrodes on the dorsal surface of the ganglion. With transmitted light it was possible to see the outlines of these somata. The presynaptic fibre was impaled by exploratory tracking with the microelectrode in the known anatomical region (§3) while the fibre was stimulated with short current pulses through the sucrose gap. The recording arrangement is shown in more detail in figure 3.

The saline bath was normally grounded with a silver–silver chloride electrode of large

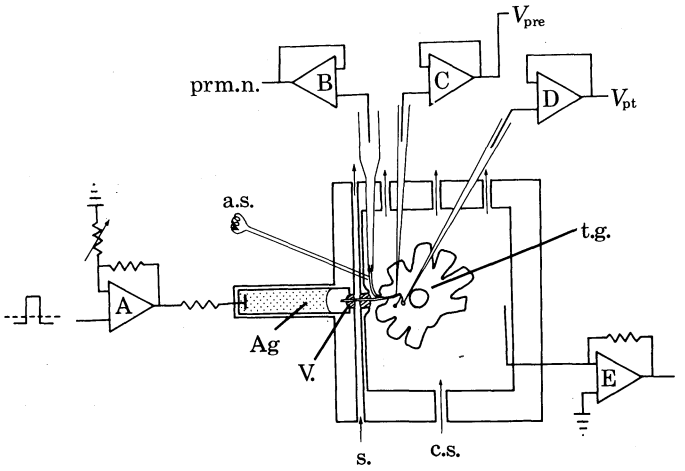

FIGURE 2. A diagram of the recording apparatus, viewed from above. The thoracic ganglion (t.g.) was pinned out on the Sylgard floor of the Perspex chamber and superfused with crab saline (c.s.) at a rate of two chamber volumes per minute. The T-fibre was isolated in the sucrose gap (s) and sealed with Vaseline (V.). Current was injected into the fibre through a current-limiting resistor and an Ag|AgCl|agar|KCl electrode (Ag) from the high-voltage amplifier, A. Amplifers, B, C and D recorded promotor nerve activity (prm. n.) and the pre- and post-synaptic potentials (V_{pre}, V_{pt}). The bath was grounded through an Ag|AgCl electrode of large surface area, connected directly to earth, or through the current monitor amplifier, E. Promotor neurons were identified by antidromic stimulation with a bipolar wire electrode (a.s.). (For clarity, the ganglion is shown at four times the scale of the chamber.)

surface area to reduce voltage artefacts from the injected current passing through the bath resistance. An additional KCl agar bridge was used only for ion-substitution experiments. With normal perfusion the resting bath potential was stable.

The glass micropipettes used for recording were generally of 6–16 MΩ resistance. The lower resistance was used for low noise presynaptic recording and current injection and the higher resistance for recording from finer motoneuron processes within the neuropil. The micropipettes were generally filled with 3 M KCl solution, saturated with fast green (Thomas & Wilson 1966), both to make the tips visible and for immediate staining of cells to check recording sites. Some recordings were made with unstained 3 M potassium acetate or citrate electrodes.

The T-fibre often became slightly depolarized in the process of dissection and desheathing and it was found necessary to restore a reasonable resting potential once the fibre was held in the sucrose gap, by means of a small, constant, hyperpolarizing current. The largest resting potential recorded from the ganglion end of the fibre in more intact preparations was about 80 mV, and this was the value taken for the imposed potential. This was also the potential around which promotor activation was usually completely suppressed. Slight depolarizations from this level generally gave responses in the lowest threshold motor units of lively preparations.

Resting potentials of motoneuron somata, were about 70 mV in isolated ganglia. Motoneurons with resting potentials less than 60 mV were rejected for recording purposes. They generally showed poor antidromic responses and did not allow stable recordings of excitatory postsynaptic potentials (e.p.s.p.). By monitoring the promotor nerve response at all times prior to the experimental recording, it was possible to be sure that the T-fibre was not damaged either in setting up or during penetration with microelectrodes. Penetration of the peripheral fibre is very difficult because of the tough sheath cells and often causes membrane damage (Mirolli

1979), but this is not the case with the intraganglionic fibre, whether monitored pre- or post-synaptically.

3. Anatomy

(*a*) *The promotor muscle*

The promotor muscle of the fourth leg in *Callinectes* is more complex in form than that of *Carcinus*, which is not modified for swimming. The muscle divides into two distinct bundles from the coxal apodeme: a medial muscle, which is white in colour and has its origin in the midline beneath the thoracic ganglion; and a more lateral muscle, which has red, small calibre fibres in the middle but white, large calibre fibres down either side, as indicated in figure 4.

The receptor muscle strand runs between red and white and inserts on the middle of the triangular apodeme. It originates at the end of a long, thin skeletal rod (figure 5) that projects from the edge of the endosternite. This attachment derives its strength mainly from the connective tissue that binds the rod to the endosternite behind. The rod itself has very little mechanical strength and if the loose connective tissue is cut the rod can be seen to bend as the promotor muscle is stretched by remotion (backward and upward movement) of the coxa. It is possible that there is some slight give in the rod during normal function. The receptors on the other walking legs of *Callinectes* attach to the smooth edge of the endosternite as they do in all the legs of *Carcinus*. The receptor-rod arrangement is similar to that described in the cheliped of *Maia* by Alexandrowicz & Whitear (1957).

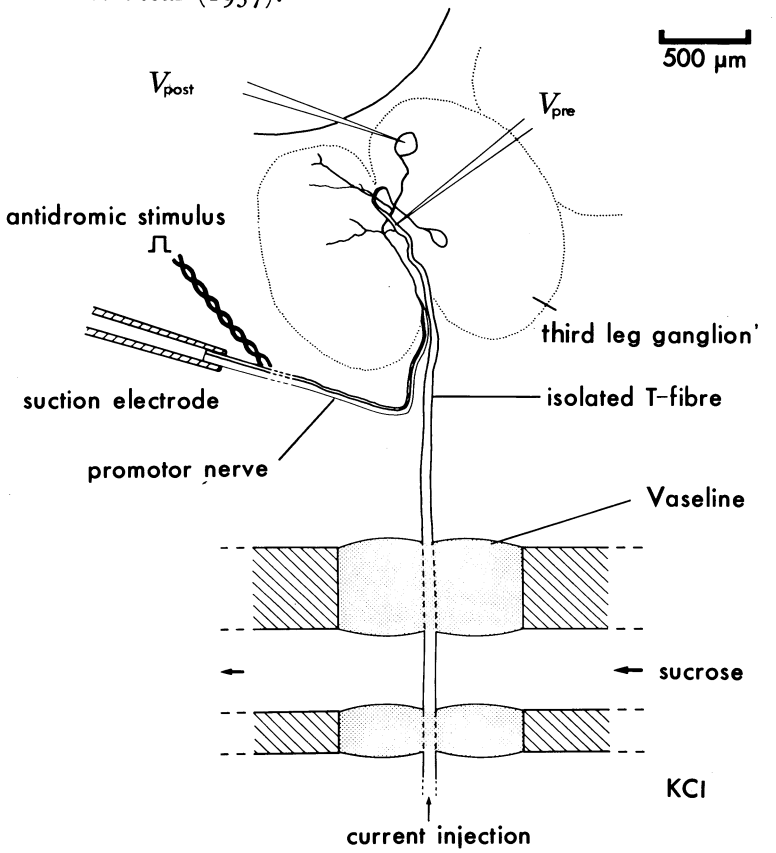

Figure 3. A diagram of the central portion of figure 2, with the usual position of the recording and stimulating electrodes indicated. The thickness of the elements of the sucrose gap is drawn to one quarter of the anatomical scale shown above.

The promotor muscle is innervated by a motor nerve that contains seven large axons and a number of very small fibres whose nature is not known (figure 10). This is surprisingly less than the number of large axons seen in *Carcinus* (Bush 1977, fig. 2). In addition, the receptor muscle is innervated by two motor axons, as in *Carcinus*, and by the two large sensory fibres, the S and T-fibres, which end, respectively, on the flanking elastic strands and the muscle tendon. The similarity of this peripheral anatomy to that already described for *Carcinus* (Alexandrowicz & Whitear 1957) was checked by methylene-blue staining, and by forward-filling of the cut receptor nerve with cobalt. The large D-fibre that accompanies the S and T in the same sheath innervates a finer receptor strand (the depressor receptor), which is involved with the coxo-basal joint.

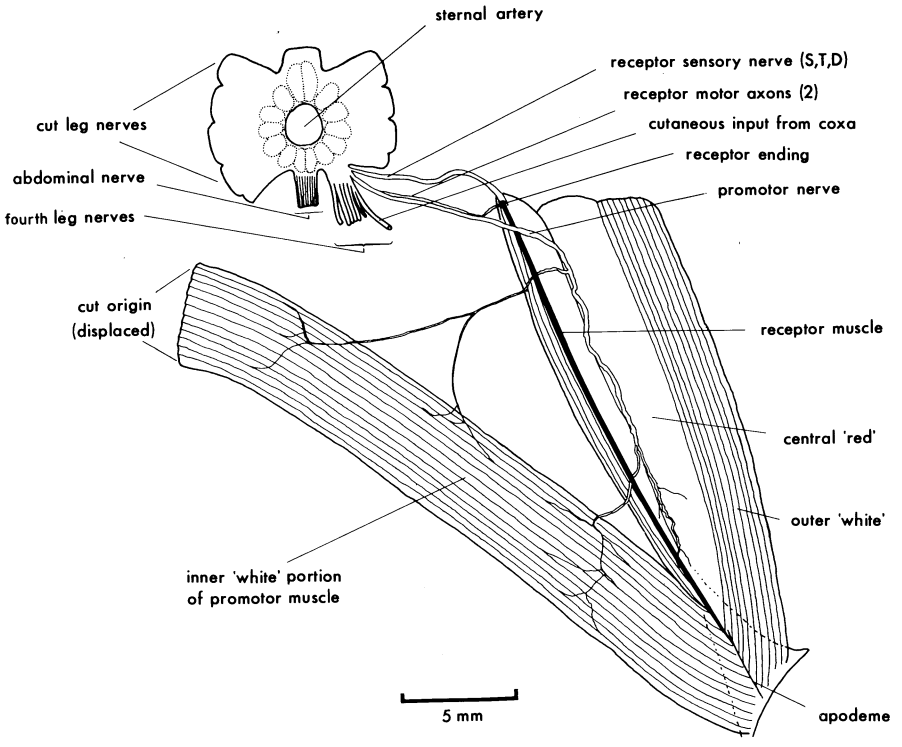

FIGURE 4. A dorsal view of the isolated thoracic ganglion and right promotor muscle, showing the innervation of the muscle and its receptor.

(*b*) *The thoracic ganglion*

The central nervous system of the crab has been little studied apart from the classical account of cell types given by Bethe (1895, 1897*a*, *b*) (see also Bullock & Horridge 1965). The ganglion is roughly annular in plan, the ganglia of the ventral chain of more elongated Crustacea having coalesced around the large sternal artery. The separate ganglia remain represented by the distinct masses of neuropil, which can be seen most clearly by transmitted light (see figure 6). Those neuropilar masses associated with the periopods (legs and chelipeds) are ellipsoidal in form, though interconnected at their inner ends (against the sternal artery) by axonal tracks (figure 7). The abdominal and oral ganglia are even more compressed. The neuronal somata lie around the outside and between the ellipsoidal masses of neuropil, in a layer that is only a few cells thick (figures 7, 15). The peripheral nerves arise from the outer faces of the ellipsoids, where the unmyelinated axons increase many times in diameter for their peripheral course.

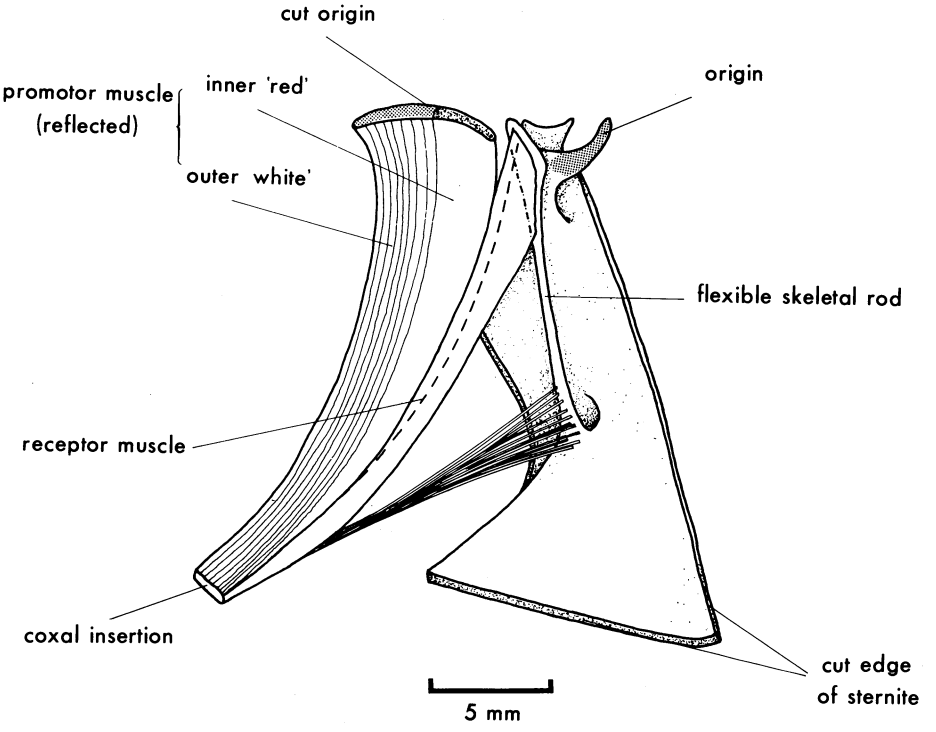

FIGURE 5. A semi-diagrammatic drawing of the promotor muscle as removed with the ganglion for subsequent isolation of the receptor. The coxal insertion has been cut and the inner white portion of the muscle (see figure 4) removed. The origin of the more lateral component of the muscle has been cut away from the sternite spur ('origin'), to allow that part to be reflected and expose the underlying skeletal rod, the flattened end of which serves as the origin of the receptor strand (dashed line) and some of the surrounding muscle fibres. A few sparse muscle fibres are seen to attach around the base of the receptor rod. The function of these is not known.

(*c*) *The promotor motoneurons*

The promotor nerve in *Callinectes* contains only seven clear axons (figure 10), and when it was back-filled with cobalt a maximum of seven somata were stained (figures 6, 7). These seven cells were consistently positioned, five being dorsal to the neuropil of the 'third leg ganglion' and two mediolateral to the neuropil of the fourth leg, though from animal to animal they were found to vary quite widely in their spacing. The four largest dorsal somata were generally close together, sometimes without intervening cells, but in one case were found to be separated by several other cell bodies. The deeper somata (6 and 7) occupied various positions between the inner (sternal artery) and outer edges of the ganglion in different preparations, though always on the medial side of the neuropil and always immediately adjacent to each other. The relative sizes of the somata were also consistent, and corresponded well with the relative diameters of axons in the nerve. Individual back-filling of the three largest peripheral axons has demonstrated that these are indeed the axons of the three largest (dorsal) somata (1–3) (see figure 8). The fact that cell bodies of fourth leg motoneurons are found over what is nominally the third leg ganglion is not necessarily surprising, since Allen (1894, 1896) showed that motoneurons of the embryonic lobster (*Homarus*) can send their axons to other segments to exit from the ventral cord.

The individually stained motoneurons of figure 8 show that the main dendritic field lies across the upper surface of the fourth leg neuropil, while two major dendritic branches run ventrally

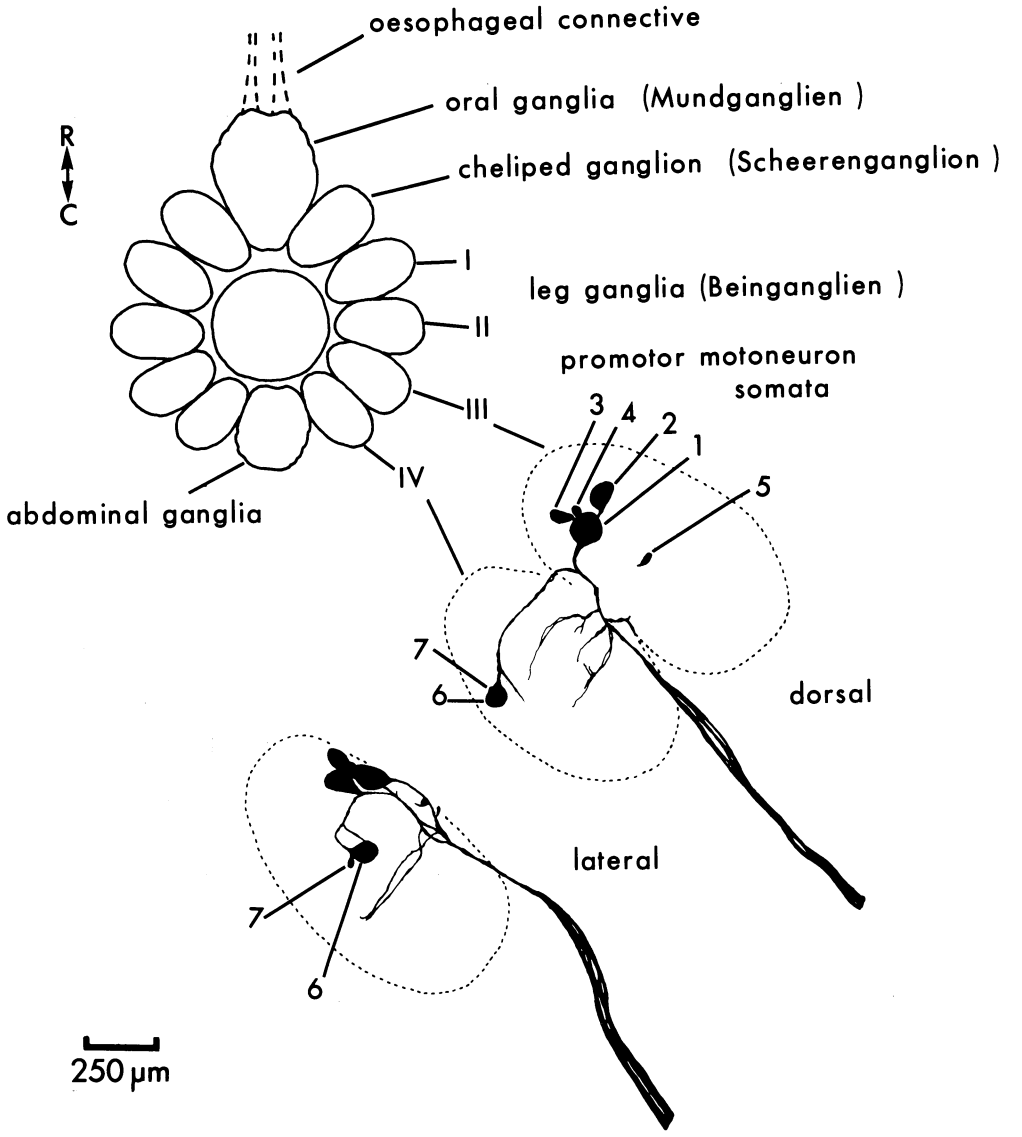

FIGURE 6. *Camera lucida* drawings of a whole mount preparation in which the promotor nerve was back-filled with cobalt, showing the seven motoneuron somata and the distribution of their major dendrites within the ganglion. The dashed lines indicate the approximate outline of the ellipsoidal masses of neuropil. Their position within the whole ganglion is shown in the upper left. The anatomical nomenclature of Bethe (1895, 1897) is given in parentheses. Abbreviations: R, rostral; C, caudal.

around the side adjacent to the third leg neuropil, one near the cell body and one near the axon. The latter branch is of some importance as it emerges from the region where the motor cell neurites are closest to the T-fibre and its synaptic zone (figures 13–15).

(*d*) *The T-fibre of the sensory nerve*

The sensory cells were also stained by back-filling with cobalt through their peripheral fibres. The S- and T-fibres were very distinct in transverse sections of the neuropil of each leg, because, unlike those axons that conduct action potentials, they maintain their large calibre far into the ganglion (figure 7). They were found to be about 50 µm in diameter at the level of closest

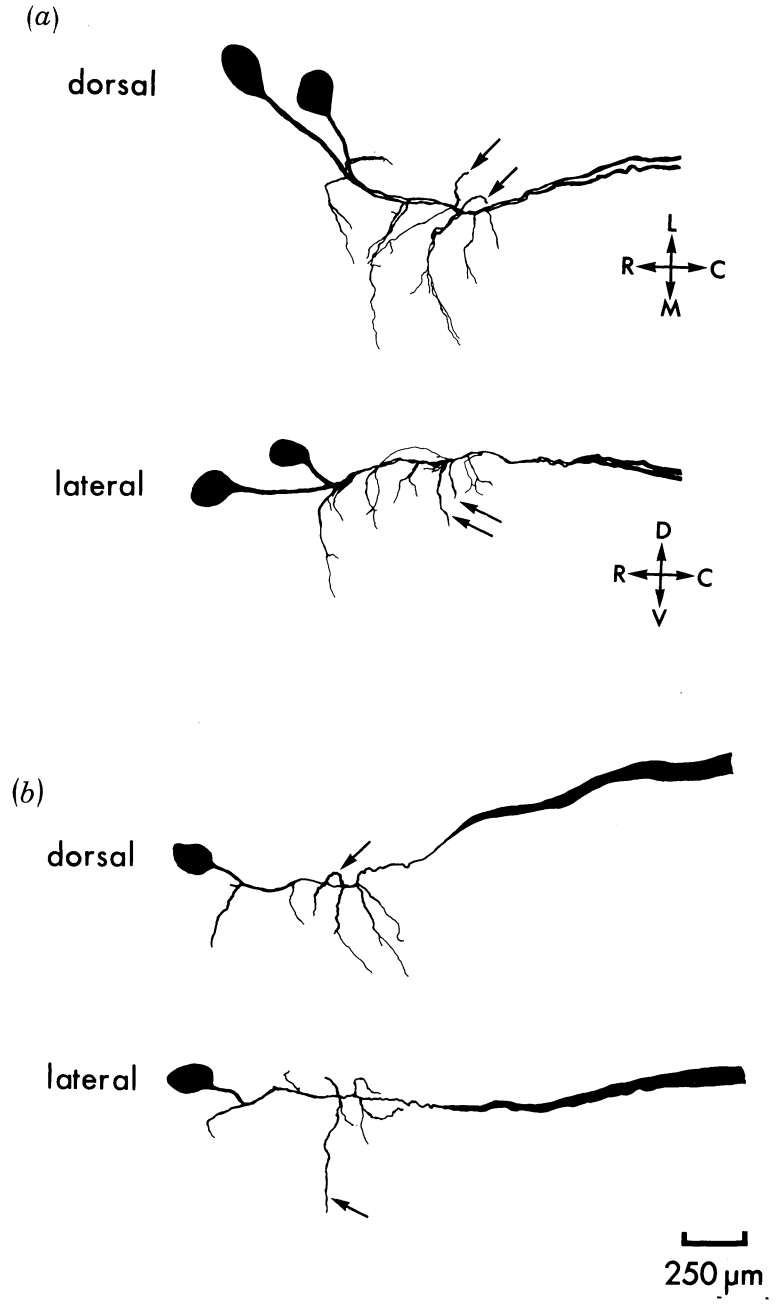

FIGURE 8. *Camera lucida* drawings of whole mount preparations of cobalt-stained promotor neurons. (*a*) Two of the large dorsal cells (1–3 of figure 6), stained together by filling two of the large axons alone. The arrows indicate the distal, ventrally-directed dendrites of the two cells, which occur at the closest apposition of the motoneurons with the sensory fibres (figure 8). (*b*) A single dorsal motoneuron, showing the main dendritic branches and the expansion of the axon once it leaves the ganglion. Abbreviations: L, lateral; M, medial, D, dorsal; V, ventral.

apposition to the promotor motoneuron dendrites (figures 13–15). Interestingly, the non-impulsive D-fibre seems not to maintain its calibre in the same way. The T-fibre has its soma on the edge of the third leg ganglion, though the large diameter portion of its neurite runs within the fourth leg neuropil (figure 9). The T-fibre branches little within the neuropil, unlike the motoneurons. It is therefore also very different from the spike-conducting stretch-receptor

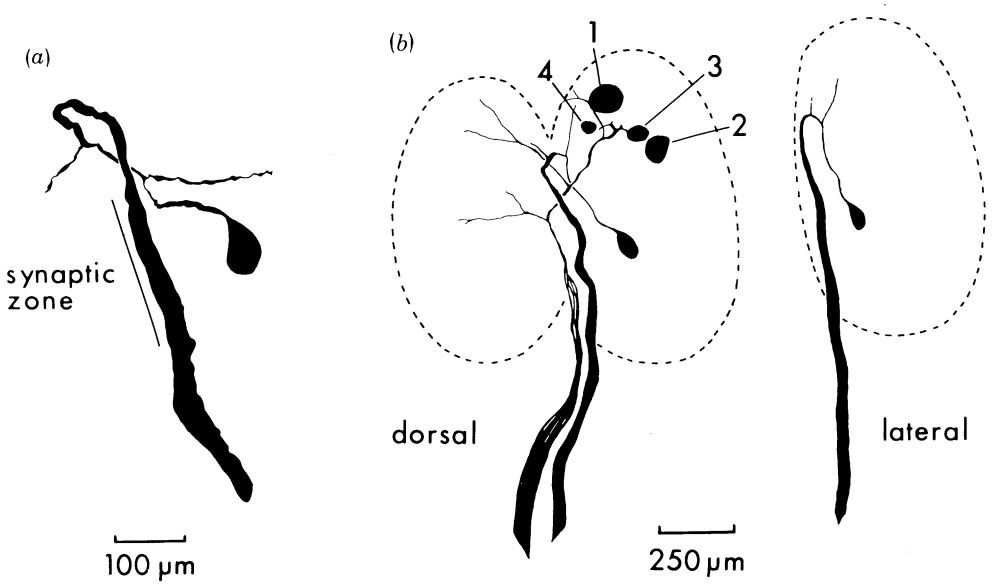

FIGURE 9. *Camera lucida* drawings of a preparation in which the T-fibre was stained darkly with cobalt and the promotor nerve filled lightly, allowing the black processes of the former to be differentiated from the light brown of the latter. (*a*) Reconstruction of the central portion of the T-fibre from 50 μm sections cut at a slightly oblique angle. (*b*) Dorsal and lateral views of the relation of the T-fibre to the third and fourth leg ganglia (dashed lines), and, in the dorsal figure, to that portion of the promotor cells (1–4) which could be seen in this partial stain.

cells examined, with similar techniques, in other invertebrates (locust, Burrows 1975 and Altman & Tyrer 1977*a*, *b*; crayfish, Bastiani & Mulloney 1978). Such cells have widespread and complex branching within the central nervous system. But the T-fibre of *Callinectes* seems also to branch more sparsely than that of *Carcinus*, as reported by Bush (1976, 1977), though cobalt

DESCRIPTION OF PLATES 1 AND 2

FIGURE 7. Photomicrographs of 2 μm plastic sections through the third and fourth leg components of the thoracic ganglion, between the inner (sternal artery) edge (top left) and the distal beginning of the synaptic zone of the T-fibre (bottom right). Sections were cut tangentially to the ganglion. The promotor nerve was backfilled with cobalt and the sections intensified with silver. The motoneuron somata (1–7) were darkly stained. Sheath cells around the outside of the ganglion also stained with the silver. The outlines of the neuropilar masses of legs III and IV are visible in all sections except the first, where third and fourth leg neuropil is joined by connective tracts (c.t.). Part of the abdominal ganglion is included on the left. The S- and T-fibres are visible in the more distal sections (S, T), and the major divisions of the motoneuron dendrites are indicated (p.m.d.). Scale bar, 250 μm.

FIGURE 10. Photomicrograph of a 2 μm plastic section through the promotor innervation about 1 mm proximal to the receptor ending, showing the seven large axons of the promotor nerve (p.m.a.), the two receptor motor axons (r.m.a.) and the three non-impulsive sensory fibres (S, T, D), surrounded by connective tissue and extrinsic muscle fibres. Toluidine blue stain.

FIGURE 11. Photomicrograph of a 2 μm plastic section through the promotor complex near the outer edge of the thoracic ganglion, showing sensory fibres (S, T, D) and the motor axons (p.m.a.) filled with horse-radish peroxidase (HRP).

FIGURE 12. Photomicrograph of a section further into the ganglion than that in figure 11, showing the most distal occurrence of synaptic mitochondria within the sensory fibres (s.m.), though at this point the motoneurons (p.m.a.) do not seem to be in close apposition.

FIGURE 13. Photomicrograph of a section through the thoracic ganglion, about 100 μm more proximal than that shown in figure 12, showing the apposition of motoneuron dendrites (p.m.d.), lightly stained with HRP, to the sensory fibres (S, T). Presynaptic mitochondria are visible in the toluidine blue counterstain.

FIGURE 14. Photomicrograph of a section a few micrometres from that shown in figure 13, showing the branching of motoneuron dendrites (p.m.d.) in the vicinity of the sensory fibres. Scale bars, 100 μm.

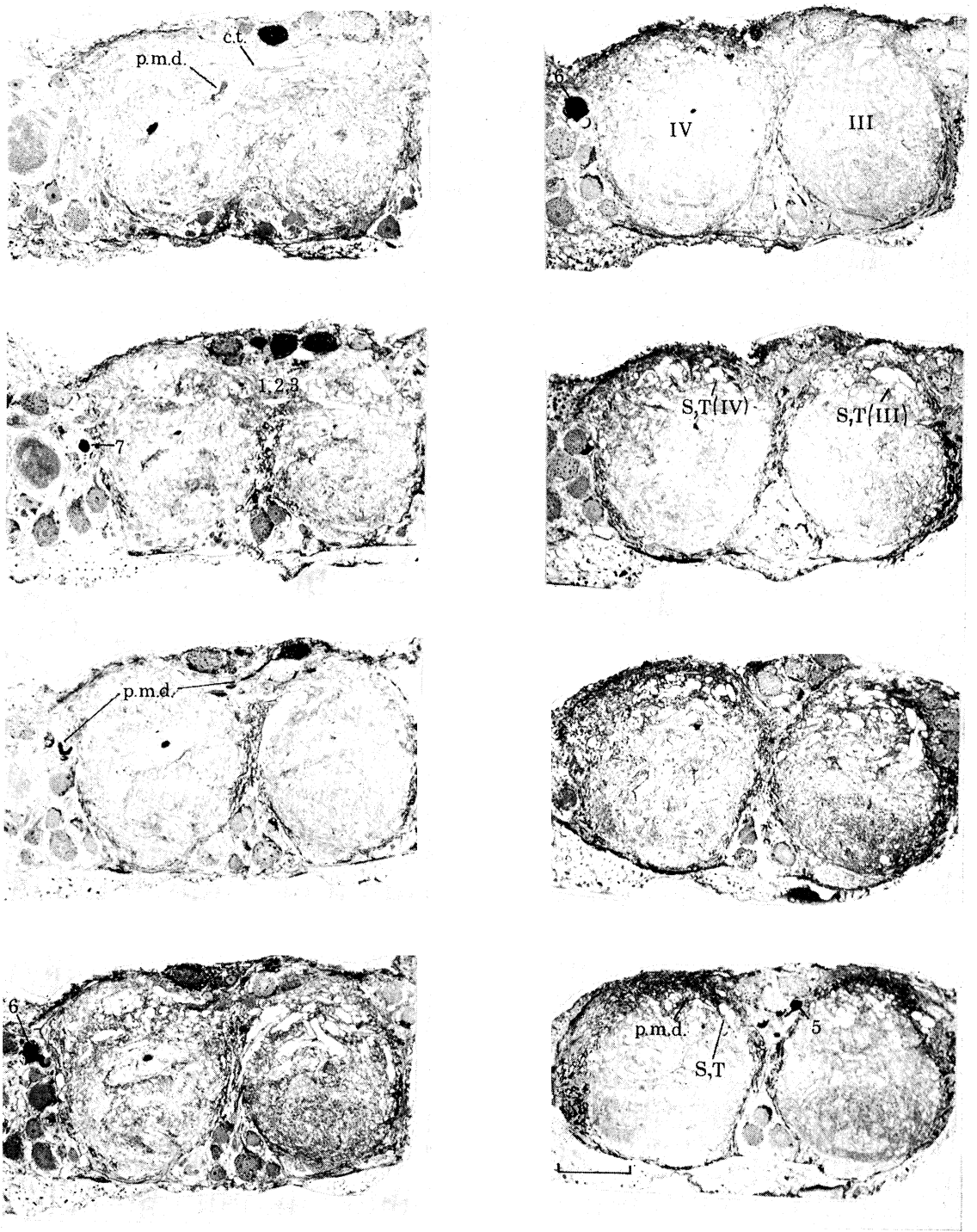

FIGURE 7. For description see opposite page.

(*Facing p.* 232)

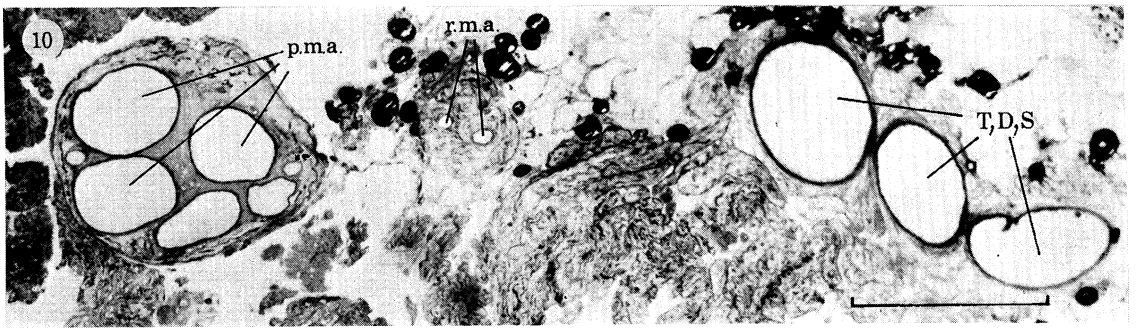

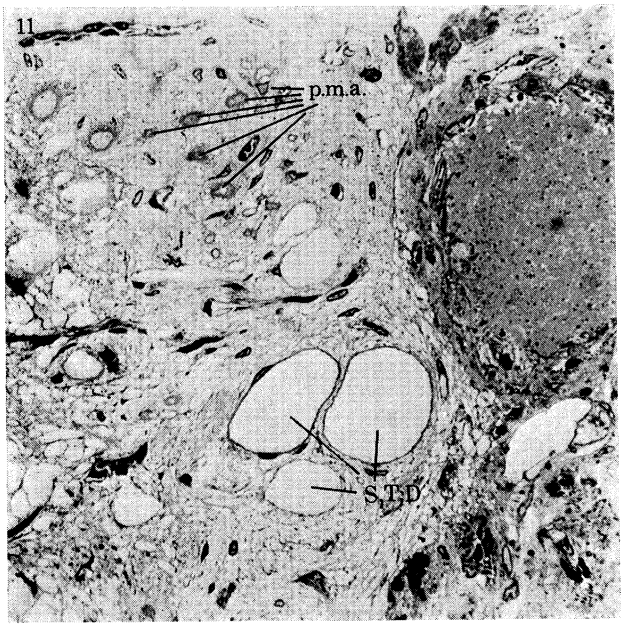

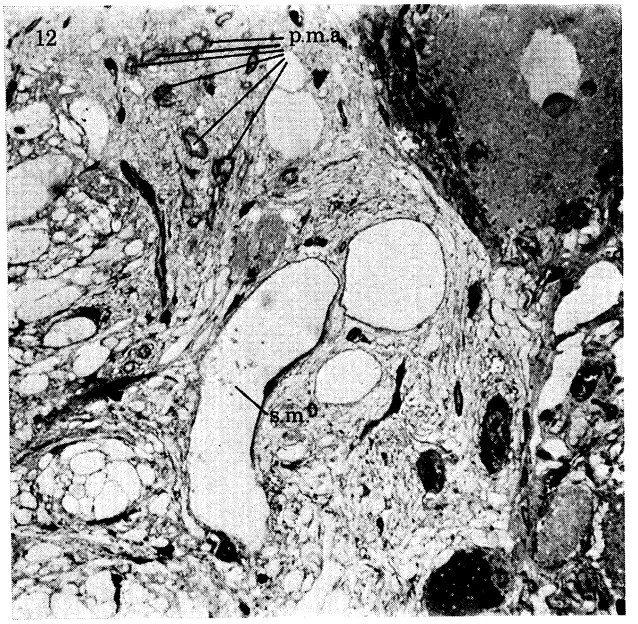

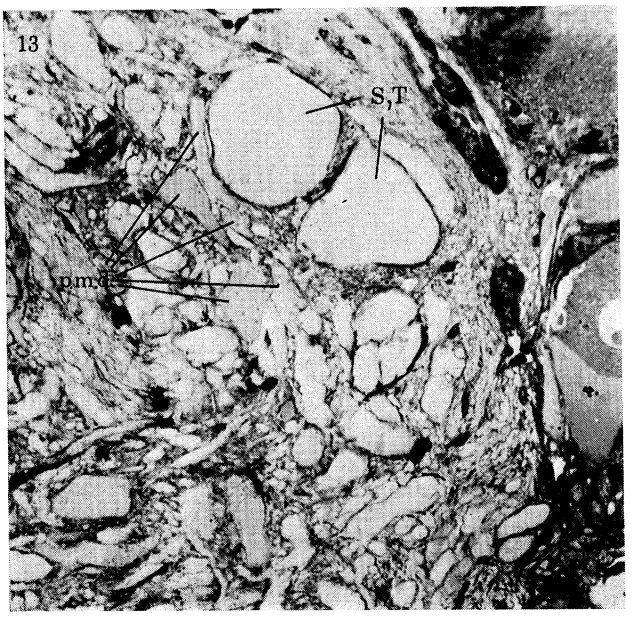

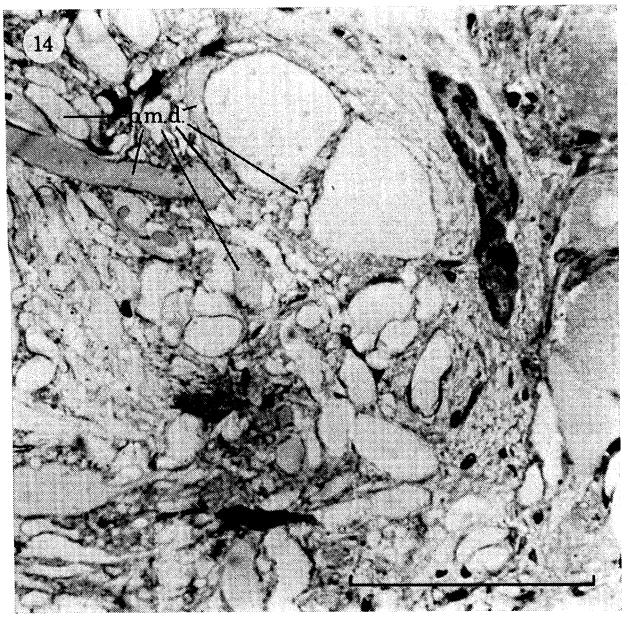

FIGURES 10–14. For description see page 232.

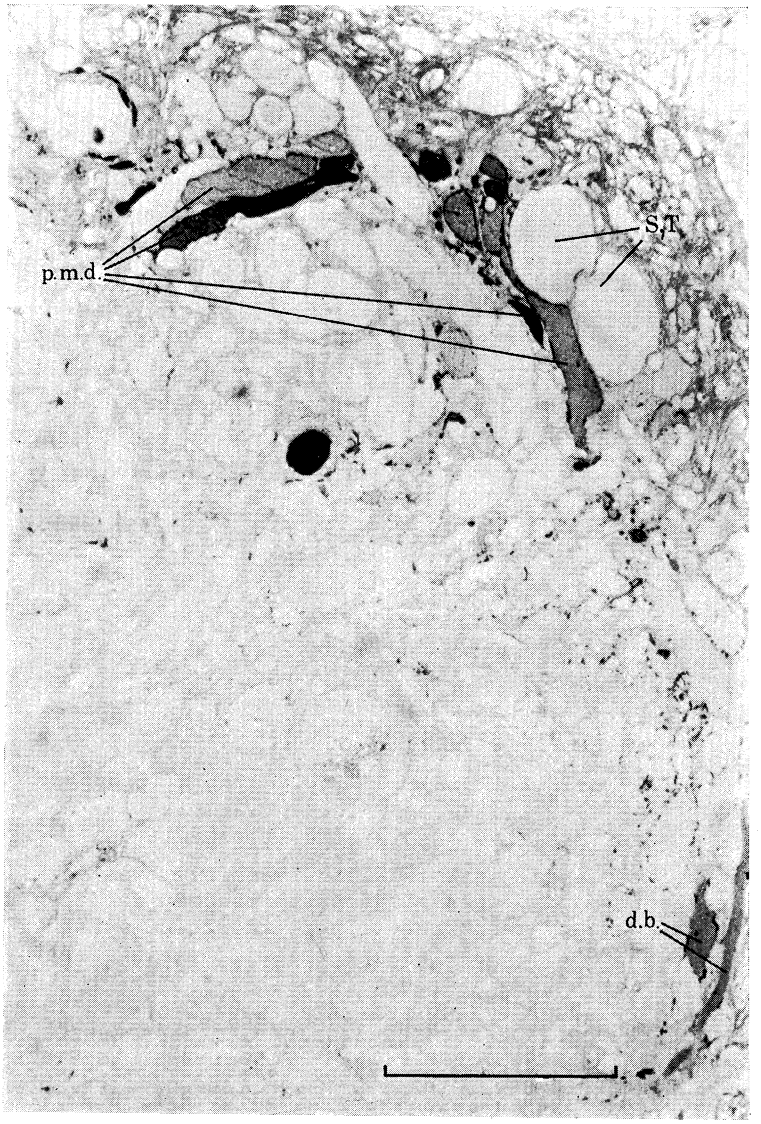

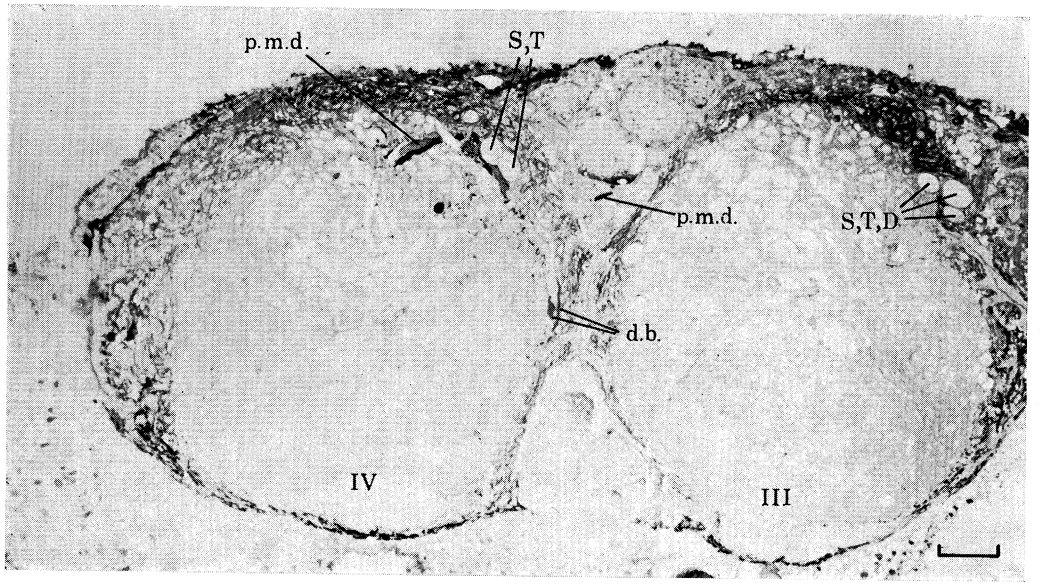

FIGURE 15. For description see page 233.

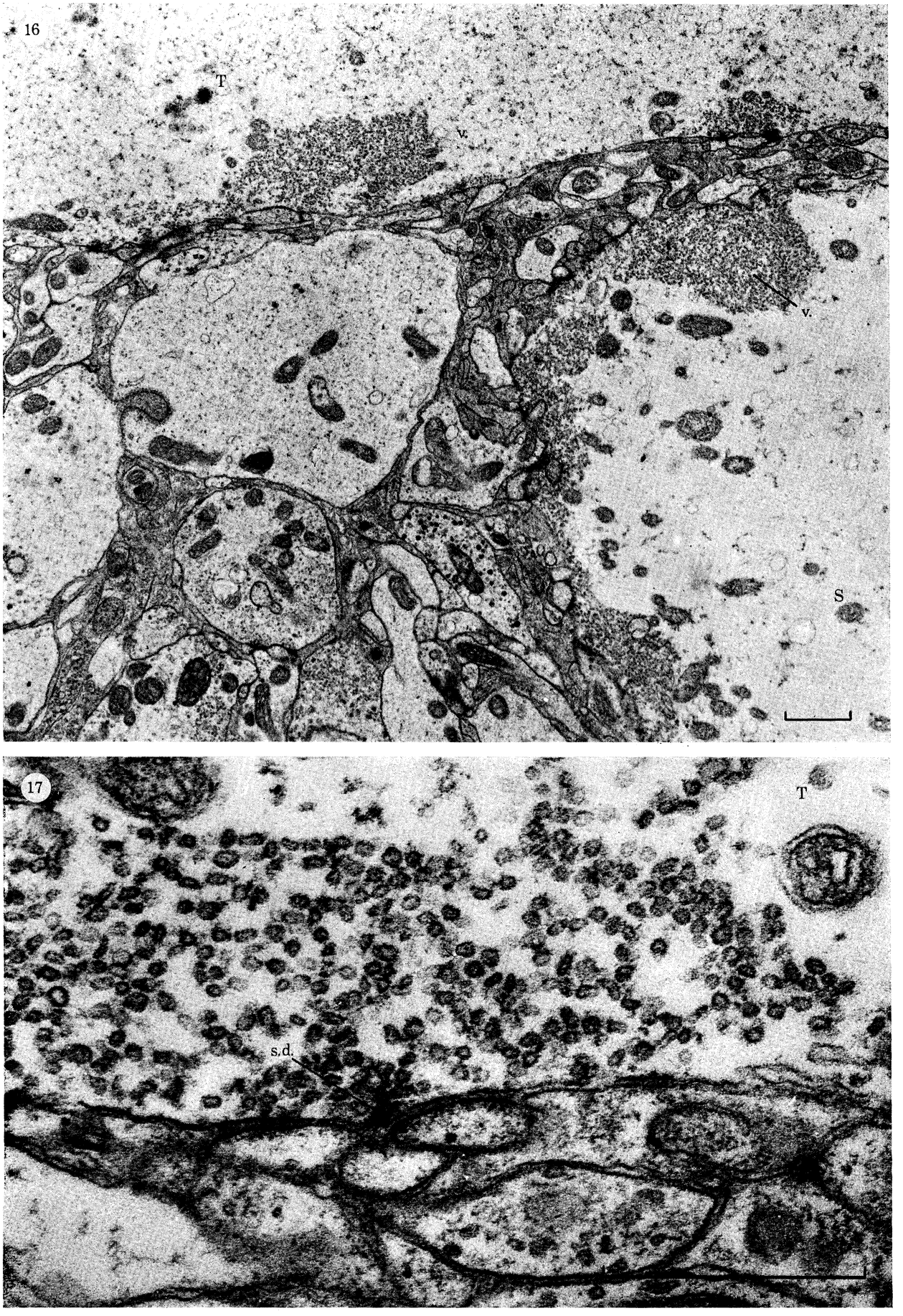

FIGURES 16 AND 17. For description see opposite.

fillings were consistent and no sign of branching was seen in thin sections. The peripheral length of the sensory fibres from the edge of the ganglion to the receptor muscle varied between 8 mm for a small (11 cm) crab to 13 mm for a large (18 cm) crab. The peripheral fibres were not routinely measured, however, in order to determine the normal variability.

In whole mounts and thin sections, the closest apposition of T-fibre and motoneurons was seen to be a third to halfway across the ganglion, where the motor neurites swing under the sensory fibres and also branch ventrally (figures 8, 9). This was therefore the region of the T-fibre that attracted most attention as being a likely site of synaptic interaction. Serial, transverse, 2 μm sections were made along the course of the sensory fibres into the ganglion, with the promotor nerve back-filled with HRP to a density visible at the light microscope level. Localized, granular staining of the sensory fibre contents was found close to the membrane, which first occurred about 100 μm distal to the crossing under of the motoneuron processes, though the greatest density of granular staining coincided with the apposition of sensory and motor cells (figures 11–15).

(*e*) *Electron microscopy of the synaptic zone*

Examined under the electron microscope, the region of sensory fibre–motoneuron junction showed large stores of synaptic vesicles within both the S- and T-fibres. These vesicles were accompanied by typically large synaptic mitochondria, which corresponded to the granular cytoplasmic contents seen with the light microscope (§3*d*). Such synaptic specializations were not seen in the more distal parts of the fibres; where only small mitochondria were found, close to the plasma membrane. Synaptic specializations were only seen on that half of the sensory fibre that faced the adjacent motoneuron processes (as identified in alternate light sections). The number of vesicles and synaptic contacts appeared to be similar in both the large sensory fibres (figure 16).

At the plasma membrane, synaptic vesicles were concentrated around presynaptic densities (figure 17), though, as can be seen in figure 16, a number of such presynaptic densities could share a fairly uniformly distributed 'cloud' of vesicles that was discretely bounded, though no details of intervesicular structures were revealed by the techniques of preservation and staining used here (osmium tetroxide, lead citrate and uranyl acetate staining: Hayat 1975). There was also no sign of the synaptic 'ribbons' seen at tonic junctions in the retina (Sjoestrand 1958) and presumably associated with the rapid turnover of the vesicle population.

The postsynaptic elements, which also stained darkly below the membrane, were mostly

---

Description of plates 3 and 4

Figure 15. Photomicrographs, at two magnifications, of a 2 μm plastic section through the thoracic ganglion showing close apposition of a promotor motoneuron dendrite (p.m.d.) to both the sensory fibres (S, T) in the synaptic zone. The promotor nerve was back-filled with cobalt and the sections intensified with silver without counterstaining. The various motoneurons stained with different intensities, so that it is possible to see some of the parallel branching. Some components of the ventrally descending dendritic branches (d.b.) can be seen. Dorsal is uppermost. Scale bars, 100 μm.

Figure 16. A low-power electron micrograph from the synaptic zone of the S and T fibres (S, T), showing large collections of synaptic vesicles in both fibres (v.), and synaptic densities associated with many small post-synaptic fibres. The large cell profile to the left was post-synaptic to the T-fibre a few sections proximally, by way of a small-calibre branch from the adjacent surface. Scale bar, 0.5 μm.

Figure 17. A higher-power electron micrograph from the same region of the T-fibre (T), showing a synaptic density (s.d.) and the clustering of vesicles around it presynaptically. Scale bar, 0.5 μm.

fibres only a fraction of a micrometre in diameter, though at least some of these could be traced back to outgrowths from larger profiles within a few serial sections. It seems likely that synapses are made with small 'spine-like' processes of larger dendrites. This would be similar to the form of the squid giant synapse (Young 1939, 1973; Hama 1962; Martin & Miledi 1975; Pumplin & Reese 1978), where the postsynaptic fibre makes contact with the presynaptic release sites by way of small knob-like extensions about 1–1.5 μm in diameter (Hama 1962). In the squid, these extensions cross the combined Schwann cell sheaths of the pre- and postsynaptic fibres. The sheath cells of the crab do not form such a continuous layer within the ganglion, though the terminal region of the sensory fibres is surrounded by a layer of fine cell processes that are not in synaptic contact with them.

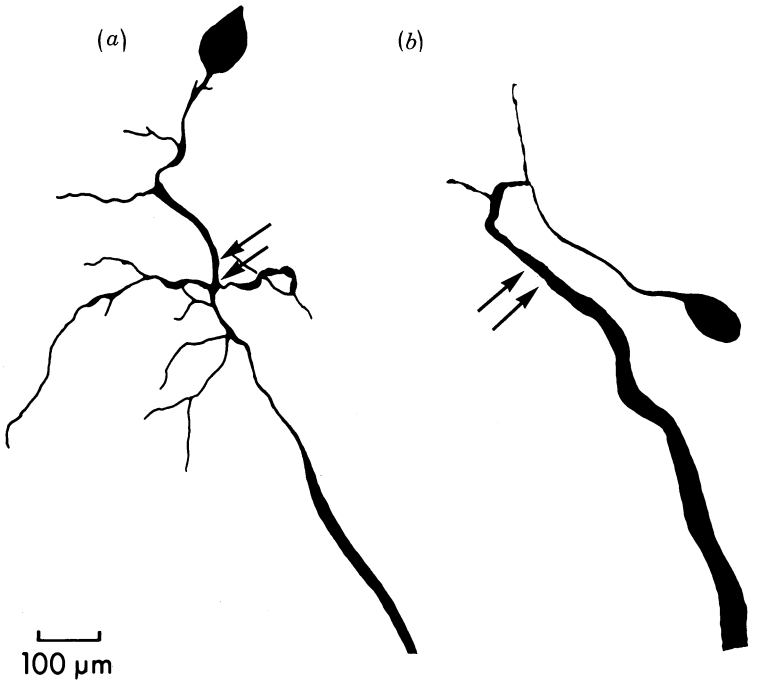

FIGURE 18. *Camera lucida* drawings of dorsal views, (*a*) of a type I motoneuron, and (*b*) a T-cell intracellularly stained with cobalt. The zones of closest apposition between sensory and motor cells is indicated by arrows. From light and electron-microscopic evidence available this is taken to be the site of synaptic interaction in the monosynaptic reflex. The two cells were stained in different ganglia.

Unfortunately, it has not been possible to obtain a sufficient density of staining with HRP in this material to identify the fine postsynaptic elements as belonging to the promotor neurons. For the moment, the identity of the synapses is assumed from the density and proximity of the larger motoneuron processes. Further efforts will be made, meanwhile, to stain, with modified techniques, the postsynaptic elements. Figure 18 illustrates the positions of the presumed sites of interaction between a type I motoneuron and the T-fibre, judging from the light-microscopical evidence of apposition.

(*f*) *Other promotor elements*

The S-fibre was not studied in detail. It has a lesser role in the stretch reflex (Bush 1976, 1977), with a smaller synaptic input to motoneurons. The responses of the S-fibre to receptor stretch have relatively little dynamic component (Bush 1977). This makes it likely that it functions

analogously with the secondary sensory endings of the mammalian spindle (see for example, Granit 1970), probably without monosynaptic input to the motoneurons themselves. The soma of the S-fibre is located on the medial side of the fourth leg ganglion, near motoneuron somata 6 and 7 (figure 6). The elements of the promotor complex therefore seem to have similar somatic locations in *Callinectes* and *Carcinus* (Bush 1976, 1977), despite differences in dendritic fields.

The two motoneurons of the receptor muscle differ from the motoneurons of the promotor muscle itself in that their peripheral axon diameter is maintained further into the ganglion and close to the synaptic zone of the sensory fibres. With cobalt staining they appear to have a dense but small dendritic field towards one edge of the fourth leg ganglion. It would be interesting to study their physiology as it is known that they receive synaptic input from the sensory fibres in *Carcinus* (Bush & Cannone 1974). The most distal of the sensory-fibre synapses (§3*e*) may be associated with these cells.

With reference to the identity of elements postsynaptic to the T-fibre, it may be noted here that many searches were made throughout the third and fourth leg ganglia for cells showing synaptic potentials generated by T-fibre stimulation. Only on very rare occasions were cells found to have synaptic input without also having a clear antidromic spike generated by promotor nerve stimulation. Input to smaller cells, difficult to penetrate with a microelectrode, cannot be ruled out by this technique, but it seems likely that the major recipients of synaptic input from the T-fibre are the promotor motoneurons.

4. Electrical behaviour of the presynaptic T-fibre

(*a*) *Length constant*

To be able to judge the accuracy with which presynaptic potentials could be recorded within the central portion of the T-fibre, it was important to obtain some measure of the degree of attenuation of electrical signals conducted through this region. Previous measurements made on the peripheral fibre had shown that the space constant could be unusually high: 5 mm (Roberts & Bush 1971) to 16 mm (Bush 1977). To check that the values were similar for the intraganglionic part of the fibre, recordings were made with two microelectrodes, one impaling the T-fibre at the usual presynaptic recording site and one just outside the ganglion. Constant-current pulses were then injected, through the sucrose gap, into the fibre (§2*e*) and the resulting voltage changes were recorded at the two electrodes. Results from such experiments are illustrated in figure 19, for both T- and S-fibre.

Unfortunately, the calculation of real membrane constants in the promotor sensory fibres is complicated. First, mathematical modelling of the system is not straightforward as we have to deal with cables that are short relative to their apparent length constants, which are tapered, and which terminate in complex membranes of unknown electrical properties. Therefore, neither the simpler infinite-cable model nor short-cable theory (Weidman 1952) can be totally satisfactorily applied. Since this work was carried out, Mirolli (1979) has published an account of the S-fibre in the Pacific crab *Scylla serrata* that approaches this problem more fully. He favours a semi-infinite model for the steady-state condition, though he finds deviations from it for the conduction of electrical transients, requiring the assumption of a short-circuit termination. Secondly, the electrical responses of these fibres to injected current involve very slow components, which, as Mirolli (1979) has illustrated, can produce voltage 'creeping' over several seconds. Therefore, neither the space constant nor time constant are open to straightforward

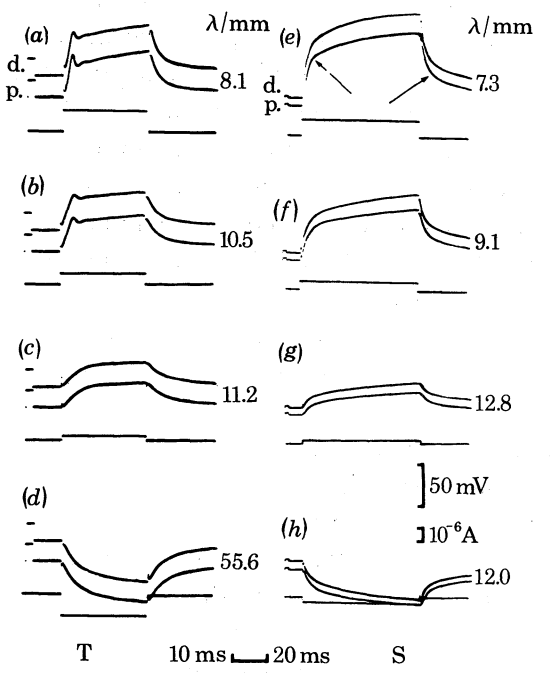

FIGURE 19. Intracellular recordings from sensory fibres, taken with a distal microelectrode (d.) in the fibre outside the ganglion and a proximal electrode (p.) in the synaptic zone within the ganglion, while injecting constant current pulses through the sucrose gap. Values of length constant, calculated on infinite-cable assumptions are given for each level of current pulse. In (*a*)–(*d*) the electrode tips were 0.65 mm apart in a T-fibre, the distal electrode 1 mm from the sucrose gap. In (*e*)–(*h*) the electrode tips were 1 mm apart in an S-fibre, the distal 1.8 mm from the sucrose gap. There is a clear transient response in the T-fibre, but only a difference of depolarizing and repolarizing time constants in the S-fibre (arrows).

analysis. Thirdly, the electrical characteristics of the sensory fibre membrane have proved to be quite variable, especially with regard to the degree of rectification and the prominence of active responses (§4*b*). This is probably owing to real differences in physiology as well as to the expected differences in the effects of experimental handling. Variability in the active component of the receptor was also noted, in *Carcinus*, by Roberts & Bush (1971).

For the purposes of the present study it was only necessary to determine whether or not the attenuation of signals in the intraganglionic fibre was sufficiently small that presynaptic potentials could be recorded with reasonable confidence in their values. Therefore the values of length constant given in figure 19 were calculated on the simple infinite cable model (length constant $= x/\ln V_0/V_x$, where V_0 and V_x are the distal and proximal changes recorded at a separation x). Voltage values were taken arbitrarily at the termination of a current pulse of duration similar to that to be used for analysis of synaptic transmission, rather than current being passed for several seconds to establish the final steady-state response. The 'apparent' length constants in the presynaptic region were found to be within the range of 3–60 mm reported for the peripheral fibre in other species (Roberts & Bush 1971; Mirolli 1979). The fibres used in these examples showed more rectification than was usual for fibres with a single intraganglionic microelectrode penetration. There was consequently a reduction of apparent length constant with depolarization. The values shown in figure 19 are probably an underestimation, therefore, as the normal setting up of the preparation did not involve the generally damaging procedure (Mirolli 1979) of penetrating the sheath of the extraganglionic fibre with a microelectrode.

In conclusion, it seems likely that recording the potential at almost any point along the length of the T-fibre within the ganglion should give a close approximation of presynaptic potential for all but very large depolarizations, where length constant may fall below 10 mm.

(*b*) *The depolarization transient, a graded spike*

As can be seen in figure 19, the response of the T-fibre to current injection is not that of a purely passive membrane or resistance–capacitance network. Above a certain threshold of depolarization, the rate of rise of the depolarization begins to exceed the rate of repolarization and this acceleration grows into a spike-like event with increasing current strength. This transient response to depolarization was variable from animal to animal. It was usually more prominent in the T-fibre than in the S-fibre, and at times was almost absent from the latter (figure 19). The largest amplitude transient was recorded from the T-fibre of an immature crab (8 cm carapace width). It is possible that spike-amplitude is consistently related with age or moulting-cycle, but this has not been investigated systematically. This large response is shown in figure 20, as it indicates the form of the spike more clearly than that more usually recorded in adult animals.

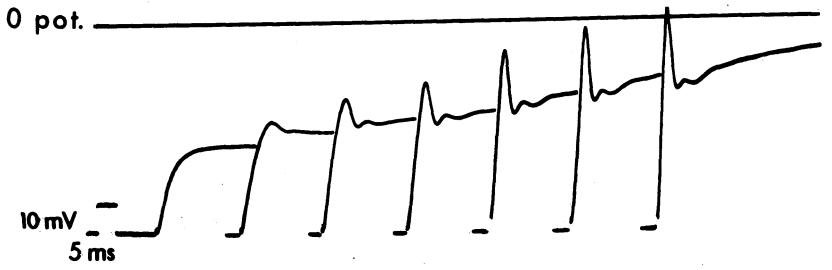

FIGURE 20. Intracellular records showing an unusually large transient voltage response to the injection of constant current pulses into the T-fibre of an immature crab. The microelectrode, within the ganglion, was about 4 mm from the sucrose gap. The rising phases of the depolarizing responses to increasing steps of current are shown. The upper line (0 pot.) in this and subsequent figures indicates the bath potential relative to the presynaptic intracellular potential.

This spike-like response is formed by a double wave of positivity, the second part of which increases and then fails in relative amplitude as the first part steadily increases with increasing current steps. With increasing amplitude, the second peak decreases in latency after the first with indications of further oscillations in membrane potential.

Figure 19*a* also shows that the spike is larger in amplitude, relative to the plateau depolarization further into the ganglion, at the level of the synapse. In figures 21 and 22 it can be seen that the response is not only relatively larger in amplitude but also reaches its peak earlier at the synapse than in the peripheral fibre. Yet the absolute amplitude of the 'spike' is larger in the fibre than in the synapse, so the event seen in the fibre is not merely conducted electrotonically from the preterminal region. Rather, it seems likely that the rising phase of the spike results from voltage-dependent conductance changes occurring initially in the peripheral fibre membrane, and that the fall is led by conductance changes occurring within the ganglion, perhaps at the synaptic level.

The duration of the depolarizing phase of the transient decreased with increasing amplitude, as can be seen more clearly in differentiated records like those of figure 23. In this figure, the responses of the same T-fibre to injected current are shown before and after the intracellular

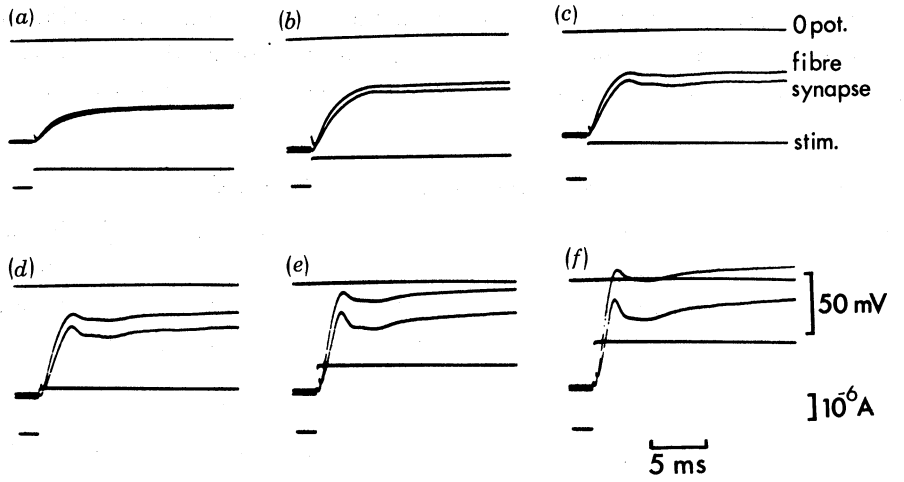

FIGURE 21. Intracellular recordings of voltage responses of the T-fibre to the injection of constant current stimulus (stim.) through the sucrose gap, with microelectrodes proximally in the synaptic zone (synapse) and just outside the ganglion in the peripheral fibre (fibre). The electrode tips were 1 mm apart and the fibre electrode was 1 mm from the sucrose gap. The transient response is larger relative to the plateau depolarization at the synaptic level than in the peripheral fibre.

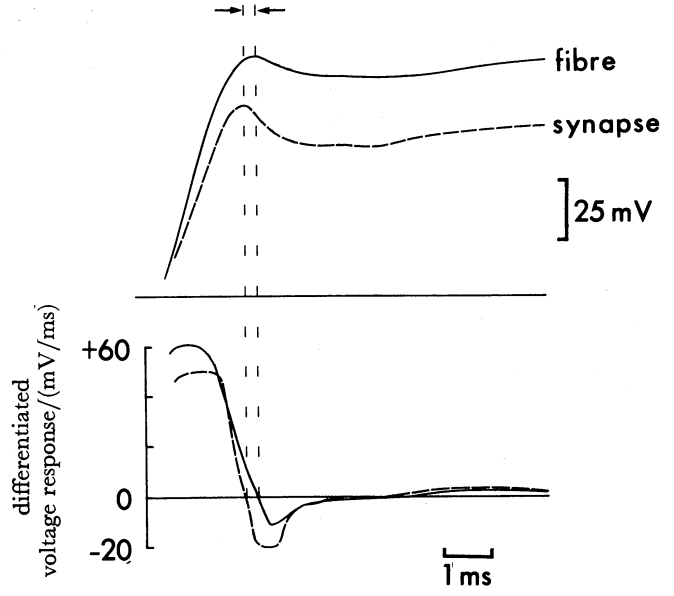

FIGURE 22. Tracings of a response shown in figure 21 at an expanded time scale and with the signals differentiated below. The reversal of voltage change at the peak of the transient response occurs 250 μs earlier at the synapse than in the fibre.

injection of TEA. At low levels of depolarization, when the membrane potential rises relatively slowly through the threshold for a transient response there is a prolonged, low amplitude 'spike'. The duration of the response is increased even more by the injection of TEA, and this may be either by a direct effect on the conductance responsible for the repolarization (see §6*h*) or because the TEA increases the time constant of the cell (by blocking voltage-dependent potassium channels (Armstrong & Binstock 1965)) and therefore decreases the rate of rise of the potential through threshold.

The time-dependence of the T-fibre membrane response was studied by recording with a microelectrode at the synaptic level while injecting sinusoidally oscillating currents through the

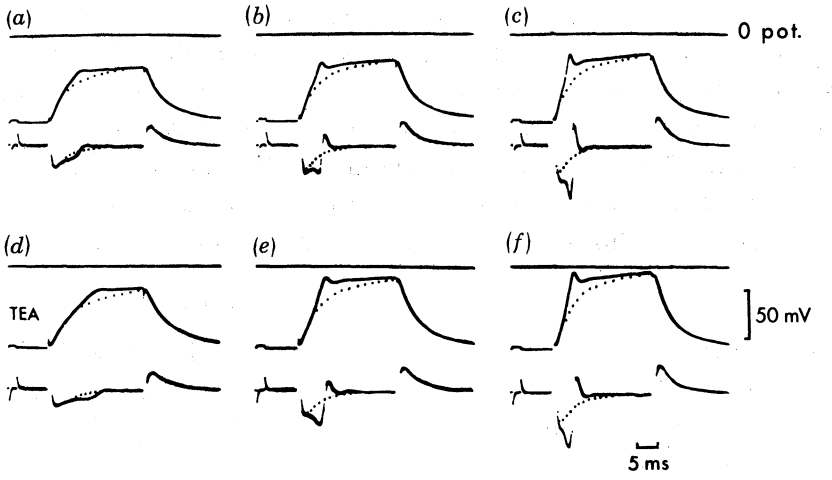

FIGURE 23. Each of the records (*a*)–(*f*) shows a recording of voltage and electrically differentiated voltage (dv/dt) from the synaptic zone of a T-fibre in response to injection of constant current pulses of three different intensities. In (*d*)–(*f*), the fibre had been injected with TEA. The dotted lines indicate the rising phases which would be symmetrical with the falling phases.

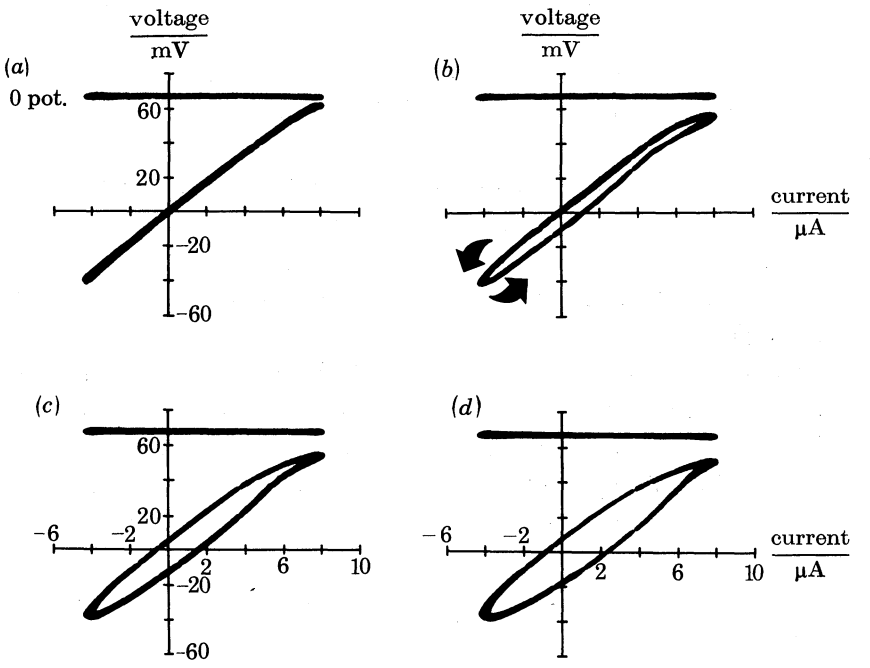

FIGURE 24. Voltage–current plots for the T-fibre, generated by applying sinusoidally oscillating currents through the sucrose gap and recording the voltage changes with a microelectrode at the synaptic level. The current signal was fed to the horizontal deflector plates of the oscilloscope. The distance from the sucrose gap to the recording electrode was 2 mm. Plots were made with the current oscillating at (*a*) 1, (*b*) 2.5, (*c*) 5 and (*d*) 9 Hz. Note the reduction of hysteresis in the depolarizing direction.

sucrose gap. In this way it was possible to determine whether the cell was likely to behave as a purely passive cable at normal frequencies of operation.

From the recordings in figure 24, it seems that the response of the fibre at a frequency of 1 Hz is purely passive, but at higher frequencies the depolarizing and hyperpolarizing responses become asymmetric. As would be expected, the capacitance of the cell membrane results in a voltage hysteresis proportional to the frequency of oscillation. But this hysteresis is reduced at

voltages above threshold for the depolarization transient, the depolarization rising faster than would be predicted for a passive cable. It seems, therefore, that there is a tendency for the depolarization of the proximal T-fibre to become regenerative, though it is only at very high frequencies (a step input) that this results in an obvious, spike-like yet graded event. This active response of the T-fibre is probably the same as that responsible for the variable 'spiky' alpha component of the receptor response to stretch described by Bush (1977). The possible functional significance of this transient will be considered later (§6*i*).

(*c*) *The ionic basis of the graded spike*

On present knowledge, the most likely mechanism for the depolarization transient is a brief alteration in ionic membrane conductance. An inward current of the kind required to produce the observed regenerative depolarization would be expected to be carried by sodium and/or by calcium. It is known that the promotor sensory fibres of *Carcinus* contain some voltage-sensitive sodium channels that are susceptible to tetrodotoxin (TTX) poisoning (Lowe *et al.* 1978), though these seem not to be operating under normal conditions. It was found in *Callinectes* that TTX had little or no effect on the amplitude of the depolarization transient at concentrations (up to 10^{-6} M) that completely blocked the motoneuron spiking, contrary to the finding of Roberts & Bush (1971) that 0.3×10^{-6} M TTX reduced the depolarization transient of the receptor potential by about 50% in amplitude in other species. However, apparently similar transients have been described from other non-spiking secretory cells, in the lobster stomatogastric ganglion (Graubard 1978) and, on a slower time scale, in the pedal gland of the slug (Kater 1977). In these cases too, the responses were shown to be unaffected by TTX. It should be stressed here that we have been concerned only with the proximal segment of the T-fibre, and it is quite possible that its membrane properties differ significantly from those of the peripheral fibre nearer the receptor ending, with its sodium-dependent responses to stretch (Roberts & Bush 1971; Bush 1977).

Figure 25 shows the effect on the transient of replacing external sodium to be quite small. There is some reduction in the amplitude of the transient and an increase in its duration, but this may be explicable by an increase in the time constant of the cell, in the same manner as in figure 23 (i.e. the amplitude of the transient is smaller and its duration longer as the underlying rate of rise of potential is decreased; a membrane normally slightly leaky to sodium would be expected to show an increased membrane resistance and therefore a larger time constant in the Tris medium). There is no reason to believe that this resistance of the transient response to removal of external sodium is due to retention of sodium in the extracellular space. Krauhs & Mirolli (1975) have demonstrated that the receptor end of the T-fibre, with its elaborate sheathing, has its extracellular space open to lanthanum ions in *Cancer*. Replacement of sodium completely suppresses the T-fibre e.p.s.p. recorded in the motoneuron soma, suggesting that the extracellular space of the synaptic end is also open to diffusion.

Initial experiments, with choline to replace sodium, suggested a much more powerful effect on the transient, which lead us, in a preliminary note (Blight & Llinás 1978), to say that the transient was sodium-dependent. These experiments proved to be unrepeatable with the more satisfactory Tris substitutions or with other stocks of choline chloride, so that the original observations probably derived from some poisoning of the T-fibre with contaminants. Nonetheless, it remains possible that the transient involves inward movement of sodium as well as calcium and more precise measurements are needed to determine the proportional significance of each ion.

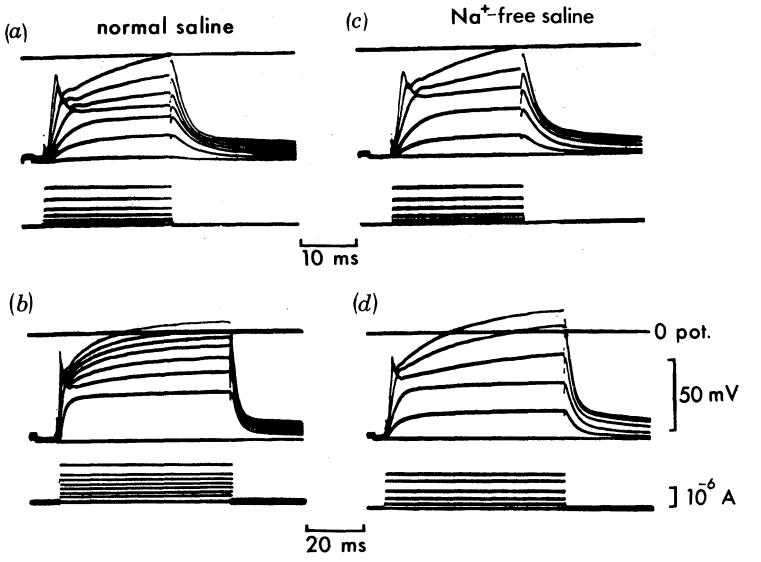

FIGURE 25. The effect of removal of external sodium ions on the depolarization transient of the T-fibre. Voltage responses to current injection through the sucrose gap were recorded with a microelectrode in the synaptic region, 2 mm from the sucrose gap. Before obtaining records (*c*) and (*d*) the ganglion was superfused for 15 min with saline in which the sodium ions had been replaced by Tris (§2*c*).

At present, however, the most probable explanation of the depolarization transient is that it represents an increased membrane conductance primarily for calcium. Unfortunately, the ability of the T-fibre to conduct depolarizing potentials was found to fall dramatically in the time needed for calcium replacement at the synapse, even in the presence of high magnesium to stabilize the membrane. However, when the preparation was superfused with saline in which calcium ions had been replaced with cadmium, there was a significant reduction in the amplitude of the depolarization transient before deterioration of conduction in the fibre and before there was much loss of calcium in the extracellular space around the synapse (as judged by postsynaptic potential (e.p.s.p.) amplitude) (figure 26).

It seems, therefore, that the calcium conductance is not limited to the synaptic membrane but is present in the fibre outside the ganglion, at least in its proximal part, as the transient is reduced in amplitude before the e.p.s.p., which suggests a reduction of extracellular calcium first in the extrasynaptic fibre. That the spike tends to *fall* earlier at the synaptic level than outside the ganglion (see figure 22) suggests that the conductance changes responsible for bringing down the spike may be predominantly synaptic. This could represent a mechanism for 'clamping' the presynaptic membrane potential from the periphery if the extraganglionic membrane tended to become regenerative and the regenerative responses were brought down at the synaptic level.

An interesting feature of the repolarizing phase of the transient can be seen in figure 25*b*, with the application of longer current pulses. The time constant for the attainment of plateau depolarization is larger than the time constant of the cell for subthreshold pulses. This is not a graded increase in time constant, but a step increase. It seems most probable that the larger time constant is that of the 'inactivation' of the conductance (presumably of potassium), which brings down the transient spike. The possible susceptibility of the repolarizing conductance to TEA is discussed later (§6*h*).

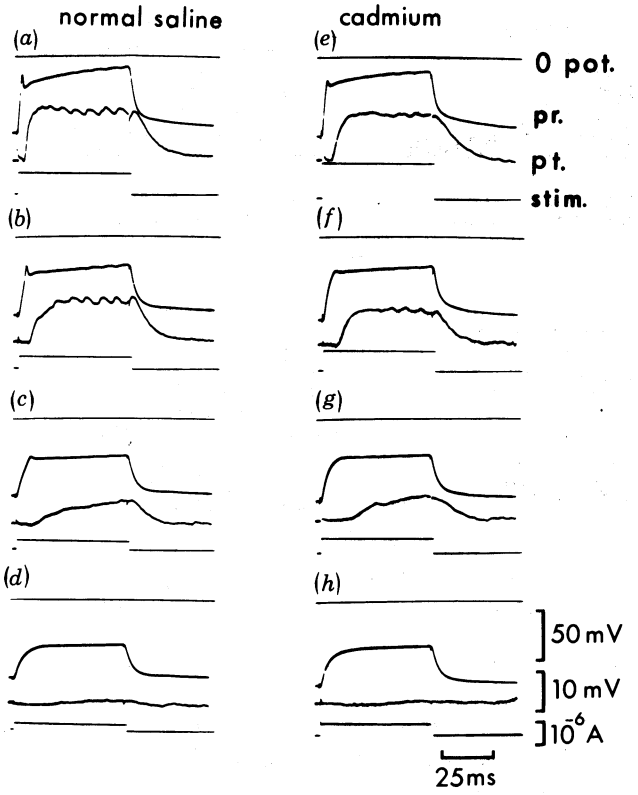

FIGURE 26. Recordings to demonstrate the effect on the presynaptic transient of replacing calcium in the superfusate with 2 mM cadmium. Records (*a*)–(*d*) show transmission characteristics of the synapse bathed in normal saline. In each block the upper line is bath potential (0 pot.) relative to the presynaptic potential (pr.), recorded from the synaptic zone of the T-fibre. The postsynaptic potential (pt.) was recorded from the soma of a type III motoneuron. Constant current stimulus pulses (stim.) were injected, through the sucrose gap, into the peripheral T-fibre. In (*e*)–(*h*) similar records are shown from the same preparation 10 min after the beginning of superfusion with cadmium saline. There is a clear effect on the peripheral transient and a smaller effect on the central transmission.

(*d*) *Capacity compensation in decremental conduction*

One of the more obvious biological problems inherent in the use of decremental conduction of analogue signals over long distances is the distortion produced by the large capacitances involved. To reduce attenuation of the signal the cell must have a relatively high membrane resistance, but this means that its time constant will also be large and electrical changes occurring at one end of a fibre will take a long time to be effective at the other. The same problem is met in the field of electronics, where to overcome the effects of distortion in analogue signals it is necessary to introduce circuit elements that do no more than compensate for the capacitance of others. The interesting feature of the depolarizing transient of the T-fibre is that it appears to be an example of biological capacity-compensation.

Figure 27 illustrates the behaviour of the proximal segment of a T-fibre to current injection, as a summary of figures 19–24. At low frequencies, the fibre responds practically ohmically, and with such slowly changing signals there is little distortion introduced from the cell capacitance. At higher frequencies, the fibre shows typical voltage hysteresis in the hyperpolarizing direction, but with depolarizations above about 30 mV the hysteresis is reduced, here almost to zero, by

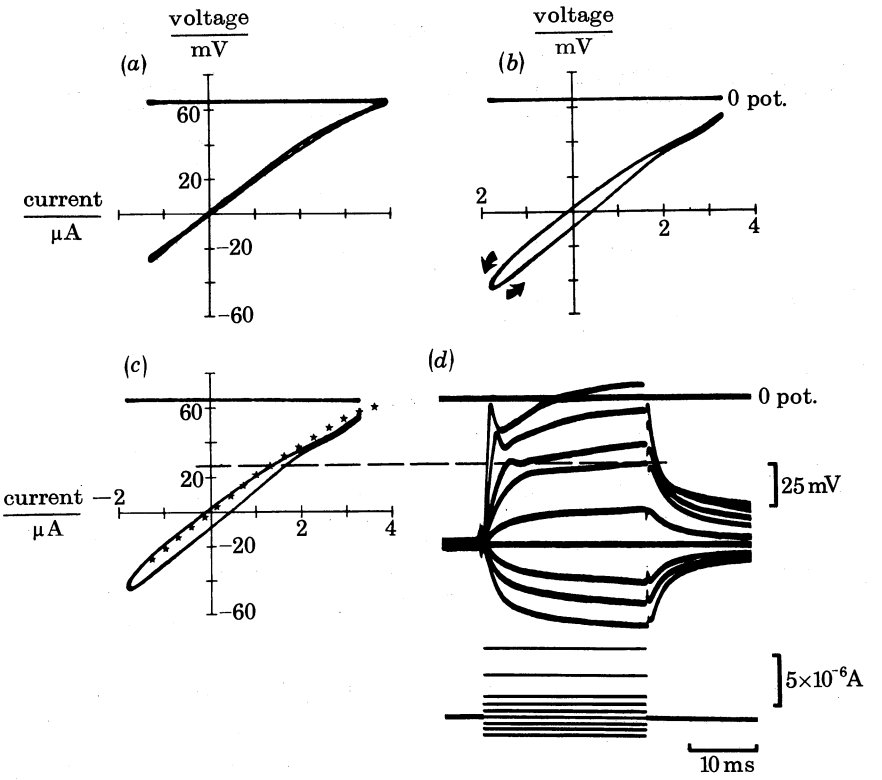

FIGURE 27. Records summarizing the effect of 'capacity-compensation' in the T-fibre. (*a*), (*b*) Continuous voltage–current plots, as in figure 24, with 1 and 6 Hz sinusoidally oscillating current respectively. The stimulus current was delivered, through the sucrose gap, at a distance of 1.7 mm from the recording electrode at the synaptic level. It consisted of a combined steady depolarizing current and sinusoidal oscillation about that level, so that the fibre was not too powerfully hyperpolarized. The responses of (*a*) and (*b*) are superimposed in (*c*), (*a*) indicated by stars. (*d*) The responses of the same fibre to injection of constant current pulses over the same range, to show that the threshold for the depolarization transient is the same as that for the reduction of hysteresis (dashed line).

the nonlinear response of the membrane to injected current. Then in (*d*) of figure 27 we can see that the effective time constant for depolarization is much reduced by the transient response to a step input, relative to the time constant for repolarization at the end of the pulse. This capacity-compensative effect has the same 'threshold' as the hysteresis reduction seen with oscillating currents.

Additionally, because the transient response is probably calcium-dependent, its role in compensating for distortion may not be limited to the presynaptic fibre. The effect of the transient on the e.p.s.p. in the motoneuron will be considered later (§6*i*).

5. PHYSIOLOGY OF THE POSTSYNAPTIC MOTONEURONS

(*a*) *The antidromic spike*

The most convenient recording sites for the postsynaptic motoneurons of the promotor system are the cell bodies that lie on the dorsal surface of the ganglion (cells 1–4 in figures 6, 7). These somata are large (over 100 μm in diameter for cells 1–3), reasonably consistent in position (§3*c*), and sometimes directly visible by transmitted light, particularly if the underside of the ganglion is desheathed to reduce light scattering. They are easily impaled and are recognized as

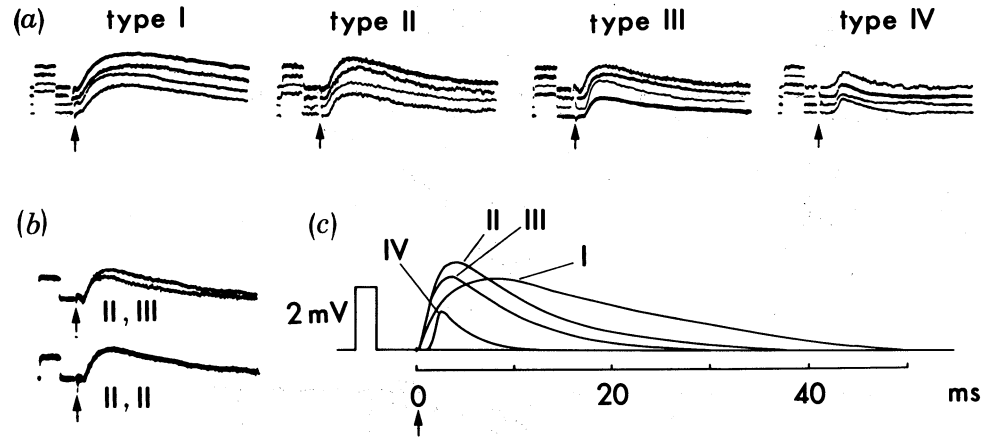

FIGURE 28. The four types of antidromic spikes recorded in the somata of motoneurones 1–4 (figure 6). (*a*) Four examples of each type, recorded from different animals to indicate the level of repeatability. (*b*) The antidromic spike was recorded in the type II cell of a ganglion, then in the type III cell of the same ganglion, then in the type II cell again to check that penetration had not altered its characteristics to appear like another type. Spikes recorded in the first and second penetration of the type II cell are shown below superimposed. Spikes from the type II and III cells are superimposed above. (*c*) Tracings of representative spikes of the four types to show their characteristics more clearly. All calibration pulses 2 mV × 2 ms.

promotor motoneurons by the presence of antidromic spikes when the peripheral promotor nerve is stimulated. After records had been made from many of these cells it was found that the antidromic spikes could be divided into three types and, with more difficulty, eventually a fourth, on the basis of their form (figure 28). These spike forms were remarkably consistent from animal to animal, even at different times of the year and in different geographical populations.

The somata of these motoneurons, together with much or all of the dendritic membrane, do not propagate action potentials. This situation is typical of invertebrate ganglia and results in very small amplitude antidromic spikes recorded at the soma. These were never above 4 mV in the largest type (I), and in the region of the 1 mV for the smallest (IV). At the same time, the spike recorded at the soma has a very long duration, reflecting the time constant of the cell.

By electrophoretic ejection of fast green (FCF) from the recording electrode, it was determined that the spike with the longest duration (type I of figure 28) was recorded from the soma of largest diameter (cell 1 of figure 6). Spikes II and III were recorded from the intermediate sized cells (2 and 3), and spike IV from the smallest (4). At the same time, on the evidence of conduction velocities and back-filling of individual axons with cobalt, type I/1 has the largest peripheral axon (figure 10), types II/2 and III/3 the two intermediate sized axons, and type IV/4 one of the smaller axons, perhaps, by extrapolation from soma size, the third smallest.

No recordings were made from the other three somata, though perhaps from their neurites. Antidromic spikes recorded in neurites could not be identified with cell types. Occasional recordings were made from fibres of promotor neurons with lower thresholds than those of types I–IV. The peripheral branching of the axons has not been studied, but presumably cell types I–III would be involved in more phasic activity of the fourth leg, such as swimming and escape responses. This would agree both with their high conduction velocities and with their relatively high thresholds for T-fibre activation (§6*b*).

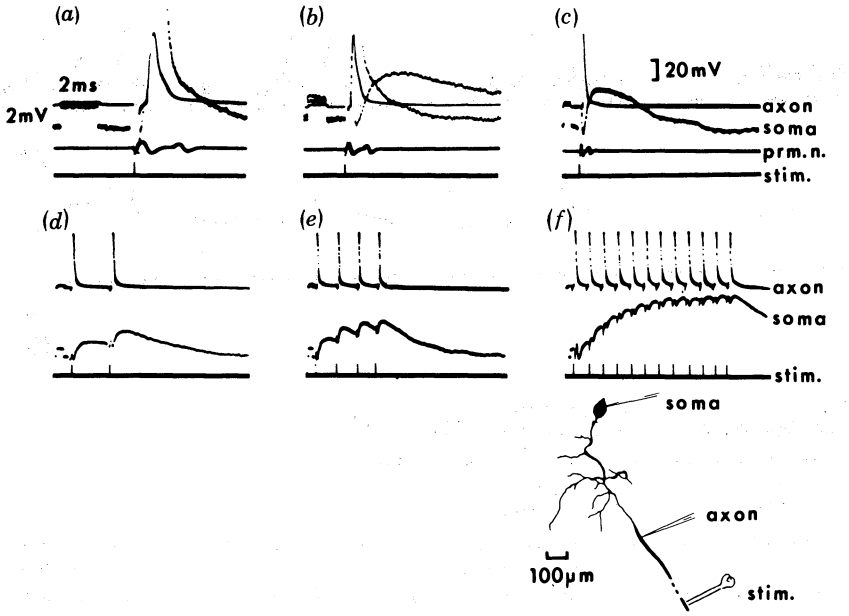

FIGURE 29. Antidromic spikes recorded simultaneously in the axon on the edge of the ganglion and in the soma of a type I motoneuron. (*a*) The spike recorded in the axon at high and low gain to show the typical form with after-depolarization. (*b*) At one-half of the sweep speed of (*a*), together with the spike recorded in the soma, showing the axonal after-potential to be short relative to the somatic potential. (*c*) At one-fifth of the the sweep speed of (*a*), to show the somatic time course. (*d*)–(*f*) Repetitive firing of increasing frequency to show the summation of somatic potentials. The inset shows the recording situation on the outline of a stained cell. A similar, 2 mV/2 ms, calibration pulse is shown in all records. Sweep speed in (*e*) and (*f*) was one-tenth that in (*a*). The compound potential recorded from the cut end of the promotor nerve at the level of the receptor ending is shown in trace labelled prm. n.

(*b*) *Dendritic depolarization by repetitive firing*

One of the consequences of the large time constant of the motoneuron somato-dendritic membrane is that antidromic spike depolarizations can sum to give steady depolarizations of quite large amplitude, even at the firing rates found in normal behaviour. This can be seen at the somatic level in figure 29, where antidromic spikes have been recorded near the initial segment of the axon and in the soma of the same cell while stimulating the peripheral nerve.

Such dendritic depolarizations may have positive-feedback effects on the spike-initiating zone of the same cell, tending to reinforce (at a fairly low gain) bursting behaviour with strong initial input. They may have more significance, however, in the light of the finding of interaction (probably dendritic) between the promotor motoneurons (§5*c*).

(*c*) *Interaction between motoneurons*

There seems to be some level of excitatory interaction between the motoneurons. In some cells it was possible to record a second, small, lower threshold, all-or-nothing event underlying the antidromic spike. This potential presumably originates from the antidromic spike of one of the other motoneurons. It was most easily recorded in the high-threshold type I cell, though not all type I cells demonstrated it (figure 30). By injecting current into type I somata and recording in neighbouring motoneurons it has not been possible to demonstrate electrical coupling between them. The junctions between the cells are therefore probably at too great an electrotonic distance from the soma to be revealed by this technique. Nonetheless, by analogy with other systems of

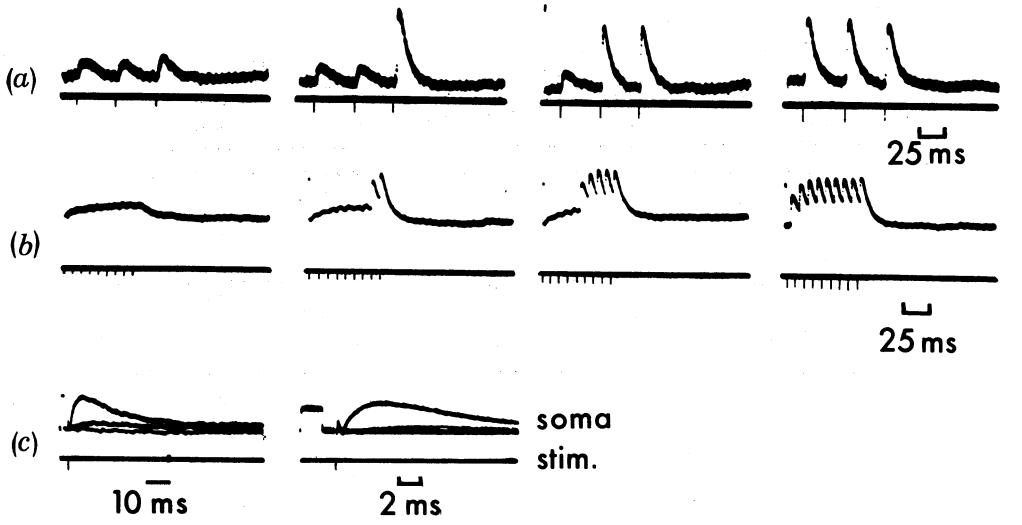

FIGURE 30. Recordings of the interaction between a lower threshold motoneuron and a type I motoneuron. All the records in (*a*), (*b*) and (*c*) show intracellular potential of a type I soma (upper trace), together with the timing of stimuli to the peripheral promotor nerve (lower trace). (*a*) Three shocks of equal intensity were delivered to the nerve and the intensity was increased slightly in each of the four cases from left to right. There were two all-or-none potentials in the soma, with different thresholds. (*b*) With increased stimulus frequency it could be shown that both all-or-none potentials could sum. (*c*) Superimposed traces of single shock stimulation with varying intensities show the two all-or-none units to have different time courses. All calibration pulses were 2 mV.

synergistic neurons, it seems likely that there are electrotonic junctions between the dendrites of the motoneurons that run in close apposition over much of their course (figure 8).

It is possible that the combination of dendritic coupling with the summation of antidromic spikes provides a mechanism whereby the threshold of more phasic motoneurons could be lowered for concerted activation with the lower threshold cells, in that repetitive firing alone (ignoring the synaptic potentials, which may be even more important if close to coupling sites) in lower threshold units would slightly depolarize the dendrites of more phasic cells and predispose them to fire (figure 30*b*).

(*d*) *Soma–dendritic membrane properties*

To understand better some of the features of the e.p.s.p. recorded in the soma, it was useful to know more about the postsynaptic membrane response to injected current. Although it was not possible to examine the postsynaptic membrane itself, the somatic and the adjacent dendritic membrane (which determines in part the voltage recorded in the soma) was open to study. To make this analysis, two microelectrodes were inserted into a motoneuron soma and their position was checked by antidromic spike recordings. Transmembrane voltage was measured through one electrode as current pulses of known amplitude were injected via the second electrode (figure 31).

Somatic current–voltage relations were linear through the resting potential for type I and II cells, but the membrane resistivity showed marked rectification with larger depolarizations. In this set of experiments, the maximum depolarizations were about 40 mV for type II cells and near 60 mV for the type I cell measured. The type III cell could not be depolarized more than 20 mV by injected currents. If the membrane properties near the soma are continued throughout the dendritic tree, then one would not expect to record an e.p.s.p. larger than 60, 40, or 20 mV in the types I, II, and III motoneurons respectively.

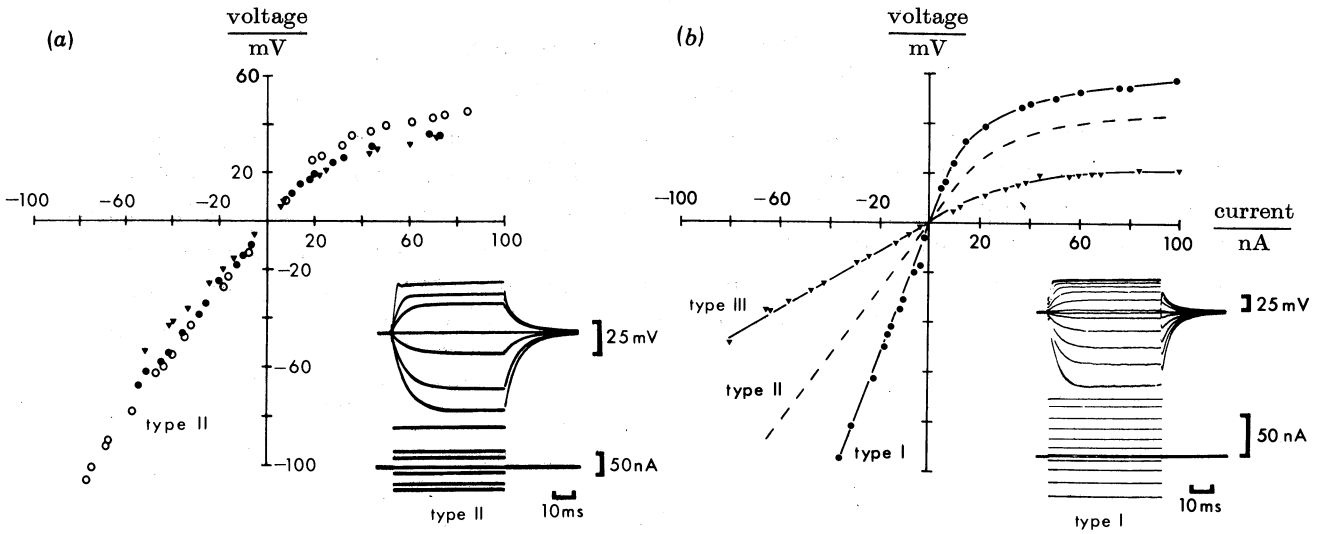

FIGURE 31. (*a*) Voltage–current plots for three type II motoneuron somata (●, ○, ▼), generated from two-electrode analysis with current pulses (inset). (*b*) Voltage–Current plot for a type I and a type III motoneuron in comparison with the mean of the type II behaviour shown in (*a*). Insets show sample records from a type II cell (*a*) and a type I cell (*b*).

(*e*) *Excitatory synaptic input*

In the isolated ganglion it was possible to analyse briefly excitatory input to the motoneurons before the experiment by recording the promotor nerve activity while cutting all the other nerves radiating from the ganglion. It was found that strong excitatory input came from injury discharges in (or electrical stimulation of) the abdominal nerve. Strong excitation, and in some subunits inhibition, derived from the ipsilateral fourth leg nerves. Very weak activation was sometimes obtained from injury to the oesophageal connective and from some parts of the ipsilateral third leg nerve. All these excitatory inputs gave only a transient effect with injury discharge. The only tonic excitatory influence following from damage was revealed by cutting the S- and T-fibres of the same leg. Even the S-fibre influence decayed to a low level within a few seconds.

One of the most powerful inputs to the promotor cells apart from the stretch receptor was found to come from the large nerve adjacent to the promotor nerve in the fourth leg bundle. In intact preparations this nerve was found to contain sensory units responding to touch on and around the coxa (figure 4). Stimulation of this nerve could be used as a test for the general reflex condition of the ganglion. Single-shock electrical stimulation gave rise to large e.p.s.p. in bursts with decay times of several seconds.

With saline containing 40 mM magnesium and 10 mM calcium the isolated ganglion generally showed little spontaneous activity except in the lowest threshold promotor unit, which often fired spontaneously, either in short bursts or, more frequently, continuously at a few spikes per second. There was much more spontaneous bursting activity, sometimes involving all seven promotor units, when the ganglion was isolated in saline containing 20 mM magnesium and 20 mM calcium. Some of this activity was clearly rhythmical and perhaps sufficiently structured to represent walking or struggling activity.

6. Synaptic transmission

(*a*) *T-fibre input to motoneurons*

It has been known for some time, from extracellular peripheral recordings, that the graded signals carried by a single T-fibre are sufficient to activate promotor neurons (Bush & Roberts 1968). However, the nature of the interaction was not apparent from this type of analysis. Recording with microelectrodes within the thoracic ganglion, we found that the action of the T-fibre on the motoneurons has the characteristics of a purely chemical synapse (§ 6*b*). Synaptic delay cannot be measured easily in this presentation because the potential at the presynaptic

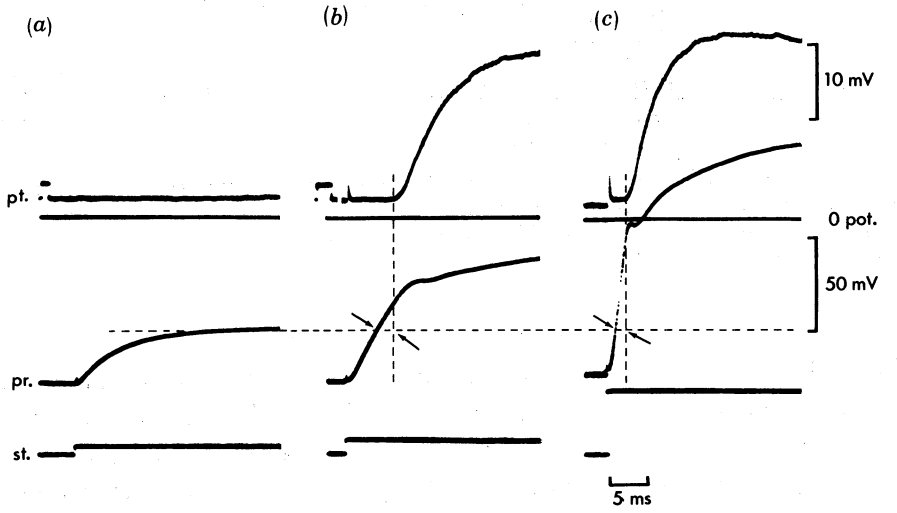

Figure 32. A measurement of synaptic delay. Presynaptic potential (pr.) was recorded in the synaptic zone of the T-fibre and postsynaptic response (pt.) was recorded in the type I motoneuron soma. (*a*) A presynaptic current pulse (st.) producing a depolarization just subthreshold for transmitter release, establishing the 'threshold' level indicated by the horizontal dashed line. (*b*), (*c*) The effect of larger current pulses giving rise to postsynaptic potential changes with latencies indicated by the vertical dashed lines and arrows. With a fast-rising potential as in (*c*), the delay in postsynaptic response from the time that presynaptic potential crosses 'threshold' appears to be between 1.3 and 1.4 ms. There is a longer apparent latency in (*b*) of about 2 ms, probably because of the difficulty of estimating the deflexion point with lower rates of rise. (The sweep speed in (*a*) was 0.4 × that in (*b*) and (*c*), to which the 5 ms scale bar refers.)

terminal rises relatively slowly and the postsynaptic recording site is at some electrotonic distance from the synapse, which gives rise to an unknown electrotonic delay.

Figure 32 shows that if we take into account the time taken by the presynaptic potential to reach the threshold for transmitter release then the delay from this point to the beginning of postsynaptic response can be as short as 1.4 ms (here recording in the soma of a type I motoneuron and therefore additionally at some electrotonic distance from the synapse). Even with precise voltage clamping experiments the delay at the squid giant synapse is at least 1 ms (Llinás 1977), and with more comparable records (see for example, Katz & Miledi 1970, fig. 4; Bloedel *et al.* 1966) the calculated delay would be nearer 1.5 ms. On this basis there is little doubt that only one chemical synapse is interposed between T-fibre and motoneuron. The regularity of the transfer characteristics of the T-fibre to motoneuron synapse, together with the lack of persistence in postsynaptic response beyond the presynaptic stimulus, means that polysynaptic pathways from T-fibre to motoneuron are generally not active in the isolated ganglion.

The e.p.s.p. recorded in the motoneuron soma in response to T-fibre depolarization was large

relative to the antidromic spike. At the soma of a type I motoneuron the maximal e.p.s.p. was about 20 mV, in types II about 5 mV, in type III about 10 mV and in type IV generally no more than 3 mV. In addition, the e.p.s.p. conductance in types I–III was usually sufficiently large to completely shunt the antidromic spike. This is demonstrated in figure 33 with simultaneous recording from a motoneuron soma and a neurite of the same cell, which was closer to the spike-initiating zone.

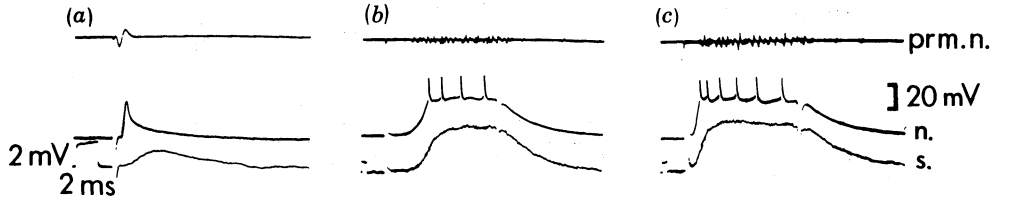

FIGURE 33. Simultaneous recordings from the soma (s.) and a neurite (n.) of a type II or type III motoneuron, demonstrating the shunting of the action potential by the e.p.s.p. conductance in the somatic recording. (*a*) Antidromic spike. (*b*), (*c*) E.p.s.p. produced by injection of constant-current pulses into the peripheral T-fibre. The extracellularly recorded promotor nerve activity is shown above (prm. n.).

This behaviour of the e.p.s.p. is in agreement with the anatomical finding that the synaptic input to the motoneurons is on the main dendrite between axon and soma. However, the degree of shunting was variable and it was possible to record orthodromically activated impulses at the soma in some animals, though at smaller amplitudes than those antidromically activated in the absence of synaptic input.

On occasions, recordings were obtained from the postsynaptic neurites in close proximity to the presynaptic fibre, though penetrations tended to be unstable and difficult to repeat. E.p.s.p. up to 35 mV in amplitude were recorded in such cases. This is consistent with the level of membrane rectification determined for the soma of type II cells (figure 31) as possibly being the maximal e.p.s.p. amplitude. If the levels of rectification recorded in the soma represent the actual limits of the e.p.s.p. in the motoneuron dendrites, then the e.p.s.p. at the soma is reduced to about 20% of its amplitude in the type II cell, and to 30–40% in the type I cell. Though 60 mV e.p.s.p. were never recorded, we cannot dismiss the possibility that postsynaptic neurites of type I motoneurons were never impaled. For the study of synaptic transmission in this preparation, the T-fibre to type I motoneuron synapse appeared to be the most useful.

(*b*) *Depolarization–release coupling at the T-fibre synapse*

From the above, it follows that the preparation allows relatively easy study of transfer characteristics by graded depolarization, even in the absence of the conductance-blocking agents TTX and TEA. Figure 34 illustrates the form of the e.p.s.p. recording in the soma of a type I motoneuron in response to stimulation of the T-fibre with constant-current pulses of increasing amplitude. Transmission showed an apparent threshold (figure 35), but this 'threshold' is partly determined by the resolution capability of the recording apparatus, as the relation between pre- and postsynaptic potentials is a continuous function. As in the voltage-clamped squid synapse (Llinás 1977), for small presynaptic depolarizations the postsynaptic response was a linearly rising potential. With larger presynaptic depolarizations, the postsynaptic response rapidly reached a plateau level. With further increase in stimulus intensity, the plateau level itself rose until it reached a maximum.

The transfer characteristics of the synapse can be plotted as the amplitude of the postsynaptic

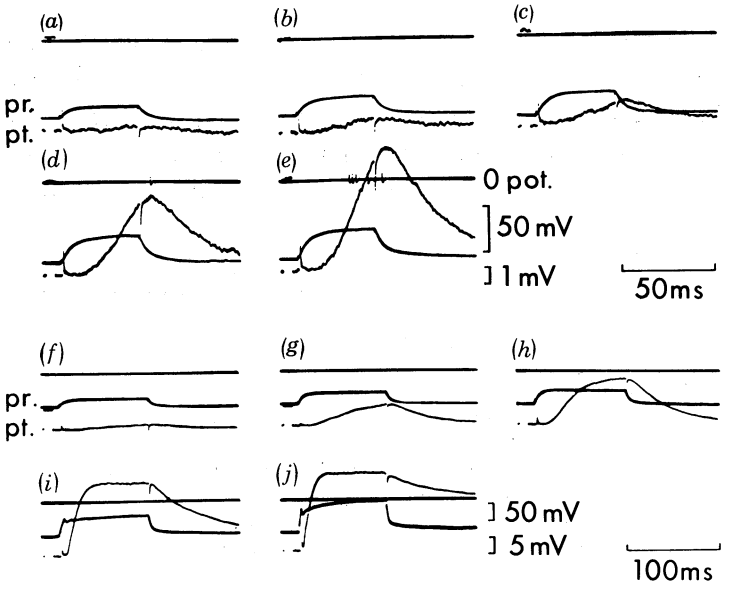

FIGURE 34. The transmission of graded signals between the synaptic zone of the T-fibre (pr.) and the soma of a type I motoneuron (pt.). Constant-current pulses of increasing amplitude were injected into the T-fibre through the sucrose gap. Bath potential relative to the presynaptic recording is shown (0 pot.). Voltage gain of the recording was changed between (*e*) and (*f*).

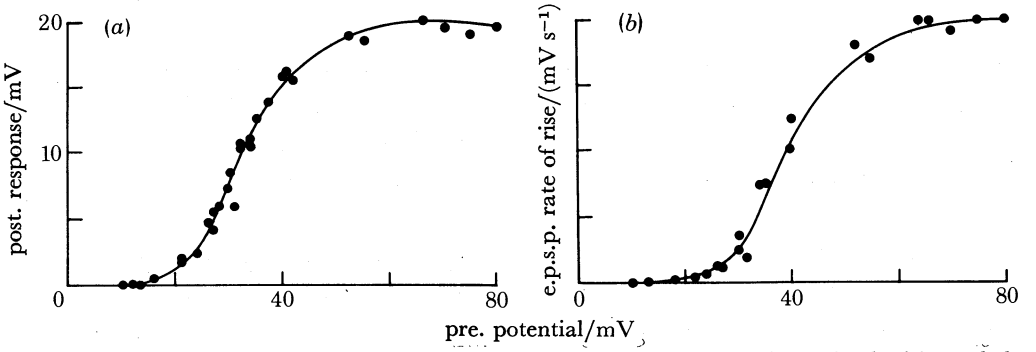

FIGURE 35. Transfer characteristics of the T-fibre/type I motoneuron synapse determined with graded constant current pulse stimulation (figure 34); (*a*) plotted as peak amplitude of postsynaptic response; (*b*) plotted as initial rate of rise of postsynaptic response against presynaptic depolarization from the holding potential of −80 mV.

response against the presynaptic potential. When this is done for the crab synapse, the relation obtained is a sigmoidal curve that is extremely similar in form to that which has been demonstrated for prolonged pulses in the squid giant synapse injected with TEA and bathed in TTX saline (Katz & Miledi 1967*b*; Kusano 1968; Llinás *et al.* 1976; figure 35). This relation is also similar in part to the mixed chemical and electrotonic junction of the lamprey Müller cell (Martin & Ringham 1975). The values of presynaptic potential at 'threshold' and at peak release, and the slope of the linear range of the transfer curve, are all within the range of those quoted for the squid giant synapse. When plotted on a logarithmic scale, the presynaptic depolarization required for an *e*-fold increase in release (as measured by postsynaptic peak potential) was found to be 5.8 mV (see also discussion in Llinás (1979)).

However, as can be seen in figures 34 and 36, the values of peak post-synaptic response for small amplitude signals of limited duration are not plateau responses but are taken arbitrarily on the linearly rising part of the potential by the termination of the pulse.

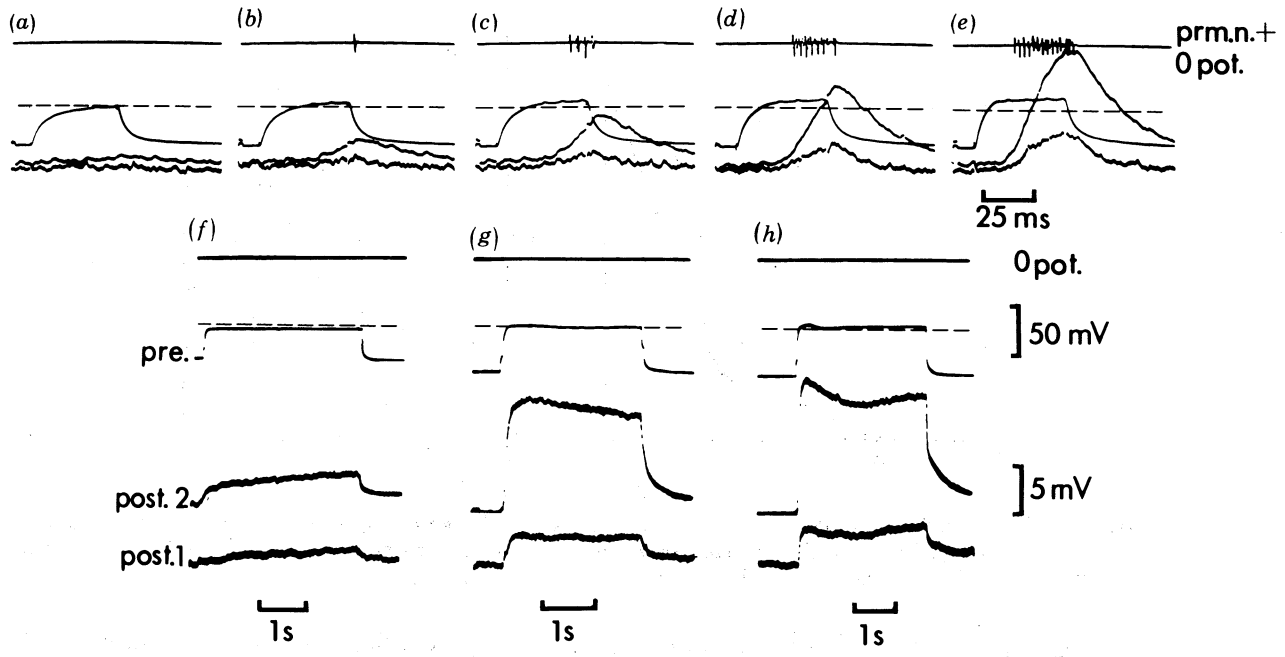

FIGURE 36. Recordings from the presynaptic zone of the T-fibre (pre.) and from two postsynaptic cells: post 1, a cell with no antidromic spike from promotor nerve stimulation, but situated in the third leg ganglion; post 2, the type I motoneuron soma. (*a*)–(*e*) Injection of 50 ms, constant-current pulses of increasing amplitude through the sucrose gap into the T-fibre, showing that the two postsynaptic cells register the same presynaptic 'threshold' (dashed line). (*f*)–(*h*) More prolonged current pulses show release occurring below the apparent 'threshold' for the short pulse and reaching plateau levels beyond its time range. Extracellular responses in the promotor (prm. n.) are shown in (*a*)–(*e*). Voltage gain calibrations apply throughout.

According to the interpretation of the e.p.s.p. form derived from computer modelling of the squid synapse (Llinás *et al.* 1980), the rate of rise of the e.p.s.p. is a more direct indicator of the calcium currents underlying transmitter release than is the plateau level, which involves additional factors, such as transmitter (vesicle) diffusion. The relation of the rate of rise of the e.p.s.p. to the presynaptic potential is shown in part *b* of figure 35. Again it is a sigmoidal curve, but slightly displaced to the right. The value of considering rate of rise rather than plateau response for the lower amplitudes can be seen in a logarithmic plot, as in figure 37. The logarithmic relation between pre. potential and post. response is consistent down to small depolarizations only for the rate of rise. The slope of the relation is similar, however, and the value of 12.5 mV of presynaptic depolarizations for a tenfold increase in postsynaptic response compares well with the value of 11.5 mV obtained in the squid synapse by Katz & Miledi (1967*b*) and that of 10 mV by Llinás *et al.* (1980).

(*c*) *Demonstration of suppression potential*

If the presynaptic depolarization was increased beyond that shown in figure 35, it was sometimes possible to demonstrate the existence of 'suppression' (Katz & Miledi 1967*b*) in the crab synapse. This is the phenomenon whereby transmission is progressively attenuated as the presynaptic potential approaches the equilibrium potential for calcium across the membrane, which has been shown to be accompanied by reduction and final cessation of the calcium current into the presynaptic terminal (Llinás & Nicholson 1975).

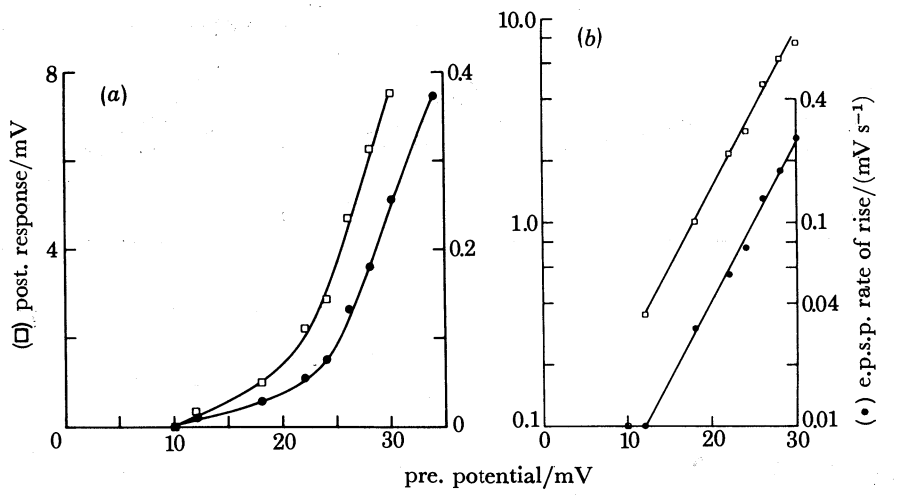

FIGURE 37. The lower parts of the range of the relations shown in figure 35, (*a*) drawn in more detail, and (*b*) plotted with logarithmic ordinates. The logarithmic relation of peak postsynaptic amplitude to presynaptic potential breaks down near zero, where the peak response is no longer a plateau response.

Recordings of suppression in the crab (figure 38) appear different from those published for the squid because of the behaviour of the depolarization transient in the T-fibre, with its accompanying increase in time constant of the attainment of plateau depolarization (§4*c*). This means that 30–40 ms are required for the presynaptic membrane potential to be raised to the suppression level, and during this time transmitter is released. The crab synapse, therefore, did not show the complete suppression of transmission during the pulse that is seen in the squid, but rather gave first a maximal 'on response', which was then suppressed as the presynaptic potential reached a high plateau level. That this was suppression rather than transmitter depletion was shown by the fact that the 'off response' immediately following the termination of the pulse was similar in amplitude to the maximal 'on response'.

Again, the value for the suppression potential shown by this recording, or at least the curve of the relation approaching suppression, is closely similar to that measured more recently in the squid (Kusano 1970; Llinás *et al.* 1976); however, this was the lowest value obtained. Furthermore, the suppression phenomenon was rather difficult to attain in the T-fibre because of the problem of increased conductance due to rectification at positive potentials (§4*a*), and it often appeared to be higher than the +50 to 60 mV shown here. This is most likely because of the difficulty in locating precisely the presynaptic site with the microelectrode. The tendency to be too distal in the T-fibre, in addition to the much reduced length constant at high current levels; would result in an over-estimation of the suppression potential. (It becomes progressively more difficult to penetrate the T-fibre as one moves into the ganglion, because of both diminishing calibre and lack of anatomical landmarks.) A similar problem was met in earlier recordings of suppression in the squid, leading to over-estimations of the value of the suppression potential (Katz & Miledi 1967*b*; Kusano *et al.* 1967).

(*d*) *Gain modulation and transmitter depletion*

Despite the practically identical transfer characteristics of the crab and squid synapses when transient signals are used, the two preparations show quite different behaviour with respect to prolonged depolarizations. This might have been expected from the fact that the squid synapse normally transmits highly phasic signals (Young 1939) while the signal from the crab is part of

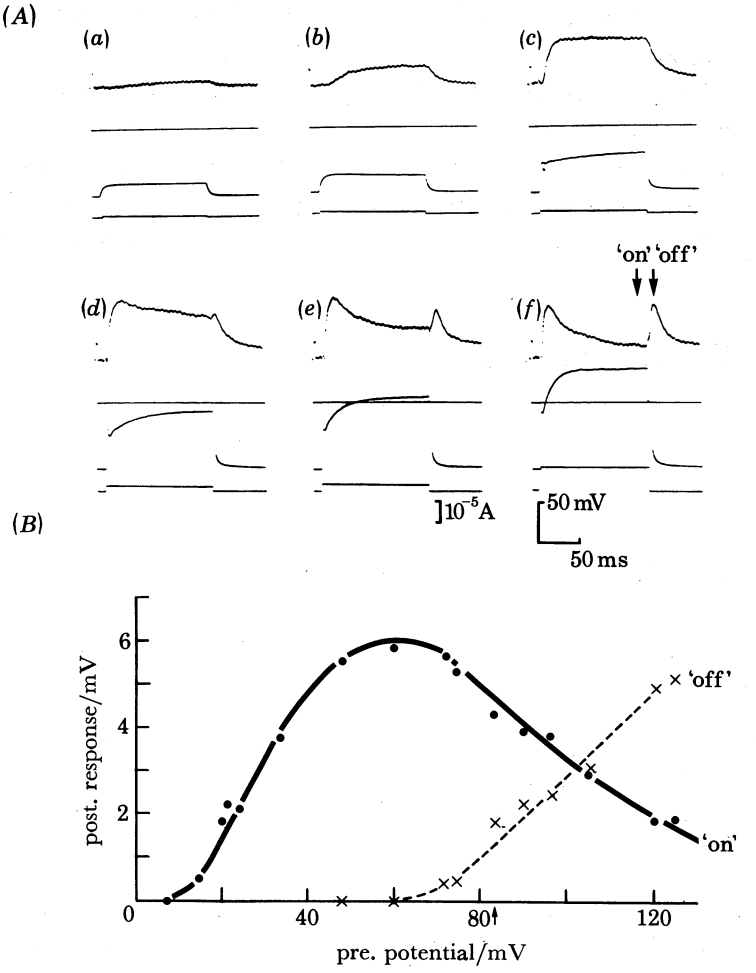

FIGURE 38. Transfer characteristics of a T-fibre/type II motoneuron synapse, demonstrating the 'suppression' of of transmitter release with high levels of depolarization. (*A*) In each of the records (*a*)–(*f*) the traces show, from top to bottom, the intracellular potential at the motoneuron soma (calibration pulse of 2 mV), the bath potential relative to the presynaptic potential shown below it, and the current injected into the T-fibre peripherally through the sucrose gap. (*B*) A plot of the relation between postsynaptic response and presynaptic depolarization from the recordings shown in (*A*). Symbols: ●, the 'on' response measured at the end of the current pulse; ×, the peak 'off' response. The prepotential was measured at the final plateau level. The arrow in (*B*) indicates bath potential.

the stretch reflex, which is likely to operate much of the time in a tonic fashion. On comparison of figures 34 and 38 here with similar constant-current data from the squid (Katz & Miledi 1967*b*, fig. 10; Kusano 1970, fig. 8; Llinás 1977, fig. 1), the crab shows no obvious depletion like that encountered in the squid, with its time course of a few milliseconds. This is shown even more clearly by comparison with voltage-clamp data (Llinás *et al.* 1976, fig. 1).

In true contrast to the postsynaptic response to sustained presynaptic depolarization in the squid synapse, that in the crab can be constant over a period of minutes though, with large amplitude depolarization, the response shows a certain amount of depression over the first second. The dependence of this depression on the amplitude of the presynaptic signal is shown in figure 39*a*. This depression might be interpreted in a number of ways: reduced quantal release, reduction of the size of each quantum, desensitization of postsynaptic receptors, or reduction of presynaptic calcium current. Without the ability to record quantal events (§ 6*g*), it is not possible

to distinguish between the first two possibilities as yet. Receptor desensitization (at least at the motor endplate) occurs at a rate that is an order of magnitude slower than the depression seen here (Katz & Thesleff 1957), though it may play a part in the slower components of the depression. There is good evidence that the synaptic calcium current does not inactivate significantly in the squid (Katz & Miledi 1971; Llinás *et al.* 1980) and there seems no reason to speculate about a possible partial inactivation contributing importantly to the depression in the crab, where slow transmitter depletion provides a more likely explanation, as it is almost certainly the

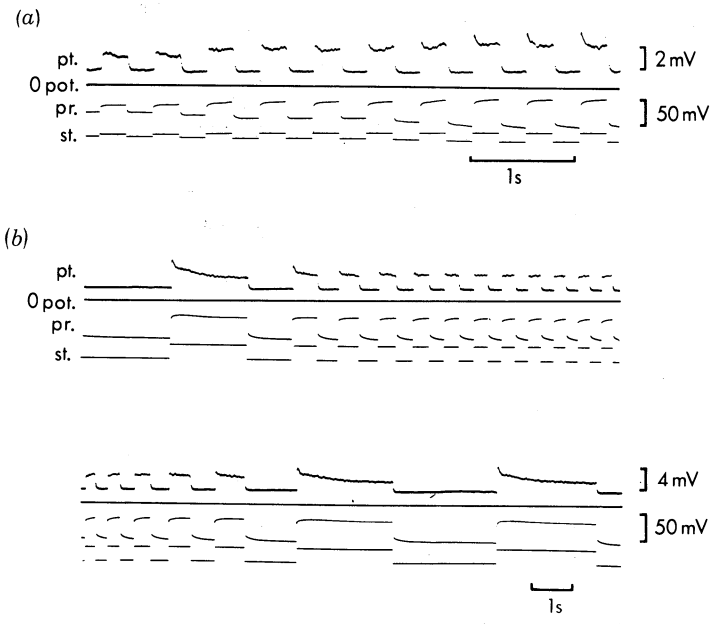

FIGURE 39. (*a*) Continuous record of synaptic response to injection of square wave current of increasing amplitude, to demonstrate the effect of stimulus amplitude on transmission depression. Simultaneous recordings were made from the synaptic zone of the T-fibre (pr.) and the soma of the type II motoneuron (pt.), while injecting the stimulus current (st.) through the sucrose gap at a distance of 1.5 mm from the (pr.) recording electrode. The bath potential (0 pot.) is shown relative to the presynaptic potential. (*b*) From the same preparation, indicating the time scale of recovery from depression. There is no visible recovery from depresssion until the periods of repolarization begin to exceed 500 ms.

cause of the analogous depression in the squid (Kusano & Landau 1975; Llinás *et al.* 1980). Any initial transient calcium current associated with the graded spike probably acts on a much shorter time scale and is filtered from the recordings by the time constant of the cell (§6*i*).

The depression in the postsynaptic response seems to be composed of at least two phases, a rapid decrease occurring within 250 ms and a slower decrease over more than a second. These two phases may represent the employment of two levels of transmitter storage. The final plateau of release would then represent the basic turnover capacity of the synapse when reserves have been depleted.

By varying the duration of the pulses it was possible to measure also the time required for recovery from depression, as in figure 39*b*. Recovery occurred within about 1.5 s, only slightly longer than the depression itself. This is faster than the rate of recovery in the squid (Kusano & Landau 1975), where the time constant of recovery was 4.9 s, or in the rat neuromuscular junction (Christensen & Martin 1970), with a time constant of 4 s. These data are not directly comparable because we have used prolonged pulses rather than the discrete pulses delivered at intervals that have to be used in the spiking synapse. But it seems likely that the T-fibre synapse

has a high vesicular turnover rate, consistent with its role in the stretch-reflex and the high plateau response for prolonged transmission. This may mean that the ability to replenish stores is also unusually high.

Though the crab synapse demonstrates depression at high amplitudes, no evidence has been found of facilitation or habituation. This too would be consistent with its tonic role. Once the stretch reflex has been set at a suitable level, there must be no autofacilitation or habituation if it is to remain adjusted to the mechanical requirements of the animal. If those mechanical requirements change then the parameters of the stretch reflex would have to change also, probably at the T-fibre synapse, but this would have to be through extrinsic modulation. In this sense it is the opposite of the condition found in the well-documented gill-withdrawal reflex of *Aplysia* (e.g. Kandel *et al.* 1975). The latter involves a phasic synapse for the mediation of a rapidly habituating reflex, which the animal would require to *sensitize* extrinsically.

The T-fibre synapse might therefore prove an ideal preparation for the analysis of the dynamics of transmitter production and vesicle recycling, as it is relatively uncomplicated by modulatory effects and is open to study with high frequency or low frequency analogue signals. This would be the case especially if miniature potentials can be recorded routinely with the refinement of recording techniques (§6*g*).

(*e*) *Synaptic properties and the stretch reflex*

As the T-fibre synapse takes part in a monosynaptic reflex, it is possible to relate directly the properties of the synaptic transmission with the behaviour of the animal. The availability of the stretch reflex of the crab to neurophysiological analysis at the membrane level is therefore unusually complete for any unit of animal behaviour. Fortunately, many of the properties of the sensory receptor and something of the reflex behaviour of the promotor complex have been described previously (reviews by Bush (1976, 1977)). A preliminary account will be given here of a striking relation between synaptic and reflex properties that emerged from the study of depression described above (§6*d*).

As can be seen in figure 40, the transmission behaviour of the T-fibre synapse with large amplitude, prolonged signals is remarkably similar to the transmission behaviour of the whole stretch reflex. Stretch to the receptor muscle provides the input to the reflex, and the output is muscle tension, which depends directly on the activation of the promotor motoneurons. The activation of these motoneurons by a square stretch stimulus to the receptor follows a typical peak–plateau course in terms of response frequency, though this pattern is mostly due to the receptor potential transient, in turn produced by the tension transient involved in a step length change (Bush & Roberts 1968; Bush 1977). It may be surprising, therefore, that behaviour is found at the level of the synaptic membrane that parallels that of the receptor potential.

However, a step depolarization is probably an abnormal signal for the T-fibre synapse and it is instructive to examine the transmission with more graded stimuli, such as sinusoidal oscillations, which may reflect the kind of input signals commonly met in nature. When such a stimulu was used, as in figure 41, we obtained the initially surprising result that it was possible for the postsynaptic signal to *lead* rather than lag behind the presynaptic signal and stimulus current in its oscillation phase.

At frequencies of oscillation higher than about 4 Hz, there was an expected synaptic delay between the peak of the presynaptic depolarization and the postsynaptic peak. Below about 3 Hz, however, the postsynaptic peak occurred earlier and the postsynaptic potential was

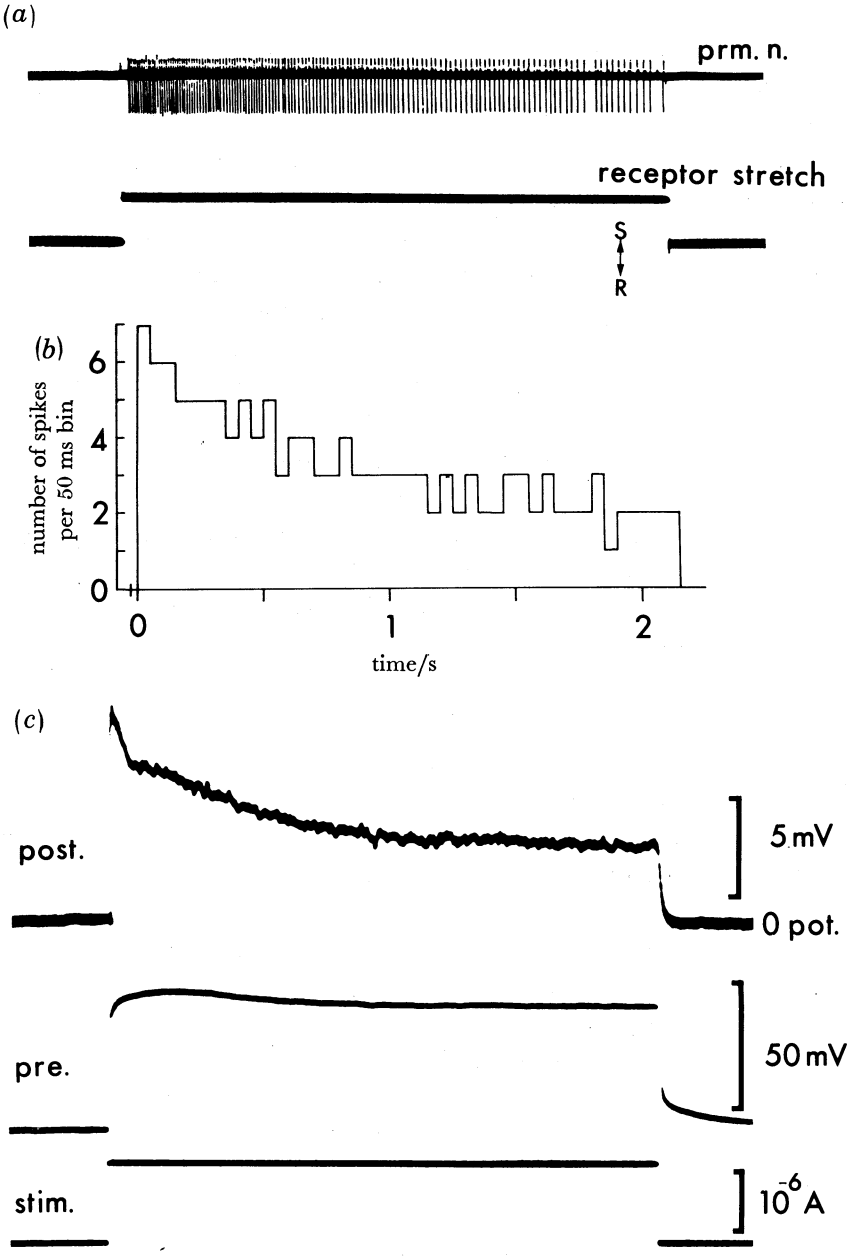

FIGURE 40. A comparison of the time course of adaptation in the overall stretch reflex and in the synaptic transmission between T-fibre and type II motoneuron. (*a*) A suction-electrode recording of the response of a unit in the promotor nerve (prm. n.) to a step length change in the receptor muscle, generated by a simple electromechanical puller (S–R, stretch–relaxation). (*b*) The unit response reduced to a frequency histogram, divided into 50 ms bins following the first spike. (*c*) The e.p.s.p. recorded in a type II motoneuron soma (post.) in response to presynaptic depolarization (pre.), generated by injection of a current pulse (stim.) into the T-fibre. The time scale is the same throughout.

already beginning to drop when the presynaptic potential reached its peak. With increasing frequency of oscillation, the amplitude of responses remained relatively constant until the oscillation became so rapid that the pre- and postsynaptic hysteresis began to reduce it, the whole system failing to follow the input signal.

Comparing again the transfer characteristics of the synapse and the whole reflex, as in figure 42, we found that they were still consistent. The output of the motoneurons normally led the

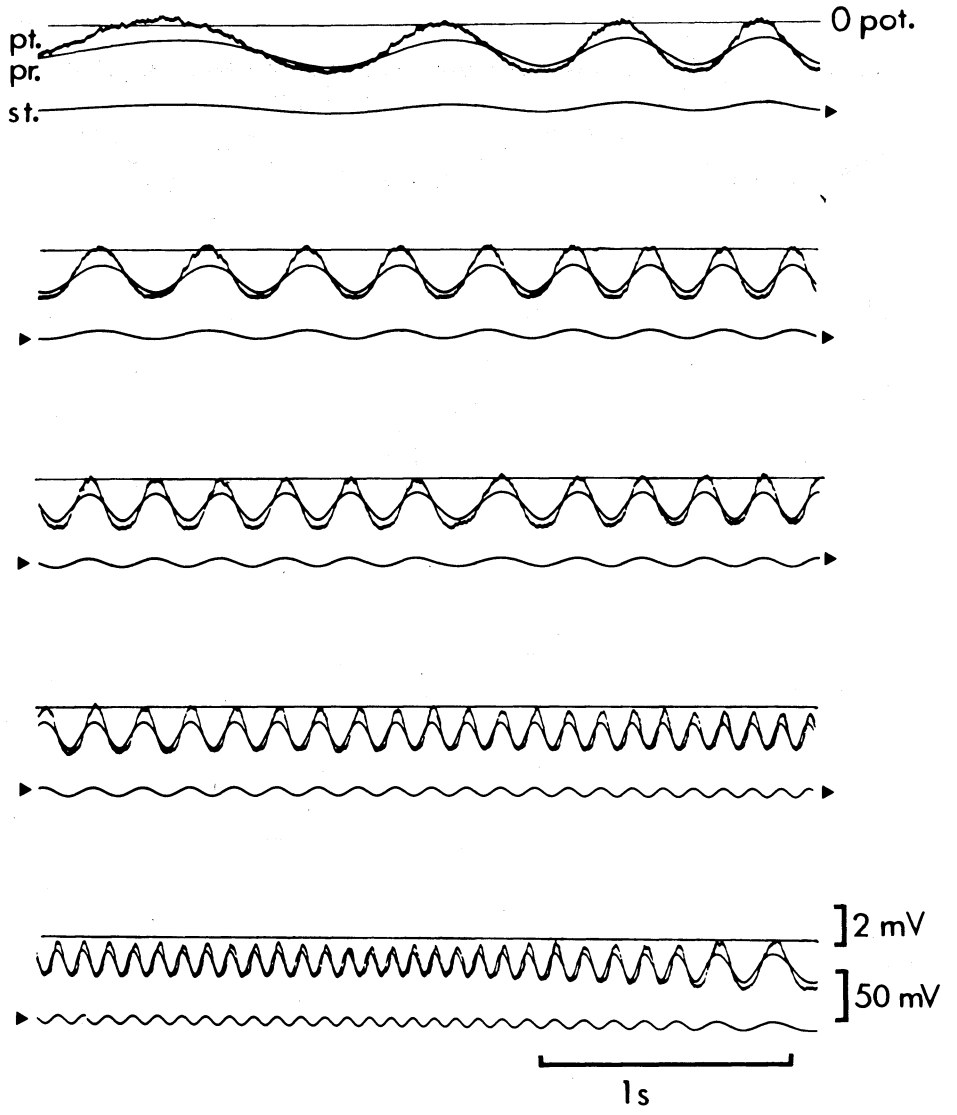

FIGURE 41. A continuous recording (left–right, top–bottom) of transmission between the T-fibre (pr.) and the type II motoneuron soma (pt.) with a constant amplitude, varying frequency oscillation of stimulus current (st.) delivered to the T-fibre through the sucrose gap. Note that the postsynaptic oscillations at lower frequencies lead in phase both presynaptic and stimulus oscillations.

input length signal, and this was presumably largely due to the fact that the receptor potential is derived from tension changes in the muscle which lead the length changes in their phase, more especially at high frequencies.

This sinusoidal data is not open to straightforward interpretation, because of the smoothness of the transitions involved. The effect that is seen with ramp stimuli (figure 43) is easier to analyse. Here the postsynaptic peak does not lead the presynaptic, but the postsynaptic waveform is distorted. It rises rapidly but flattens out before the peak and then drops rapidly after the peak.

It appears that the gain of the transmission simply falls with time; and this is directly associable with the depression seen with the square pulse. When we compared oscillations at different frequencies in the three waveforms (square pulse, ramp and sinusoid; figure 44), it was clear

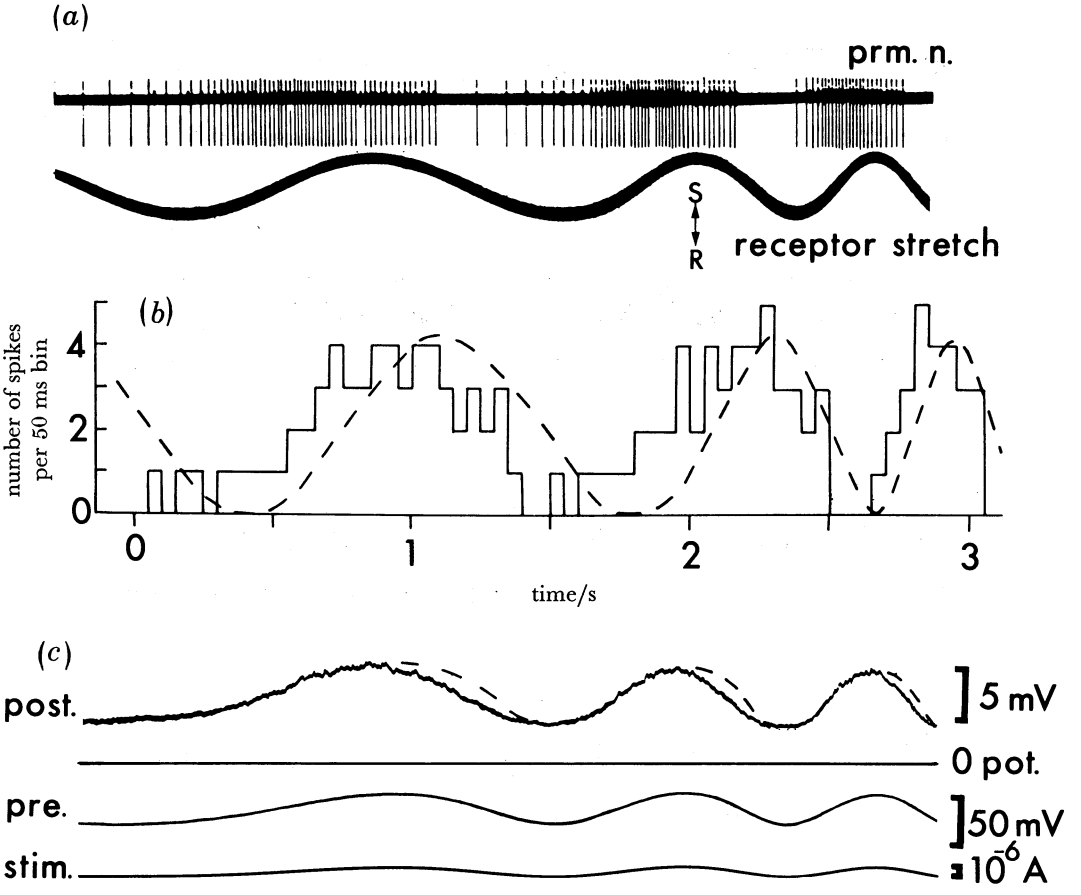

FIGURE 42. As in figure 40, a comparison of stretch reflex and synaptic transmission. (*a*) The response of a promotor nerve unit (prm. n.) to receptor muscle length oscillations of increasing frequency. (*b*) Frequency histograms constructed from recording in (*a*). The dashed line indicates the stimulus form at equalized amplitude. (*c*) The potential recorded at the type II motoneuron soma (post.) in response to oscillations of the presynaptic potential (pre.). The dashed line indicates the presynaptic oscillation at an equalized amplitude. Note that it is especially the falling phase that leads postsynaptically. The time scale is the same throughout.

that the sinusoidal phase lead and the skewing of the ramp signal were attributable to the same phenomenon as the depression of the square pulse, i.e. transmitter depletion (§6*d*).

At frequencies of oscillation (about 1.5 Hz here) where there is no peak on the square pulse postsynaptically, there is also little distortion of the ramp and little phase lead on the sinusoid. The depression phenomenon allows the e.p.s.p. to 'mimic' the behaviour of the receptor potential at low frequencies and high amplitudes of stimulation. In terms of the depletion hypothesis, because the transmitter supply decreases with time, the gain of the transmission wanes during the course of a long stimulus, with a similar time course to the waning of muscle tension and receptor potentials. It seems likely, however, that the nonlinear calcium-current properties of the presynaptic fibre (§4*b*) contribute to the time differentiation of the input signal at frequencies above about 1 Hz, and thereby decrease postsynaptic lag in that range, even in the absence of a depletable transmitter store. (figure 41 shows phase lead maintained up to about 4 Hz in this same preparation with sinusoidal input.)

It would be interesting to know if this behaviour of the transmission had functional meaning within the stretch reflex. However, it would be necessary to record the receptor potential phase gain at different frequencies of stretch to answer this question fully, and this has not yet been

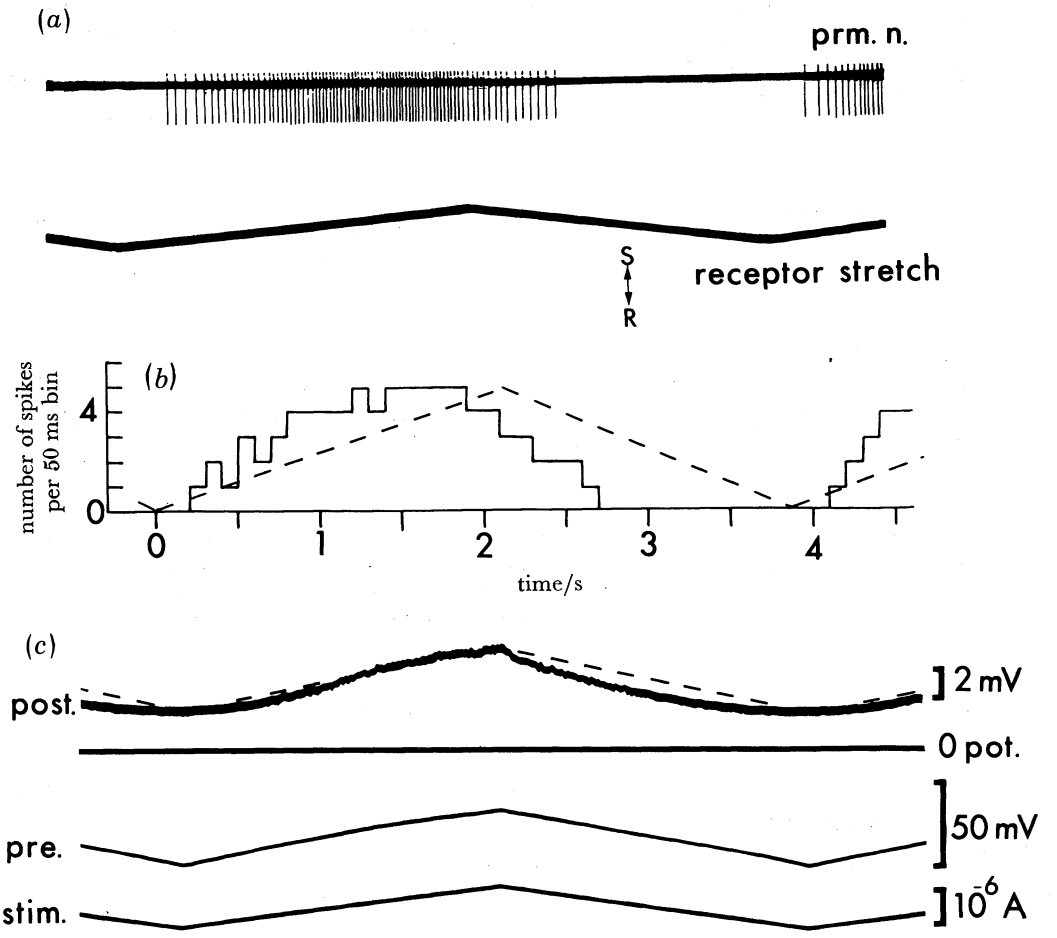

FIGURE 43. As in figures 40 and 42, a comparison of stretch reflex and synaptic transmission. (*a*) The response of a promotor nerve unit (prm. n.) to ramp stretch (S) and relaxation (R) of the receptor muscle. (*b*) Frequency histogram constructed from the recording in (*a*). (*c*) The potential recorded at the type II motoneuron soma (post.) in response to ramp depolarization and repolarization of the presynaptic T-fibre (pre.), generated by the stimulus current (stim.). The time scale is the same throughout.

done. Nevertheless, if we examine a Bode plot for the transmission in the whole reflex and for the synaptic transmission of sinusoidal signals (figure 45), we see that the phase lead of the motoneuron discharge decreases at those lower frequencies at which the phase lead of the e.p.s.p. is increasing. Therefore, it seems likely that the phase lead of the receptor potential drops even more strongly at these low frequencies, where muscle tension is more in phase with muscle length because of the small dynamic contribution, and that the synaptic phase lead partially makes up for the loss.

Therefore, it seems a reasonable function for the depletable transmitter store at this synapse that it should provide some maintenance of derivative response in the stretch reflex, allowing the motoneuron discharge to lead the muscle stretch over a wider range of input frequencies. If this is the case then it is an interesting example of the extension of the operating range of a reflex by the use of different but complementary strategies at either end of the range. Phase lead is generated at high frequencies by the signal *rising* faster than the stimulus at the level of the receptor potential (and the presynaptic potential), and is partly preserved at lower frequencies by the signal *falling* faster than the stimulus at the level of the postsynaptic potential. Further-

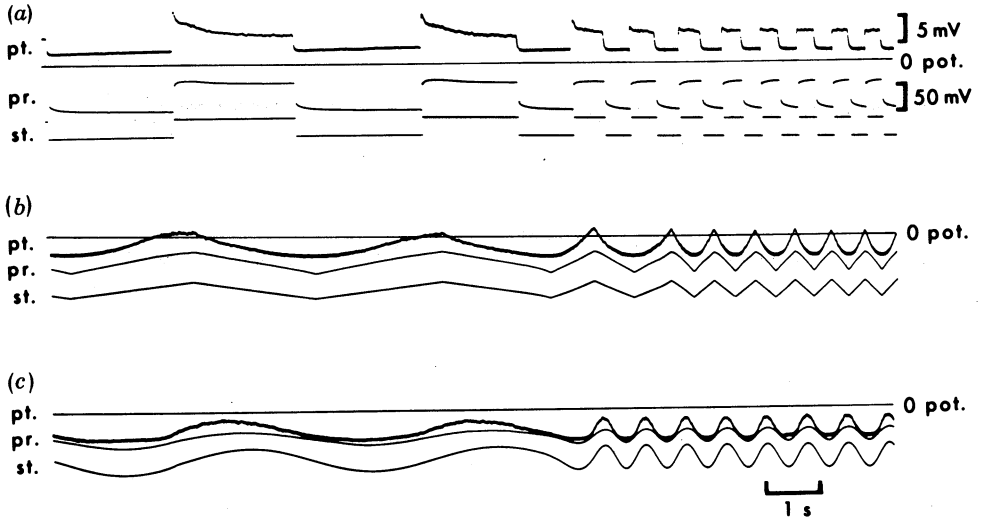

FIGURE 44. Records illustrating the transfer characteristics of the T-fibre type II motoneuron synapse for presynaptic stimuli of different wave forms at different frequencies. Traces (*a*), (*b*) and (*c*) are records taken from the same preparation of the potential recorded in the motoneuron soma (pt.), and in the presynaptic zone of the T-fibre (pr.) relative to the bath potential (0 pot.). Note that distortion of transmission occurs only at lower frequencies.

more, this is a role for depletion that would not by its nature be restricted to non-impulsive synapses.

Unfortunately, we have little knowledge about the normal stretch-reflex activity in the behaviour of Crustacea in general (Evoy & Fourtner 1973; Mill 1976; Marrelli & Larimer 1978) and nothing of *Callinectes* in particular with which to judge accurately the physiological relevance of these observations. The behavioural study by Paul (1976), on the role of the non-impulsive receptors in the sand crab, *Emerita*, suggests a rather specialized function in the timing of the power stroke for the ballistic tail-flip, and it is not easy to equate this directly with *Callinectes* in the absence of behavioural studies of its swimming mechanism.

We can only say that the present recordings demonstrate the possibility that is open to the nervous system, of employing depletable transmitter stores for the generation of derivative functions that play a more refined role in behaviour than that already seen in the rapid habituation of whole defensive acts, as in the hatchetfish (Auerbach & Bennett 1969; Highstein & Bennett 1973) or *Aplysia* (Castellucci *et al.* 1970).

(*f*) *Testing for cholinergic transmission*

There is evidence that acetylcholine is used as a transmitter by at least some crustacean sensory cells (reviewed by Florey (1973) and Gerschenfeld (1973)). A study was made by Bush *et al.* (1974) and Emson *et al.* (1976) on the levels of choline acetyltransferase in different crab nerves, including the promotor stretch-receptor fibres. It was concluded that there was good evidence for acetylcholine synthesis and therefore presumably utilization in the sensory fibres. Tests were therefore carried out in the *Callinectes* preparation, with conventional blockers of cholinergic transmission, to see if further evidence could be provided for the role of acetylcholine in the transmission between T-fibre and motoneurons.

Superfusion of the ganglion with 3×10^{-5} M atropine sulphate, 10^{-3} M hexamethonium bromide or 5×10^{-5} M *d*-tubocurarine chloride (all from Sigma) for periods of up to 25 min was

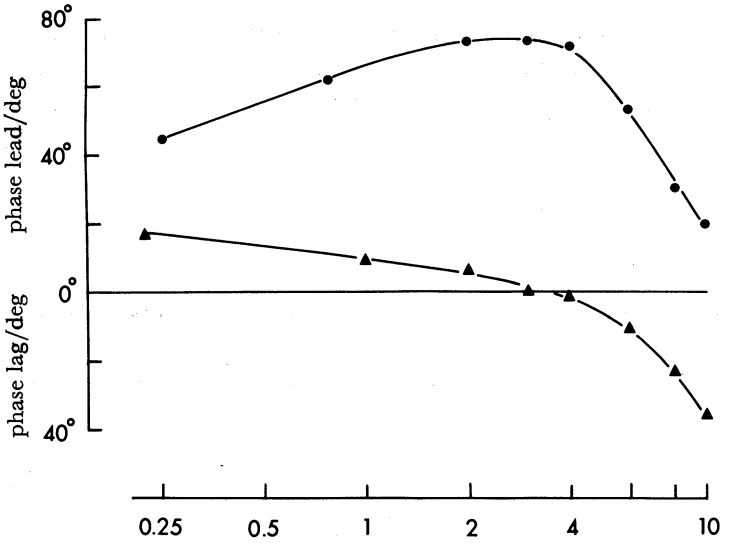

FIGURE 45. Bode plots of the phase relations of the middle of the motoneuron burst response to different frequencies of sinusoidal stretching of the muscle receptor (●), and the peak of the postsynaptic response recorded in the soma of the type II motoneuron in response to sinusoidal oscillation at different frequencies of the presynaptic potential in the T-fibre (▲). In the upper part of the frequency range the phase lead on the whole reflex and the synaptic response fail together as the conduction time of the neural elements becomes a significant fraction of the period of the oscillation. In the lower part of the frequency range the phase lead of the whole reflex response begins to decrease gradually, though the phase lead on the synaptic transmission increases. Reflex and synaptic data were obtained from different preparations.

found to have no observable effect on the transmission characteristics of the T-fibre synapses. Similar levels of these drugs have been found to have significant depressant effects on acetylcholine responses in cells of the stomatogastric ganglion of the crab *Cancer pagurus* by Marder & Paupardin-Tritsch (1968).

There is evidence here, then, that leads us to question the evidence for acetylcholine being the transmitter of the T-fibre. The promotor receptor cells are quite different from most crustacean sensory cells, both in their non-impulsive physiology and in having their somata located within the central nervous system rather than peripherally. It may be that they are also pharmacologically distinct; so support from analogy with other systems cannot carry much weight. The demonstration of very high choline acetyltransferase levels mentioned above is more concrete but not conclusive evidence. Meanwhile, there is a note of warning concerning our own data. Barker *et al.* (1972) found, in a study of lobster sensory neurons, that they required high concentrations and long superfusion times of anticholinergic agents to show depressant effects on e.p.s.p. It may be that diffusion of these drugs is restricted within the ganglion, in which case the identification of transmitter substances is made very difficult.

(*g*) *Looking for miniature potentials*

A frustrating limitation with the squid giant synapse preparation is that it is difficult to record miniature potentials; so quantal analysis of the e.p.s.p. is cumbersome (Miledi 1967; Mann & Joyner 1978). The crab preparation seems, unfortunately, to share to some extent the same characteristic, in that it has not been possible to measure quantal size of e.p.s.p., as miniature events are generally not seen at the normal recording site. This is partly owing to the

low input resistance of the postsynaptic cell, partly to the distance from the synapse to the postsynaptic recording site. When recording closer to the synapse in the finer neurites of the motoneurons, it was possible to see miniature potentials (figure 46), and the amplitude of the e.p.s.p. with small stimulating currents showed a 'jitter', which may represent quantal failure.

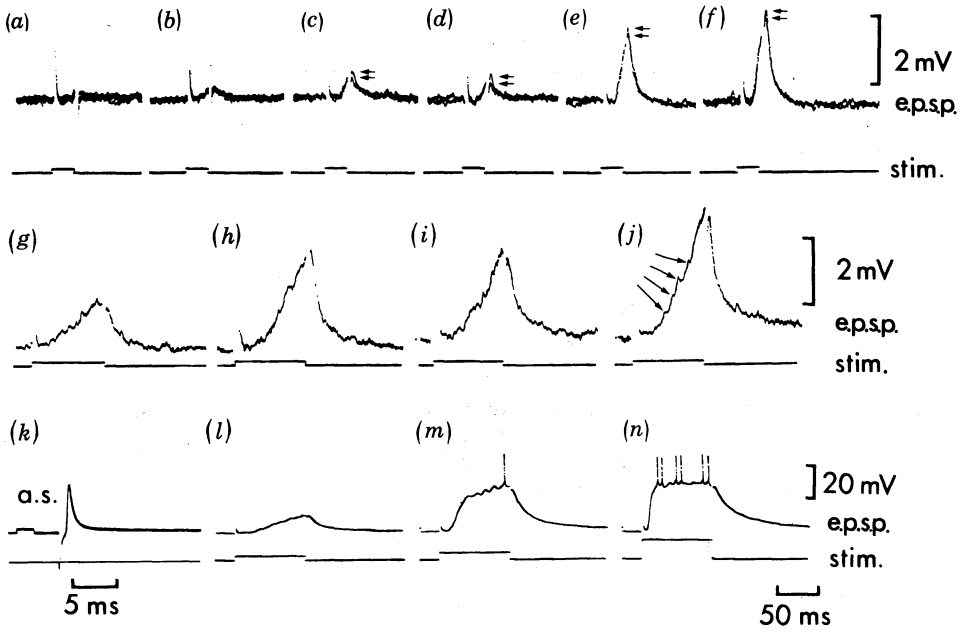

FIGURE 46. E.p.s.ps recorded from a promotor motoneuron within the neuropil close to the T-fibre presynaptic zone. (*a*)–(*f*) Superimposed traces, each showing the responses to three repeated stimuli of equal current strength (stim.) of the presynaptic T-fibre. The amplitude of the e.p.s.p. shows a 'jitter' of about 150 μV (arrows). (*g*)–(*j*) Low amplitude e.p.s.ps at faster sweep speed to show miniature activity (arrows), some of which may be part of the e.p.s.p. itself. (*k*) The antidromic spike at this recording site. (*l*)–(*n*) E.p.s.ps recorded with larger current pulses to demonstrate the maximal amplitude at this site.

From the recordings available, the maximal size of miniature potentials at the level of the synapse is less than 200 μV, but may be as much of 150 μV (figure 46), in which case they would still be an order of magnitude *larger* than those in the squid, which might be expected from the smaller size of the postsynaptic cell. With low-noise recording techniques it may be possible to measure the quantal size of e.p.s.p. in the crab.

Nonetheless, it is clear that the quantal *content* of the T-fibre e.p.s.p. is large, and this is consistent with ultrastructural data showing dense vesicle stores and multiple release sites. This also means that the capacity of the T-fibre for vesicle turnover must be quite high, in the light of the depletion data presented above (§6*d*). If we make a generous estimate of the size of the miniature potential at 200 μV, with a simplified right-triangle form and a half-width of 5 ms and assume that the miniature potentials sum linearly (all of which will result in an underestimate of numbers), then for an e.p.s.p. 30 mV in amplitude and 1 s in duration about 30 000 vesicles would be required. If we assume that the numbers are similar for all seven motoneurons and ignore the known input to the receptor motoneurons and the unknown input to other cells in the ganglion, then the T-fibre would release some 210000 vesicles per second at this relatively high amplitude of stimulation. This would represent 588 μm^2 of new membrane (with vesicles of 300 Å diameter) in a terminal region with a surface area of 10000–20000 μm^2. This calcula-

tion gives a release rate of 210 quanta per millisecond from an area of about 10^{-4} cm^2, but, when all the factors tending to give an underestimation of numbers are taken into account, the real rate of release at the crab synapse should be closer to that, estimated for the frog neuromuscular junction, of 250 quanta per millisecond from an area of 2.5×10^{-5} cm^2 (Katz & Miledi 1969*b*).

(*h*) *Presynaptic potassium conductance: effect of* TEA

The voltage-dependent calcium conductance of the presynaptic terminal has, by its nature, a tendency to become regenerative. The opening of the channels is produced by a depolarization and the inward current of calcium ions that results will give rise to a further depolarization, as does the sodium or calcium current of a neuronal action potential. In addition, the synaptic calcium conductance does not appear to inactivate in the way that sodium or calcium currents of action potentials do. It is therefore important for the cell that it should be able to control the entry of calcium. Part of the stability appears to come from the relatively small conductances involved in normal transmission, but there is generally also a counter-current of potassium ions, which tends to prevent regenerative calcium entry into the synapse. Katz & Miledi (1969*a*) were able to show that when the potassium conductance of the squid synaptic terminal is blocked by internal TEA ions then it is possible to demonstrate regenerative calcium entry.

In neurons that fire action potentials, much of this potassium-mediated control can originate from the normal voltage-dependent potassium channels of the action potential mechanism, though it is now clear that neurons can also demonstrate outward potassium currents that are dependent upon either the influx of calcium across the membrane (Heyer & Lux 1976*a*, *b*; Lux & Heyer 1979) or the concentration of calcium below the membrane (Meech 1972, 1974; Meech & Standen 1975; Eckert & Tillotson 1978). However, there appears to be little delayed rectification of the kind produced by voltage-dependent potassium conductance in the crab T-fibre (figure 24). The functional significance of this may be that the cell relies on a maintenance of membrane resistance with depolarization to be able to conduct receptor potentials from the periphery into the ganglion (though the system could be more sensitive to low-amplitude signals if it compressed the voltage range of receptor potentials by rectification of the kind found in the non-spiking *Limulus* photoreceptor (Pepose & Lisman 1978)). The large synaptic complex present at the central end of the T-fibre involves the operation of synaptic calcium currents, which in turn will need to be controlled by opposing potassium currents if the cell is to avoid the possibility of explosive calcium entry and transmitter release, such as is seen at the frog neuromuscular junction (Katz & Miledi 1967*a*) or the squid giant synapse (Katz & Miledi 1969*a*) when the voltage-dependent potassium is blocked and the external calcium concentration is relatively high.

The crab terminal is therefore likely to be of some interest for the study of the problem of calcium current control in non-spiking cells and regions of neurons that lack delayed rectification. A few observations have already been made that bear upon the calcium–potassium system of the proximal T-fibre. Square pulses of current injected into the fibre, producing depolarizations below the 'threshold' for calcium entry (transmitter release), give voltage changes that indicate the primary time constant of the cell membrane. Larger current pulses reveal a second, larger time constant for the attainment of plateau depolarization, which follows the initial graded 'spike' (figure 25).

An interpretation of this second, distinct time constant is that it represents the inactivation of the initial potassium current triggered by the sudden rise of potential or by the rapid calcium

entry that accompanies it. The possibility that this is an inactivating, voltage-dependent potassium current is especially interesting in that it would answer the evolutionary needs of the T-fibre: a sudden, explosive entry of calcium could be prevented, or only partially allowed, while the cell would show little delayed rectification when depolarized relatively slowly. This would leave a more slowly responding calcium-activated potassium conductance of smaller amplitude to control the lower frequency calcium currents involved in gradual and sustained depolarization, without great reduction of membrane resistance.

Additionally, the T-fibre may profit functionally from the delay involved in the activation of the potassium conductances. First, enough of the initial regenerative response of the calcium conductance could be allowed to occur for the production of the capacity-compensating spike with step depolarizing currents (§4*d*) and also to provide a postsynaptic derivative response for compensating postsynaptically (§6*i*). Secondly, there is evidence that slower depolarizations can become slightly regenerative (figures 24, 50), which can help to overcome hysteresis effects in conduction, and, if based on calcium influx, may aid in the production of phase lead in responses to slow signals (§6*e*). The crab may therefore benefit from instabilities in the calcium influx mechanism when the potassium control does not entirely dominate it.

In the absence of voltage-clamp studies, there is, however, little that can be done to elucidate the nature of the potassium currents, apart from application of known potassium-current blockers. Extracellular application of TEA (10 mM) or the aminopyridines 3-AmP(5 mM) and 4-AmP(2 mM) was found to have no clear effect presynaptically, though the form of the e.p.s.p. was modified. Intracellular iontophoretic injection of TEA was found to produce some modification of the presynaptic membrane response, after typically long periods of injection.

The records in figure 47 show that with large amplitude current pulses in the T-fibre injected with TEA there is a variable regenerative response. (The presynaptic voltage was already sufficiently elevated at the occurrence of these responses that their presence had very little effect on the e.p.s.p., which was already at its maximal amplitude.) These regenerative responses were still graded, however, and the membrane voltage was restored to ohmically determined levels before the end of the current pulse. It is possible that larger injections of TEA could have a more profound effect on the membrane response, but it would be expected to have less effect than in the squid terminal, which has more marked delayed rectification.

Susceptibility to TEA is often taken as an indication of the voltage dependency of potassium currents, but work on molluscan neurons indicates that this is not always true (Meech & Standen 1975). There is clearly considerable variability in the properties of neuronal potassium currents, and voltage-clamp analysis of the T-fibre may throw light on some of the functional significance of that variability. At the moment it is not clear whether the effect of TEA shown in figure 47 involves a specific effect on the conductance responsible for the repolarizing phase of the graded spike, or possibly an unspecific effect on the increased membrane conductance at higher levels of depolarization.

(*i*) *Adaptations for speed in a non-impulsive system*

One of the advantages of the 'more normal', impulsive mode of transmission of neural information is that it allows the development of high speed with low distortion. The electrical properties of neurons generally make them very poor conductors of analogue signals. The advantages of non-impulsive transmission are more difficult to define, although it appears to have evolved independently in a number of systems. Of the advantages discussed by Pearson

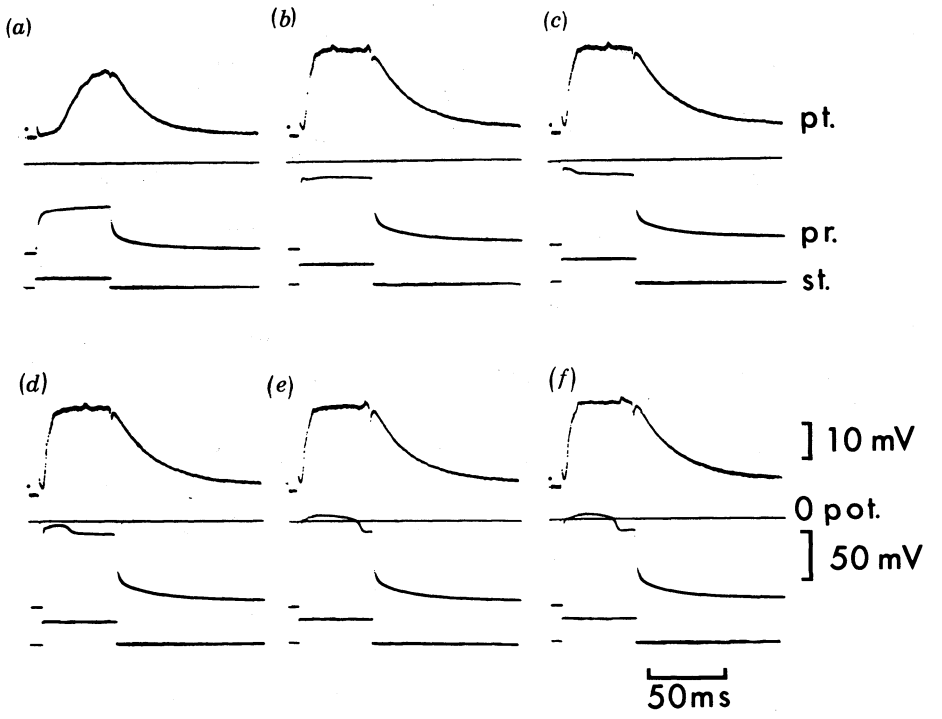

FIGURE 47. Intracellular recordings from the T-fibre synaptic region (pr.) and the soma of a type I motoneuron (pt.) after presynaptic injection of TEA (20 nA pulses, 500 ms every second for 50 min, electrodes filled with 1M TEA chloride and 1M potassium citrate). (*a*)–(*f*) Responses to injection of current pulses of increasing amplitude (st.). A regenerative response begins to appear in (*c*). In (*d*)–(*f*) the presynaptic voltage response increases substantially but transiently with little change in injected current.

(1976), only the ability to drive the output motoneurons smoothly through a wide range of frequencies, with only one or two cells supplying input, seems to apply convincingly to the crab stretch-receptor fibres. (Though this leaves us with the question of why the number of sensory elements is so restricted).

Having evolved a non-impulsive system, on the basis of an as yet unknown positive selection, the thoracic–coxal stretch receptor was faced with the associated disadvantages of slow speed and capacitative distortion, which would have been made even worse by the increase in membrane resistance needed to reduce attenuation of the signal in the long, leaky cable. The behaviour of the T-fibre includes a number of features tending to increase the speed of response in the reflex arc, almost all of them restricted to the positive phase (i.e. stretch or depolarization) of the input signal.

(1) *The receptor potential*

As demonstrated by Bush & Godden (1974), the S- and T-fibre-receptor potentials 'reflect tension more closely than length changes'. This means that the T-fibre response to stretch contains information not only about muscle length but also about the velocity and acceleration of stretch. In the S-fibre this differentiated information is found also in the falling phase of the signal (Bush & Roberts 1971), but it is found to a much lesser extent in the T-fibre. This kind of derivative response is typical of compensatory reflexes and is found also in spiking stretch receptors, like that of the crayfish abdominal muscle (Nakajima & Ondera 1969). Such responses

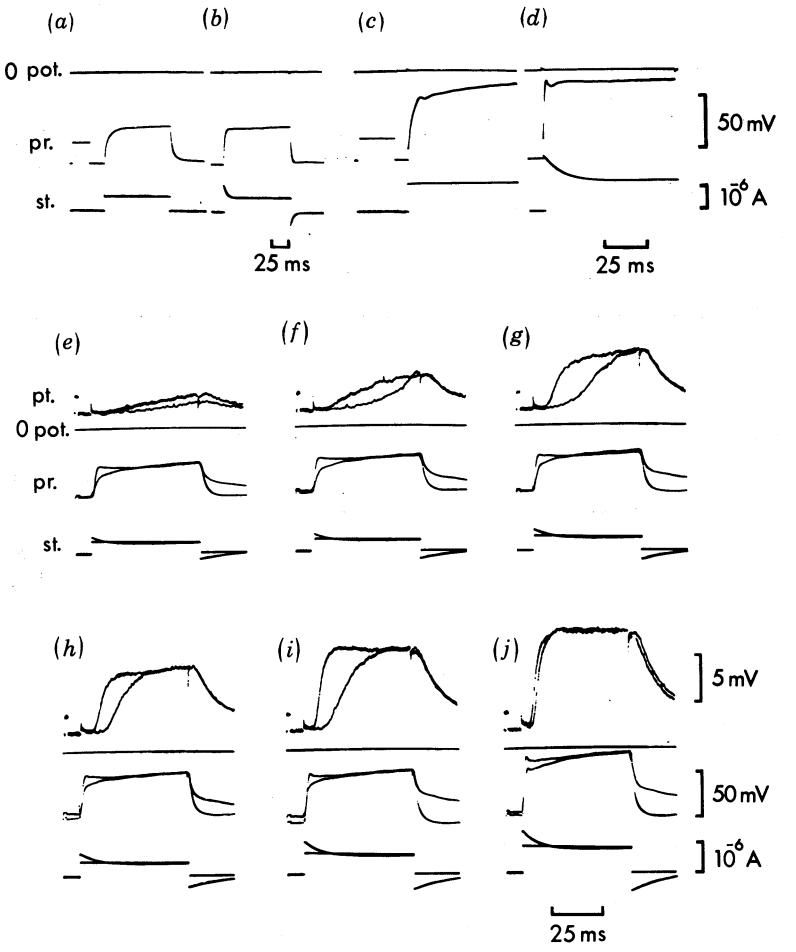

FIGURE 48. Records to show partial voltage clamping of the presynaptic terminal obtained by stimulating with a square current pulse modified by the addition of derivative responses (see text). (*a*) and (*b*) demonstrate the time constant of the passive T-fibre membrane and its clamping with a derivative current stimulus (st.). The intracellular potential (pr.) was recorded in the synaptic zone while injecting current into the peripheral fibre through the sucrose gap. (*c*), (*d*) Similarly demonstrate the effect with the secondary time constant that follows the initial depolarizing response at high amplitudes. The records (*e*)–(*j*) show pre- and postsynaptic responses to square current pulses with and without derivative signal, superimposed to illustrate the effect of the presynaptic potential form on the postsynaptic potential (pt.) recorded in the soma of the type II motoneuron.

serve in the stabilization of behaviour, by compensating for the slow speed of neural responses and in helping to overcome the oscillations that result from the perturbation of a system with a long response time for compensation.

In reflexes involving spiking neurons, however, the derivative responses mostly play their part at the level of the effector muscle by increasing the rate of rise of contraction (Buller & Lewis 1965), or at the motoneuron (see Heyer & Llinás 1977), because the form of the receptor potential will be represented fairly faithfully at the central integrating sites by the spike discharge in the synaptic terminals of the sensory fibres. The situation is somewhat different in non-spiking cells, since here the time constant of decay of the derivative response to a step tension change is of the same order as the time constant of the cell (Roberts & Bush (1971) give values for both). Clearly, then, the receptor potential will not be faithfully represented at the presynaptic level, and, in fact, one of the functions of the derivative response will be the preliminary

charging of the central end of the fibre in a time shorter than its normal time constant. In effect, the receptor potential will tend to 'voltage clamp' the terminal.

This effect can be shown experimentally by injecting current pulses into the T-fibre that are not square but contain a superimposed derivative signal (obtained by passing a parallel pulse through a resistance–capacitance (*R–C*) circuit and adding the resultant derivative to the stimulus pulse) as in figure 48. The derivative signal serves to 'clamp' the terminal region fairly well when the time constant of the *R–C* circuit is adjusted to a suitable level, either for the cell time constant or for the longer, perhaps potassium-mediated time constant seen with higher amplitude pulses (§6*h*).

It is interesting to note at the postsynaptic level that the clamping effect is found only on the rising phase. Even though the presynaptic fibre is restored more rapidly to its resting polarization, the e.p.s.p. shows the same rate of fall. This rate must therefore be determined by postsynaptic time constants. This may be linked with the fact that the T-fibre has little derivative response in the hyperpolarizing direction and has not evolved a mechanism for a hyperpolarizing transient to match the depolarizing transient. As the postsynaptic cells would not respond to its increased speed there can have been no evolutionary pressure for it to do so. In the light of this it is interesting that the S-fibre does have a hyperpolarizing derivative response in its receptor potential (Bush 1976, 1977). If this is to be reflected postsynaptically, it suggests that the S-fibre may make electronic synapses centrally as well as the chemical synapses that have been seen with the electron microscope (§3*e*).

(2) *The fibre transient and its postsynaptic effect*

The role of the partial regenerative response in capacity compensation within the T-fibre has been discussed above (§4*d*). However, the depolarization transient will have an additional postsynaptic effect if, as has been suggested (§4*c*), it is based on a sudden influx of calcium ions. At the level of the terminal itself, such an influx would be expected to give rise to the release of an initial pulse of transmitter in excess of the pulse that would be released if the voltage transient were merely based on the influx of some other ion, like sodium. Such an initial transient in the e.p.s.p. would have a similar effect in tending to 'clamp' the postsynaptic membrane as the T-fibre transient has presynaptically.

Such a postsynaptic transient is not found in the somatic e.p.s.p., but almost all recordings made near the synapse, within the neurites of the motoneurons, have shown clear transients on the rising phase of the e.p.s.p., with thresholds similar to that of the presynaptic transient. It is unfortunately unusual to be able to record presynaptically at the same time as recording in the motoneuron neurites. Figure 49 shows a single case in which it was possible to correlate the pre- and postsynaptic transients, showing that they have the same 'threshold' for appearance and that they are related to a dramatic increase in the rate of rise of the e.p.s.p. with relatively little increase in its amplitude. The promotor nerve record simultaneously demonstrates the effect of the transients on the latency of the reflex discharge.

(3) *Membrane responses and depletable transmitter*

Response speed may be an important feature of the system not only in relation to high frequency (step) inputs, but also in relation to signals of large amplitude. The nonlinear response of the T-fibre membrane to injected current at intermediate frequencies of oscillation was

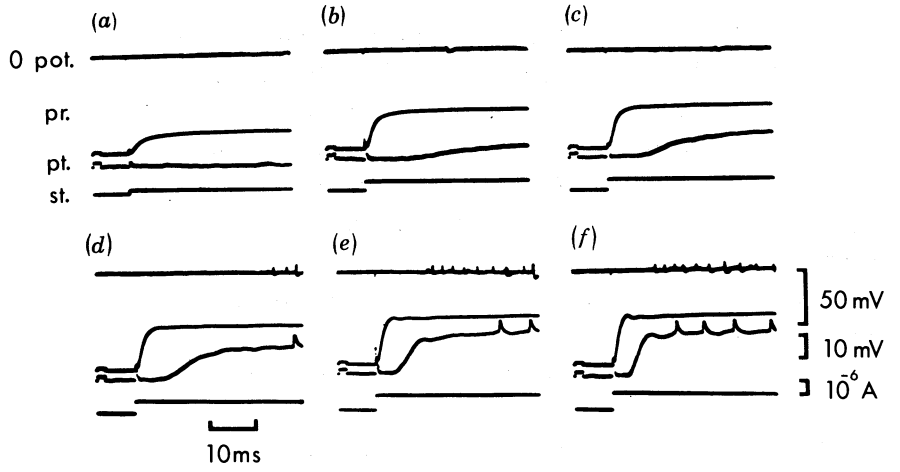

FIGURE 49. The postsynaptic effect of the presynaptic depolarization transient is seen in these recordings taken from the T-fibre synaptic zone (pr.) and a motoneuron neurite close to the synaptic zone (pt.) The effect in shortening the reflex latency is illustrated by the promotor nerve suction electrode record superimposed on the bath potential trace (0 pot.). Axonal spikes are seen in (*d*)–(*f*) on the postsynaptic recording.

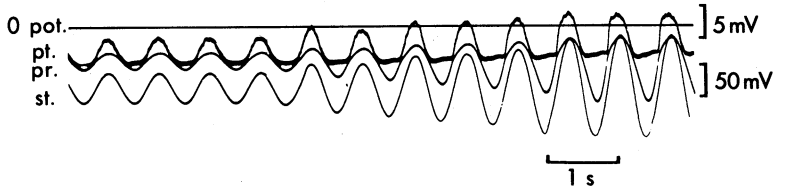

FIGURE 50. A recording of the pre- and postsynaptic responses to sinusoidal current injection of increasing amplitude. Both pre. and post. responses (pr. and pt. respectively) are skewed towards the rising phase at higher stimulus amplitudes (st.). Microelectrode recordings from the T-fibre synaptic zone and the soma of a type II motoneuron.

discussed above (§4*d*), as was the effect of the depletable transmitter store (§6*e*). These two features of the presynaptic fibre are summarized in figure 50.

This recording illustrates the relation between reaction speed and increased stimulus amplitude. The amplitude information itself is lost at the postsynaptic level when we reach the maximal level for the release coupling, but the increased amplitude of current oscillations results in an increased phase lead on the postsynaptic potential peak and the skewing of the presynaptic oscillations towards the rising phase by the non-ohmic response of the fibre to the current. The steeper rise of the postsynaptic potential to peak is due to the partial regenerative response presynaptically, and its early decline from peak, increasing the phase lead, has been interpreted as being caused by transmitter depletion (§6*e*), here initiated by the increased release during the rising phase.

(*j*) *High-gain and low-gain synaptic transmission*

At the junctions between receptor cells and sensory neurons, chemical transmission can mediate the translation of small-amplitude presynaptic voltage changes into large variations in postsynaptic firing frequency. Such informational amplification has been demonstrated for fish electroreceptors (Bennett 1968, 1971*a*, *b*) and barnacle photoreceptors (Ross & Stuart 1978). The T-fibre of the crab was known similarly to be able to produce large changes in motoneuron firing rate with small changes in membrane potential (Bush & Roberts 1968; Bush 1977). Without the ability to record pre- and postsynaptic potentials directly, it was not possible to determine

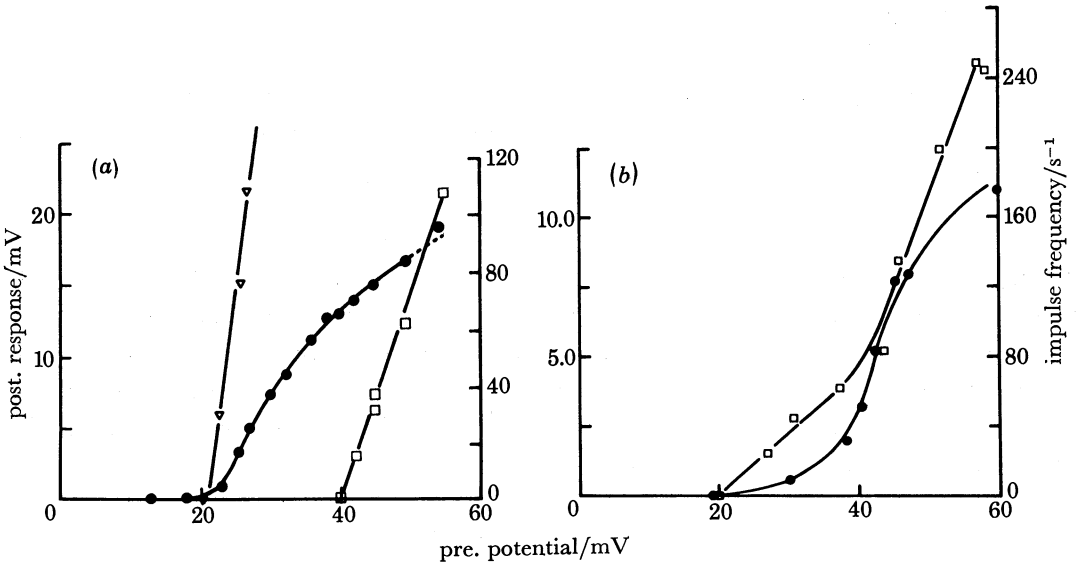

FIGURE 51. Graphs comparing the spike responses of different promotor units to T-fibre depolarization. In (*a*) are shown the peak postsynaptic response of a type I motoneuron (●) and the frequency of spike discharges in the same neuron (□) (from spike interval) in response to 50 ms current pulses injected into the T-fibre through the sucrose gap. The frequency response of another unit with a very low threshold, recorded from the promotor nerve with a suction electrode is shown for comparison (▽). In (*b*) is shown similar data for the intermediate threshold type III cell (without the lower threshold unit). In this case, presynaptic potential was recorded at the edge of the ganglion, causing a slight displacement of the transfer curves to the right. Note that the difference in spike output is not reflected at the level of the synaptic transmission.

whether the physiology of such interactions is based on a 'high-gain' transmitter release presynaptically, a high sensitivity to released transmitter postsynaptically, or a high sensitivity of the postsynaptic spike-generating mechanism to the membrane polarization affected by the e.p.s.p.

Recordings given here of the transfer characteristics of some of the crab synapses indicate that there is no difference between the voltage-dependent properties of presynaptic release in the T-fibre and those of the squid giant synapse. The presynaptic 'threshold' for release was found to be the same for all postsynaptic cells, either by recording the e.p.s.p. directly or by the threshold for axonal spiking, which was always above the threshold for e.p.s.p. generation in those cells where it could be measured. The difference between the more phasic and the more tonically responding motoneurons seemed chiefly to reside in the sensitivity of the spike-generating mechanism to the e.p.s.p. produced by the T-fibre depolarization. The phasic type I motoneuron, for instance, did not begin to spike until the e.p.s.p. was about 60% of its maximal amplitude (figure 51), whereas the more tonic type III motoneuron produced action potentials from depolarizations of the T-fibre that gave e.p.s.p. barely discernible at the soma.

For the normal functioning of the T-fibre control of motoneuronal firing, one would therefore expect that the presynaptic membrane potential would be held above threshold for release (probably by tonic activity in the receptor muscle efferents). This would depolarize but not activate the phasic elements and produce a resting discharge such as is normally recorded in the tonic units. Small changes in membrane potentials produced by muscle stretch or relaxa-

tion would strongly modulate the firing of the tonic units, in a similar way to that seen in 'high-gain' synapses.

It is not evident from this data, of course, whether all junctions of the 'high-gain' type have a similar depolarization-release coupling to squid and crab, particularly in those sensory relays where the postsynaptic cell thresholds are more uniform. However, the data do add to the growing picture of depolarization–release coupling in cells, which so far indicates a unique and rather invariant mechanism.

7. General discussion

Various aspects of the crab promotor stretch-receptor complex have been discussed with regard to previous work during the course of this account. Some of the more general principles of neuronal physiology to which the preparation has related have also been considered under the relevant sections (§§ 4*d*, 5*b*, 6*e*, *h–j*). Here we will summarize some of the possibilities for the future study of this preparation, for the examination of its own unusual characteristics and of the properties that it shares with other neural systems.

(*a*) *The stretch reflex*

The concept of the monosynaptic reflex arc from stretch-receptor neuron to motoneuron seems one of the most basic in neurophysiology, yet its precise functional role remains elusive. This is particularly because of the complications introduced by the sensory receptor having its own motor innervation. (Burke (1978) gives an account of the continuing history of this concept in relation to human muscle spindles.)

From the technical point of view, the crab promotor system is probably unsurpassed in the opportunity that it provides for electrophysiological analysis of a monosynaptic reflex. There is a single cell, the T-cell, that serves as the transducer and transmitter of information from one muscle that is analogous to that carried by the primary sensory fibres of vertebrate spindles. The sensory and motor cells are open to microelectrode penetration through much of their extent. It would be possible to record simultaneously the receptor potential, the pre- and post-synaptic potentials at the sensorimotor synapse, and the motor output. Taking these elements separately and in more detail, it would be possible to provide for the first time an analysis of a complete chain of transfer characteristics for the membrane processes involved in the flow of information from an environmental stimulus, stretch, to a behavioural response, reflex muscle tension.

The monosynaptic feedback control system presumably acts in the correction of perturbations of movement introduced by the environment, as seems most likely for other arthropod proprioceptors (see, for example: Evoy & Cohen 1971; Barnes *et al.* 1972; Möhl 1979). An understanding of the overall functional significance of our detailed knowledge at the cellular level may be more difficult to obtain. In this regard, intracellular recording from sensory fibres in more intact preparations showing spontaneous movements of the limbs would be potentially very rewarding, providing the data needed for a more comprehensive model that would allow us to check our interpretations of the relation between neuronal properties and the production of behaviour (see also the discussion in Bush (1977)). In the absence of data on the signals normally carried by the T-fibre, much of our speculation on its physiological adaptation has to remain in the abstract.

Other details of the system that need to be approached include the role of the S-fibre, which

has receptor characteristics (Bush & Roberts 1971; Bush 1977) similar to those of vertebrate spindle 'secondary' endings (Cooper 1959, 1961) in having little dynamic component, and which may therefore also have only polysynaptic input to motoneurons. The synaptic input from the T-fibre to the receptor efferent cells is known to be excitatory (Bush & Cannone 1974; Bush 1977), but intracellular recordings from these cells are needed to determine whether this positive feedback is a monosynaptic excitation or whether it comes by way of some potentially more modifiable polysynaptic route.

(*b*) *Synaptic transmission*

The analysis of synaptic properties that has been possible in the crab preparation has provided support for the general applicability of our present understanding of chemical transmission derived from other systems, particularly the squid giant synapse and the frog neuromuscular junction. Such confirmation is clear in the similarity of the relation between pre- and postsynaptic potential (figures 35, 38) to that determined in the squid preparation (see, for example, Llinás & Heuser 1977). This agreement is especially important in that the crab junctions are part of a relatively 'high-gain' system (§6*j*) engaged in tonic transmission, while that of the squid is perhaps even an extreme example of a phasic, impulsive synapse. It seems, therefore, that the basic potential-dependent characteristics of the calcium conductances of synaptic terminals can be employed, unmodified, in the mediation of electrical signals of widely different amplitudes and durations.

The differences between the transfer characteristics of crab and squid synapses appear to relate to processes other than the potential-dependent calcium conductances. Most obviously, the rate of depression of postsynaptic response to prolonged presynaptic depolarization is much slower in the crab (§6*d*), which is no doubt related to the function of transmitting postural signals of long duration and locomotory signals of high-frequency repetition. This is a difference that seems to be accounted for adequately by modifications of transmitter mobilization. Transmitter synthesis, storage and recycling rates form an important set of variables in synaptic transmission. The crab promotor synapses offer the opportunity to study these processes with maintained depolarizations (§6*d*) and provide a suitable contrast to the squid, where similar maintained signals are possible after suppression of the spike mechanism.

A second difference exhibited by the non-impulsive synapse is the presence of a presynaptic active calcium response to abruptly depolarizing currents, and this tends to increase the speed of both pre- and postsynaptic voltage changes (§4*b*, *c*, *d*; §6*i*). Such a mechanism would be of considerable importance for the functioning of otherwise 'passive' neuronal membrane, in dendrites and non-spiking axonal terminals, in improving the speed and the fidelity of transmission, by compensating for the membrane capacitance of the cell (§4*d*). The 'graded spike' of the crab T-fibre is therefore a phenomenon requiring more detailed analysis, particularly with the aid of the voltage clamp to determine the nature of the underlying conductances. To determine the real significance of these active responses for the representation of the receptor potential at pre- and postsynaptic membrane, it will be necessary also to use the intact sensory fibre and natural stimulation as well as more distal injection of current pulses. The stretch receptor fibres of the crab provide a very useful model system for the study of 'dendritic' transmission and dendro-dendritic synaptic interaction.

The study of chemical synaptic transmission still faces numerous unanswered or partially answered questions, for which the promotor system may provide clarification of the answers,

mostly by providing contrast with and confirmation of data from other preparations. These include questions like the dependence of transmission on external calcium concentration (see, for example, Katz & Miledi 1970; Crawford 1974; Llinás *et al.* 1980) and on temperature (see, for example, Ward *et al.* 1972), and the control of internal calcium levels, which must be of particular importance in the S- and T-cells, with their sustained high levels of synaptic calcium current. There is also the strong possibility (§6*g*) that with some refinement of recording technique it will be routinely practicable to record quantal events at the T-fibre synapses, thereby combining some of the advantages of both giant synapse and neuromuscular junction.

This work was supported by a N.A.T.O. fellowship (to A.R.B.) from the Science Research Council and by United States Public Health Service grant no. NS-13742 from the National Institute of Neurological and Communicative Disorders and Stroke. We would like to thank Dr Brian Bush for his useful comments and suggestions on this work and also Dr Mutsuyuki Sugimori for his kindness in designing electronic apparatus.

References

Allen, E. J. 1894 Studies on the nervous system of Crustacea. I. Some nerve elements of the embryonic lobster. *Q. Jl microsc. Sci.* **36**, 461–482.

Allen, E. J. 1896 Studies on the nervous system of Crustacea. IV. Further observations on the nerve elements of the embryonic lobster. *Q. Jl microsc. Sci.* **39**, 33–50.

Alexandrowicz, J. S. & Whitear, M. 1957 Receptor elements in the coxal region of decapod Crustacea. *J. mar. biol. Ass. U.K.* **36**, 603–628.

Altman, J. S. & Tyrer, N. M. 1977*a* The locust wing hinge stretch receptors. I. Primary sensory neurones with enormous central arborisations. *J. comp. Neurol.* **172**, 409–430.

Altman, J. S. & Tyrer, N. M. 1977*b* The locust wing hinge stretch receptors. II. Variation, alternative pathways and 'mistakes' in the central arborisations. *J. comp. Neurol.* **172**, 431–440.

Armstrong, C. M. & Binstock, L. 1965 Anomalous rectification in the squid giant axon injected with tetraethylammonium chloride. *J. gen. Physiol.* **48**, 859–872.

Auerbach, A. A. & Bennett, M. V. L. 1969 Chemically mediated transmission at a giant synapse in the central nervous system of a vertebrate. *J. gen. Physiol.* **53**, 183–210.

Bacon, J. P. & Altman, J. S. 1977 A silver intensification method for cobalt-filled neurons in whole-mount preparations. *Brain Res.* **138**, 359–363.

Barker, D. L., Herbert, E., Hildebrand, J. G. & Kravitz, E. A. 1972 Acetylcholine and lobster sensory neurones. *J. Physiol., Lond.* **226**, 205–229.

Barnes, W. J. P., Spirito, C. P. & Evoy, W. H. 1972 Nervous control of walking in the crab *Cardiosoma guanhumi*. II. Role of resistance reflexes in walking. *Z. vergl. Physiol.* **76**, 16–31.

Bastiani, M. & Mulloney, B. 1978 Central anatomy of the crayfish stretch receptor neurons. *Soc. Neurosci. Abstr.* **4**, 387.

Bennett, M. V. L. 1968 Similarities between chemically and electrically mediated transmission. In *Physiological and biophysical aspects of nervous integration* (ed. F. D. Carlson), pp. 73–128. Englewood Cliffs: Prentice Hall.

Bennett, M. V. L. 1971*a* Electroreception. In *Fish physiology* (ed. W. S. Hoar & D. S. Randall) vol. 5 pp. 493–574. New York: Academic Press.

Bennett, M. V. L. 1971*b* Electrolocation in fish. *Ann. N.Y. Acad. Sci.* **188**, 242–269.

Bethe, A. 1895 Studien über das Centralnervensystem von *Carcinus maenas* nebst Angaben über ein neues Verfahren der Methylenblaufixation. *Archs mikrosk. Anat.* **44**, 579–622.

Bethe, A. 1897*a* Das Nervensystem von *Carcinus maenas*, ein anatomisch-physiologischer Versuch: I Theil, I Mittheil. *Archs mikrosk. Anat.* **50**, 460–546.

Bethe, A. 1897*b* Das Nervensystem von *Carcinus maenas*, ein anatomisch-physiologischer Versuch: I Theil, II Mittheil. *Archs mikrosk. Anat.* **50**, 589–639.

Blight, A. R. & Llinás, R. 1978 Depolarization–release coupling at a synapse lacking regenerative spikes. *Soc. Neurosci. Abstr.* **4**, 577.

Bloedel, J., Gage, P. W., Llinás, R. & Quastel, D. M. J. 1966 Transmitter release at the squid giant synapse in the presence of tetrodotoxin. *Nature, Lond.* **212**, 49–50.

Buller, A. J. & Lewis, D. M. 1965 The rate of tension development in isometric tetanic contractions of mammalian fast and slow skeletal muscle. *J. Physiol., Lond.* **176**, 337–354.

Bullock, T. H. & Horridge, G. A. 1965 *Structure and function in the nervous system of invertebrates*, vol. 2. San Francisco: W. H. Freeman.

Burke, D. 1978 The fusimotor innervation of muscle spindle endings in man. *Trends Neurosci.* **1**, 89–92.

Burrows, M. 1975 Monosynaptic connexions between wing stretch receptors and flight motoneurons of the locust. *J. exp. Biol.* **62**, 189–219.

Burrows, M. 1979 Graded synaptic interactions between local premotor interneurons of the locust. *J. Neurophysiol.* **42**, 1108–1123.

Burrows, M. & Siegler, M. V. S. 1976 Transmission without spikes between locust interneurones and motoneurones. *Nature, Lond.* **262**, 222–224.

Burrows, M. & Siegler, M. V. S. 1978 Graded synaptic transmission between local interneurones and motoneurones in the metathoracic ganglion of the locust. *J. Physiol., Lond.* **285**, 231–255.

Burton, R. F. 1975 *Ringer solutions and physiological salines.* Bristol: Wright Scientechnica.

Bush, B. M. H. 1976 Non-impulsive thoracic–coxal receptors in crustaceans. In *Structure and function of proprioceptors in the invertebrates* (ed. P. J. Mill) pp. 115–151. London: Chapman & Hall.

Bush, B. M. H. 1977 Non-impulsive afferent coding and stretch reflexes in crabs. In *Identified neurons and behaviour of arthropods* (ed. G. Hoyle), pp. 439–460. New York, London: Plenum Press.

Bush, B. M. H. & Cannone, A. J. 1973 A stretch reflex in crabs evoked by muscle receptor potentials in non-impulsive afferents. *J. Physiol., Lond.* **232**, 95*P*–96*P*.

Bush, B. M. H. & Cannone, A. J. 1974 A positive feedback-reflex to a crustacean muscle receptor. *J. Physiol., Lond.* **236**, 37*P*–39*P*.

Bush, B. M. H., Emson, P. C. & Joseph, M. H. 1974 Transmitter enzymes and amino acid levels in sensory and motor nerves of the shore crab. *J. Physiol., Lond.* **245**, 6*P*–7*P*.

Bush, B. M. H. & Godden, D. H. 1974 Tension changes underlying receptor potentials in non-impulsive crab muscle receptors. *J. Physiol., Lond.* **242**, 80*P*–82*P*.

Bush, B. M. H., Godden, D. H. & MacDonald, G. A. 1974 Voltage clamping of non-impulsive afferents of the crab thoracic–coxal muscle receptor. *J. Physiol., Lond.* **245**, 3*P*–5*P*.

Bush, B. M. H. & Roberts, A. 1968 Resistance reflexes from a crab muscle receptor without impulses. *Nature, Lond.* **218**, 1171–1173.

Bush, B. M. H. & Roberts, A. 1971 Coxal muscle receptors in the crab: The receptor potentials of S and T fibres in response to ramp stretches. *J. exp. Biol.* **55**, 813–832.

Castellucci, V., Pinsker, H., Kupferman, H. I. & Kandel, E. R. 1970 Neuronal mechanisms of habituation and dishabituation of the gill-withdrawal reflex in *Aplysia. Science, N.Y.* **167**, 1745–1748.

Christensen, B. N. & Martin, A. R. 1970 Estimates of probability of transmitter release at the mammalian neuromuscular junction. *J. Physiol., Lond.* **210**, 933–945.

Cooper, S. 1959 The secondary endings of muscle spindles. *J. Physiol., Lond.* **149**, 27*P*–28*P*.

Cooper, S. 1961 The responses of the primary and secondary endings of muscle spindles with intact motor innervation during applied stretch. *Q. Jl exp. Physiol.* **46**, 389–398.

Crawford, A. C. 1974 The dependence of evoked transmitter release on external calcium ions at very low mean quantal contents. *J. Physiol., Lond.* **240**, 255–278.

Davidoff, R. A. & Sears, E. S. 1975 Effects of synthetic buffers on reflexes in the isolated frog spinal cord. *Am. J. Physiol.* **229**, 831–837.

Eckert, R & Tillotson, D. 1978 Potassium activation associated with intraneuronal free calcium. *Science, N.Y.* **200**, 437–439.

Emson, P. C., Bush, B. M. H. & Joseph, M. H. 1976 Transmitter metabolising enzymes and free amino acid levels in sensory and motor nerves and ganglia of the shore crab (*Carcinus maenas*). *J. Neurochem.* **26**, 779–783.

Evoy, W. H. & Cohen, M. J. 1971 Central and peripheral control of Arthropod movements. *Adv. comp. Physiol. Biochem.* **4**, 225–266.

Evoy, W. H. & Fourtner, C. R. 1973 Crustacean walking. In *Control of posture and locomotion* (ed. R. B. Stein, K. G. Pearson, R. S. Smith & J. B. Redford), pp. 477–493. New York: Plenum.

Fahrenbach, W. H. 1968 The morphology of the eyes of *Limulus*. I. Cornea and epidermis of the compound eye. *Z. Zellforsch. mikrosk. Anat.* **87**, 278–291.

Florey, E. 1973 Acetylcholine as sensory transmitter in Crustacea. New evidence from experiments demonstrating release of ACh during sensory stimulation. *J. comp. Physiol.* **83**, 1–16.

Gallyas, F., Lénárd, L. & Lázar, G. 1978 Improvement of cobalt transport in axons by complexing agents. *Neurosci. Lett.* **9**, 213–216.

Gerschenfeld, H. M. 1973 Chemical transmission in invertebrate central nervous system and neuromuscular junction. *Physiol. Rev.* **53**, 1–119.

Granit, R. 1970 *The basis of motor control.* London: Academic Press.

Graubard, K. 1978 Synaptic transmission without action potentials. Input–output properties of a nonspiking presynaptic neuron. *J. Neurophysiol.* **41**, 1014–1015.

Graubard, K. & Calvin, W. H. 1979 Presynaptic dendrites: Implications of spikeless synaptic transmission and dendritic geometry. In *The neurosciences: fourth study program* (ed. F. O. Schmitt & F. G. Worden), pp. 317–331. Cambridge: M.I.T. Press.

Hama, K. 1962 Some observations on the fine structure of the giant synapse in the stellate ganglion in the squid, *Doryteuphis bleekeri. Z. Zellforsch. mikrosk. Anat.* **56**, 437–444.

Hayat, M. A. 1975 *Positive staining for electron microscopy*. New York: Van Nostrand Reinhold.

Hays, E. A., Lang, M. A. & Gainer, H. 1968 A re-examination of the Donnan distribution as a mechanism for membrane potentials and potassium and chloride distributions in crab muscle fibres. *Comp. Biochem. Physiol.* **26**, 761–792.

Heyer, C. B. & Llinás, R. 1977 Control of rhythmic firing in normal and axotomized cat spinal motoneurons. *J. Neurophysiol.* **40**, 480–488.

Heyer, C. B. & Lux, H. D. 1976*a* Properties of facilitating calcium current in pace-maker neurones of the snail, *Helix pomatia*. *J. Physiol., Lond.* **262**, 319–348.

Heyer, C. B. & Lux, H. D. 1976*b* Control of the delayed outward potassium currents in bursting pace-maker neurones of the snail, *Helix pomatia*. *J. Physiol., Lond.* **262**, 349–382.

Highstein, S. M. & Bennett, M. V. L. 1973 Fatigue at the Mauthner fiber–giant fiber synapse of the hatchet fish. *Fedn Proc. Fedn Am. Socs exp. Biol.* **32**, 443

Kandel, E. R., Brunelli, M., Byrne, J. & Castelluci, V. 1975 A common presynaptic locus for the synaptic changes underlying short-term habituation and sensitization of the gill-withdrawal reflex in *Aplysia*. *Cold Spring Harb. Symp. quant. Biol.* **40**, 465–482.

Kater, S. B. 1977 Calcium electroresponsiveness and its relationship to secretion in molluscan exocrine gland cells. *Society Neurosci. Symp.*, vol. 2 (ed. W. M. Cowan & J. A. Ferendelli), pp. 195–214. Bethesda: Society for Neuroscience.

Kater, S. B. & Nicholson, C. (ed.) 1973 *Intracellular staining in neurobiology*. New York, Heidelberg, Berlin: Springer-Verlag.

Katz, B. & Miledi, R. 1967*a* The release of acetylcholine from nerve endings by graded electric pulses. *Proc. R. Soc. Lond.* B **167**, 23–38.

Katz, B. & Miledi, R. 1967*b* A study of synaptic transmission in the absence of nerve impulses. *J. Physiol., Lond.* **192**, 407–436.

Katz, B. & Miledi, R. 1969*a* Tetrodotoxin-resistant electric activity in presynaptic terminals. *J. Physiol., Lond.* **203**, 459–487.

Katz, B. & Miledi, R. 1969*b* Spontaneous and evoked activity of motor nerve endings in calcium Ringer. *J. Physiol., Lond.* **203**, 689–706.

Katz, B. & Miledi, R. 1970 A further study of the role of calcium in synaptic transmission. *J. Physiol., Lond.* **207**, 789–801.

Katz, B. & Miledi, R. 1971 The effect of prolonged depolarization on synaptic transfer in the stellate ganglion of the squid. *J. Physiol., Lond.* **216**, 503–512.

Katz, B. & Thesleff, S. 1957 A study of the 'desensitization' produced by acetylcholine at the motor endplate *J. Physiol., Lond.* **138**, 63–80.

Krauhs, J. M. & Mirolli, M. 1975 Morphological changes associated with stretch in a mechanoreceptor. *J. Neurocytol.* **4**, 231–246.

Kusano, K. 1968 Further study of the relationship between pre- and post-synaptic potentials in the squid giant synapse. *J. gen. Physiol.* **52**, 326–345.

Kusano, K. 1970 Influence of ionic environment on the relationship between pre- and post-synaptic potentials. *J. Neurobiol.* **1**, 435–457.

Kusano, K. & Landau, E. M. 1975 Depression and recovery of transmission at the squid giant synapse. *J. Physiol., Lond.* **245**, 13–32.

Kusano, K., Livengood, D. R. & Werman, R. 1967 Correlation of transmitter release with membrane properties of the presynaptic fiber of the squid giant synapse. *J. gen. Physiol.* **50**, 2579–2601.

Llinás, R. 1977 Calcium and transmitter release in squid synapse. In *Society Neurosci. Symp.* (ed. W. M. Cowan & J. A. Ferendelli), vol. 2, pp. 139–160. Bethesda: Society for Neuroscience.

Llinás, R. 1979 The role of calcium in neuronal function. In *The neurosciences: fourth study program* (ed. F. O. Schmitt & F. G. Worden), pp. 601–615. Cambridge: M.I.T. Press.

Llinás, R. & Heuser, J. E. 1977 Depolarization–release coupling systems in neurons. *Neurosci. Res. Progr. Bull.* **15**, 557–687.

Llinás, R. & Nicholson, C. 1975 Calcium role in depolarisation-secretion coupling: An aequorin study in squid giant synapse. *Proc. natn. Acad. Sci. U.S.A.* **72**, 187–190.

Llinás, R., Steinberg, I. Z. & Walton, K. 1976 Presynaptic calcium currents and their relation to synaptic transmission: Voltage clamp study in squid giant synapse and theoretical model for the calcium gate. *Proc. natn. Acad. Sci. U.S.A.* **73**, 2918–2922.

Llinás, R., Steinberg, I. Z. & Walton, K. 1980 Presynaptic calcium currents in squid stellate ganglion: a voltage clamp study. (Submitted for publication.)

Lowe, D. A., Bush, B. M. H. & Ripley, S. H. 1978 Pharmacological evidence for 'fast' sodium channels in nonspiking neurons. *Nature, Lond.* **274**, 289–290.

Lux, H. D. and Heyer, C. B. 1979 A new electrogenic calcium-potassium system. In *The neurosciences: fourth study program* (ed. F. O. Schmitt & F. G. Worden), pp. 601–615. Cambridge: M.I.T. Press.

Mann, D. W. & Joyner, R. W. 1978 Miniature synaptic potentials at the squid giant synapse. *J. Neurobiol.* **9**, 329–335.

Marder, E. & Paupardin-Tritsch, D. 1978 The pharmacological properties of some crustacean neuronal acetycholine, γ-aminobutyric acid, and L-glutamate responses. *J. Physiol., Lond.* **280**, 213–247.

Marrelli, J. D. & Larimer, J. L. 1978 Proprioceptive shaping of a centrally initiated motor program during movement of the crayfish claw. *Soc. Neurosci. Abstr.* **4**, 300.

Martin, A. R. 1977 Junctional transmission. II. Presynaptic mechanisms. In *Handbook of physiology: the nervous system*, vol. 1 (1) (ed. E. R. Kandel), ch. 10, pp. 329–355. Bethesda, Maryland: American Physiological Society.

Martin, R. & Miledi, R. 1975 A presynaptic complex in the giant synapse of the squid. *J. Neurocytol.* **4**, 121–129.

Martin, A. R. & Ringham, G. L. 1975 Synaptic transfer at a vertebrate central nervous system synapse. *J. Physiol., Lond.* **251**, 409–426.

Maynard, D. M. & Walton, K. D. 1975 Effects of maintained depolarization of presynaptic neurons on inhibitory transmission in lobster neuropil. *J. comp. Physiol.* **97**, 215–243.

Meech, R. W. 1972 Intracellular calcium injection causes increased potassium conductance in *Aplysia* nerve cells. *Comp. Biochem. Physiol.* **A42**, 493–499.

Meech, R. W. 1974 The sensitivity of *Helix aspersa* neurones to injected calcium ions. *J. Physiol., Lond.* **237**, 259–277.

Meech, R. W. & Standen, N. B. 1975 Potassium activation in *Helix aspersa* neurones under voltage clamp: A component mediated by calcium influx. *J. Physiol., Lond.* **249**, 211–239.

Miledi, R. 1967 Spontaneous synaptic potentials and quantal release of transmitter in the stellate ganglia of the squid. *J. Physiol., Lond.* **192**, 379–406.

Mill, P. J. (ed.) 1976 *Structure and function of proprioceptors in the invertebrates.* London: Chapman & Hall.

Mirolli, M. 1979 The electrical properties of a crustacean sensory dendrite. *J. exp. Biol.* **78**, 1–27.

Möhl, B. 1979 High-frequency discharge of the locust wing hinge stretch receptor during flight. *Naturwissenschaften* **66**, 158–159.

Nakajima, S. & Onodera, K. 1969 Adaptation of the generator potential in the crayfish stretch receptors under constant length and constant tension. *J. Physiol., Lond.* **200**, 187–204.

Paul, D. H. 1976 Role of proprioceptive feedback from nonspiking mechanosensory cells in the sand crab, (*Emerita analoga*). *J. exp. Biol.* **65**, 243–258.

Pearson, K. G. 1976 Nerve cells without action potentials. In *Simple networks and behaviour* (ed. J. C. Fentress), pp. 99–110. Sunderland, Massachusetts: Sinauer Ass. Inc.

Pepose, J. S. & Lisman, J. E. 1978 Voltage-sensitive potassium channels in *Limulus* ventral photoreceptor. *J. gen. Physiol.* **71**, 101–120.

Pumplin, D. W. & Reese, T. S. 1978 Membrane ultrastructure of the giant synapse of the squid, *Loligo pealei*. *Neuroscience* **3**, 685–696.

Raper, J. A. 1979 Nonimpulse-mediated synaptic transmission during the generation of a cyclic motor program. *Science, N.Y.* **205**, 304–306.

Reingold, S. C. 1975 Temperature effects on axonal conduction in *Callinectes sapidus* (Rathbun) and *Carcinus maenas* (L.). *Comp. Biochem. Physiol.* **A51**, 195–199.

Ripley, S. H., Bush, B. M. H. & Roberts, A. 1968 Crab muscle receptor which responds without impulses. *Nature, Lond.* **218**, 1170–1171.

Roberts, A. & Bush, B. M. H. 1971 Coxal muscle receptors in the crab: The receptor current and some properties of the receptor nerve fibres. *J. exp. Biol.* **54**, 515–524.

Ross, W. N. & Stuart, A. E. 1978 Voltage sensitive calcium channels in the presynaptic terminals of a decrementally conducting photoreceptor. *J. Physiol., Lond.* **274**, 173–191.

Schmitt, F. O., Dev, P. & Smith, B. H. 1976 Electrotonic processing of information by brain cells. *Science, N.Y.* **193**, 114–120.

Shepherd, G. M. 1979 Functional analysis of local circuits in the olfactory bulb. In *The neurosciences: fourth study program* (ed. F. O. Schmitt & F. G. Worden), pp. 129–143. Cambridge: M.I.T. Press.

Sherman, R. G. & Atwood, H. L. 1972 Correlated electrophysiological and ultrastructural studies of a crustacean motor unit. *J. gen. Physiol.* **59**, 586–615.

Sjoestrand, F. S. 1958 Ultrastructure of retinal rod synapses of the guinea pig eye as revealed by three-dimensional reconstruction from serial sections. *J. Ultrastruct. Res.* **2**, 122–170.

Székely, G. & Gallyas, F. 1975 Intensification of cobaltous sulphide precipitate in frog nervous tissue. *Acta biol. hung.* **26**, 175–188.

Takeuchi, A. 1977 Junctional transmission. I. Postsynaptic mechanisms. In *Handbook of physiology: The nervous system* (ed. E. R. Kandel), vol. 1 (1), ch. 9, pp. 295–327. Bethesda: American Physiol. Society.

Thomas, R. C. & Wilson, V. J. 1966 Marking single neurons by staining with intracellular microelectrodes. *Science, N.Y.* **151**, 1538–1539.

Tyrer, N. M. & Bell, E. M. 1974 The intensification of cobalt-filled neurone profiles using a modification of Timm's sulphide-silver method. *Brain Res.* **73**, 151–155.

Ward, D., Crowley, W. J. & Johns, T. R. 1972 Effect of temperature at the neuromuscular junction. *Am. J. Physiol.* **222**, 216–219.

Weidmann, S. 1952 The electrical constants of Purkinje fibers. *J. Physiol., Lond.* **118**, 348–360.
Whitear, M. 1965 The fine structure of crustacean proprioceptors. II. The thoracic-coxal organs in *Carcinus*, *Pagurus* and *Astacus*. *Phil. Trans. R. Soc. Lond.* B **248**, 437–456.
Young, J. Z. 1939 Fused neurons and synaptic contacts in the giant nerve fibres of cephalopods. *Phil. Trans. R. Soc. Lond.* B **229**, 465–505.
Young, J. Z. 1973 The giant synapse of *Loligo*. *Brain Res.* **57**, 457–460.

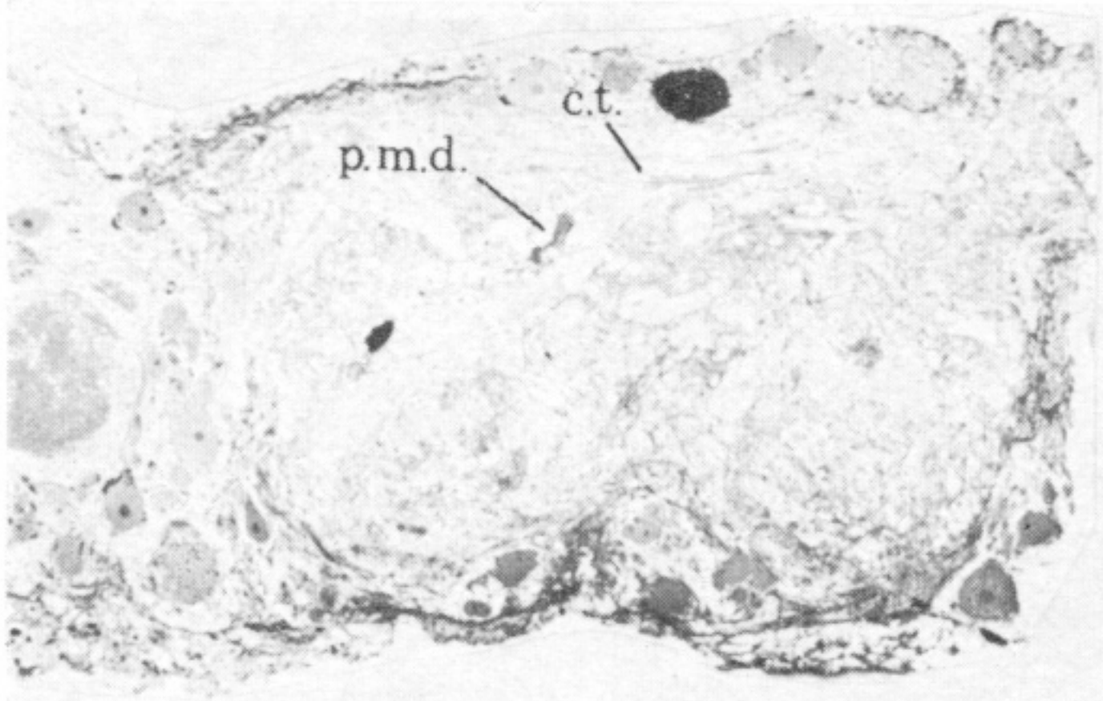

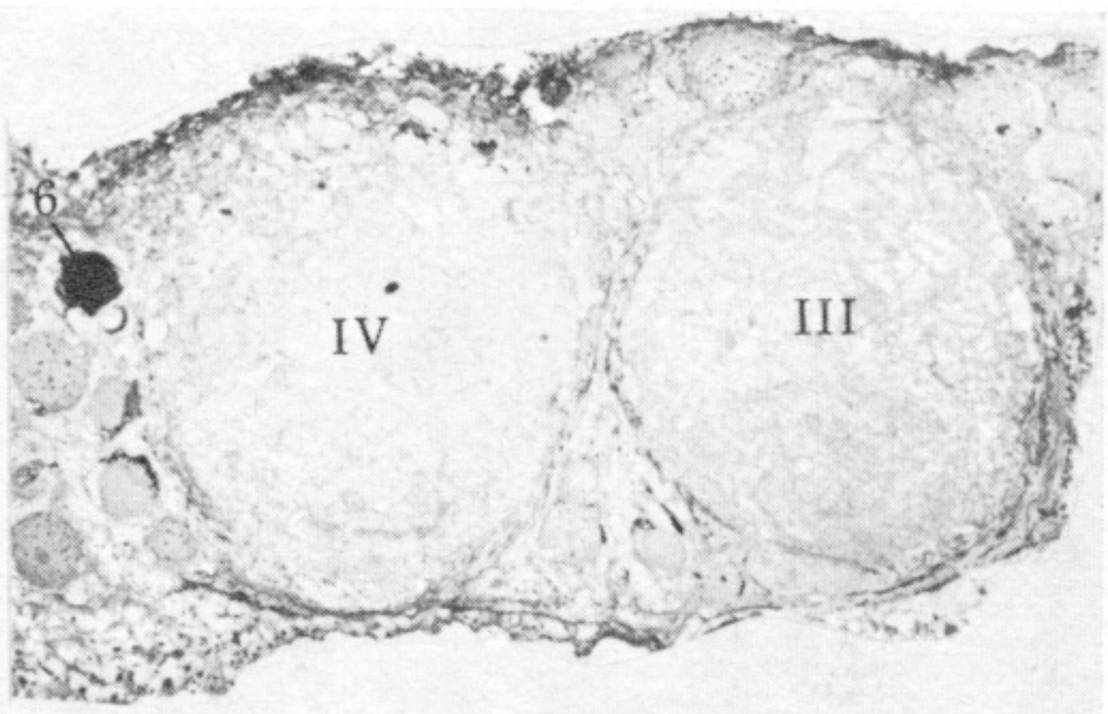

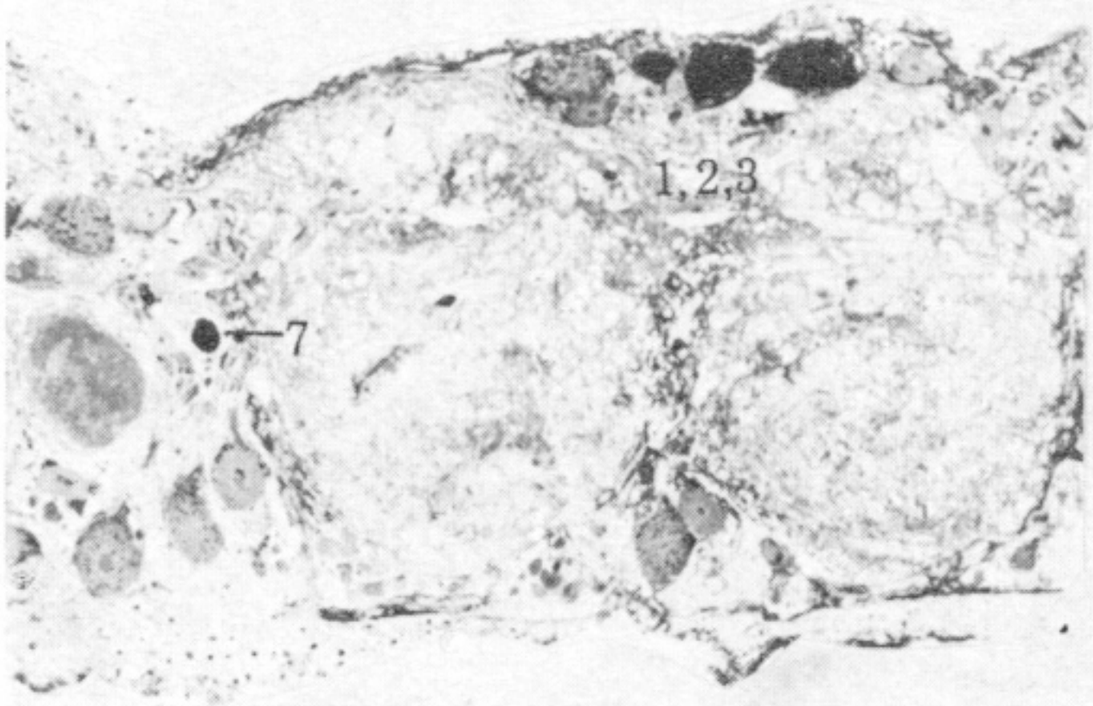

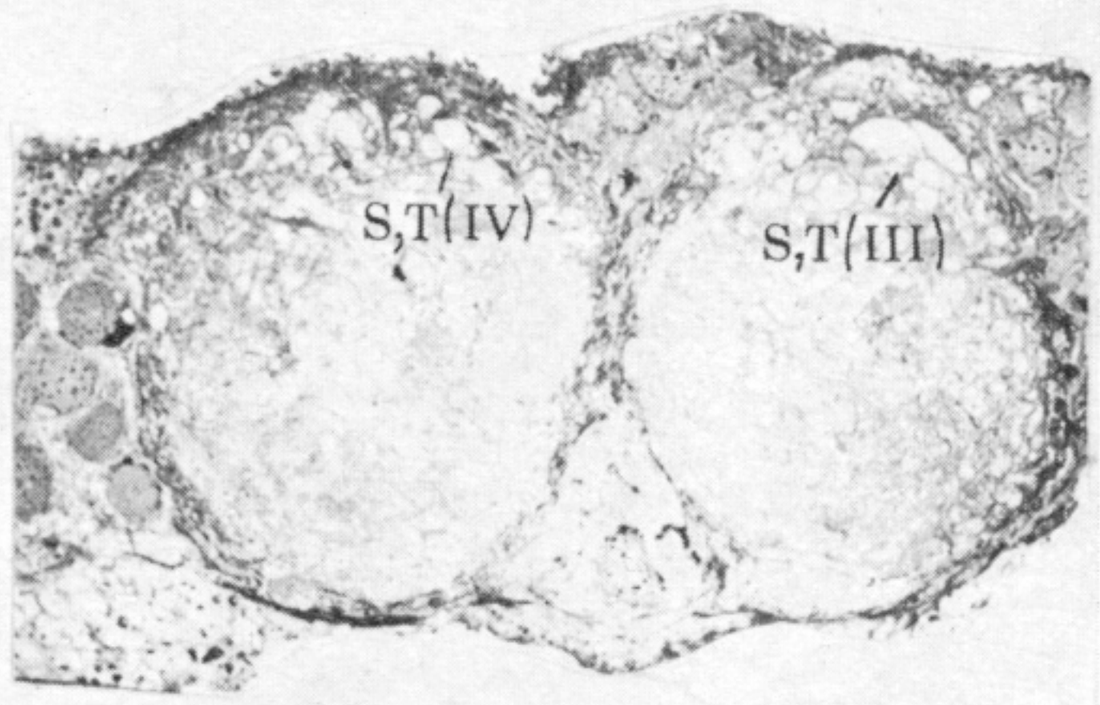

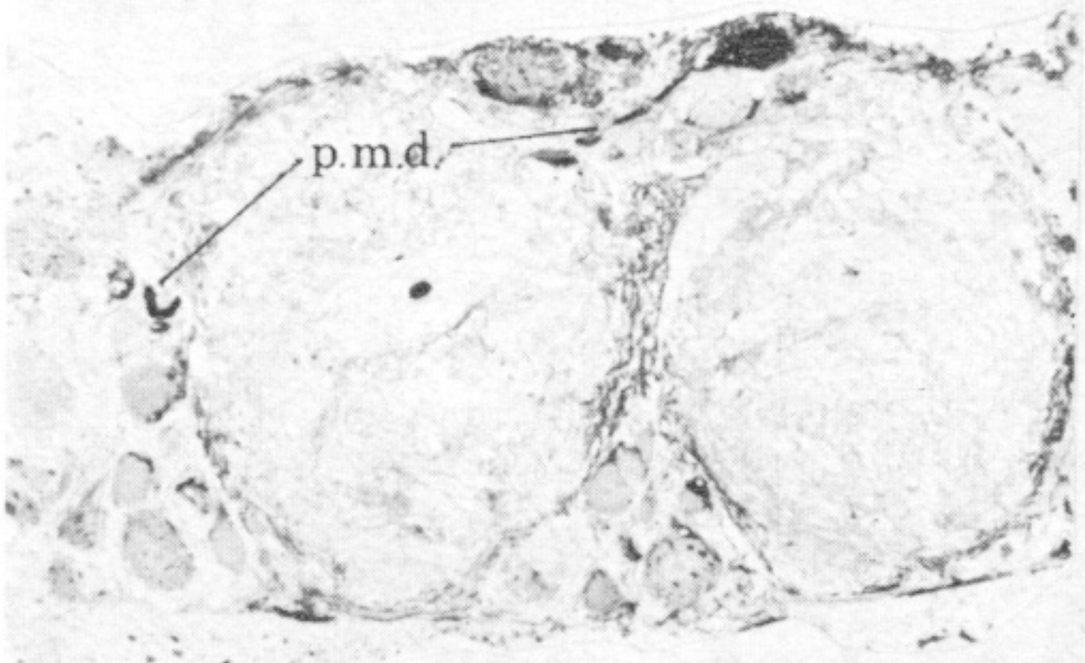

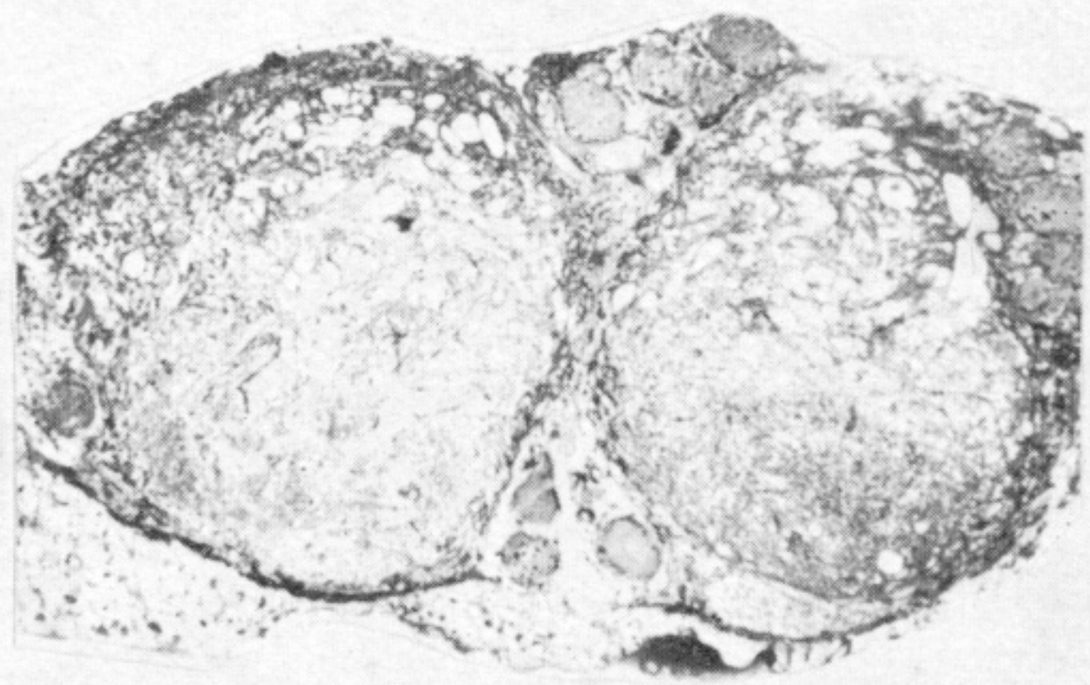

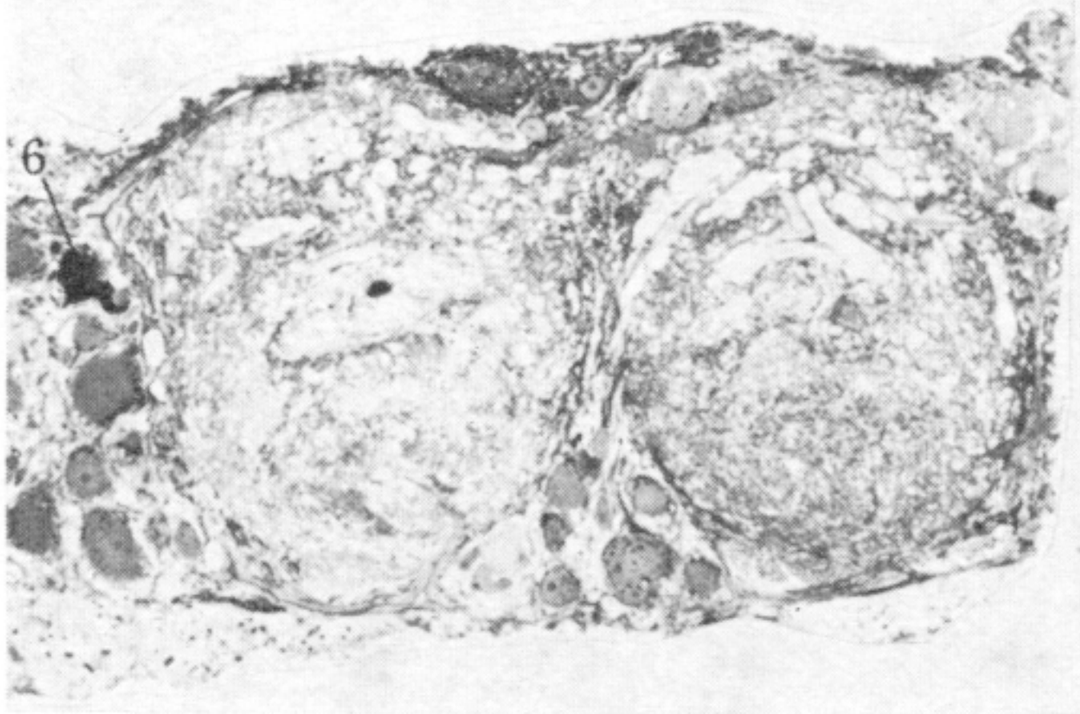

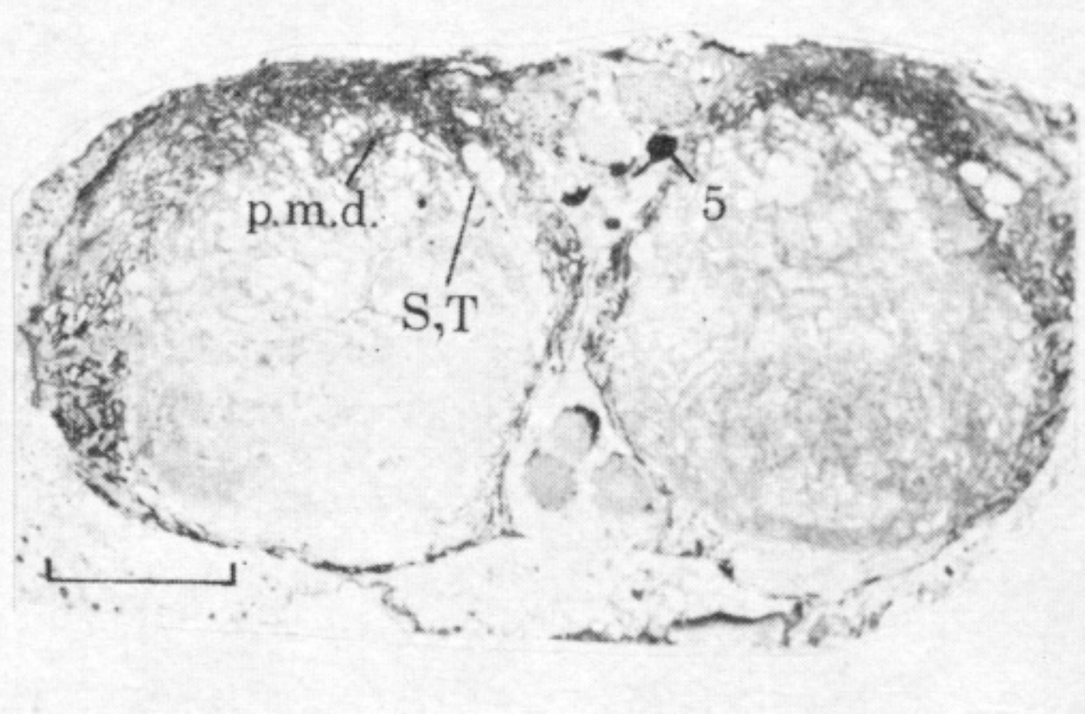

FIGURE 7. For description see opposite page.

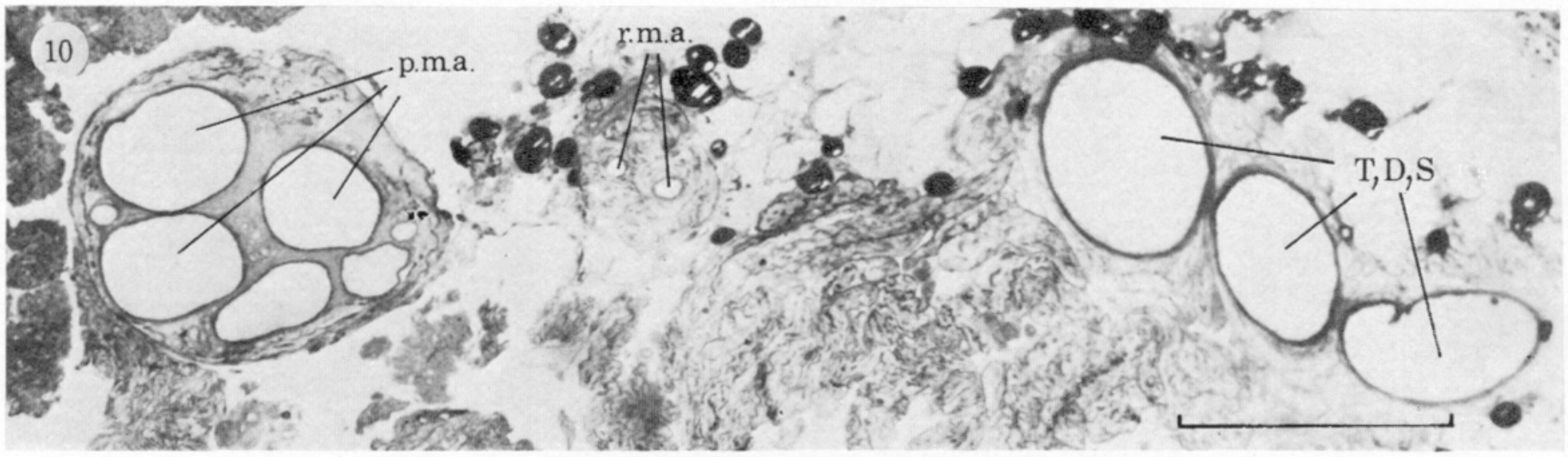

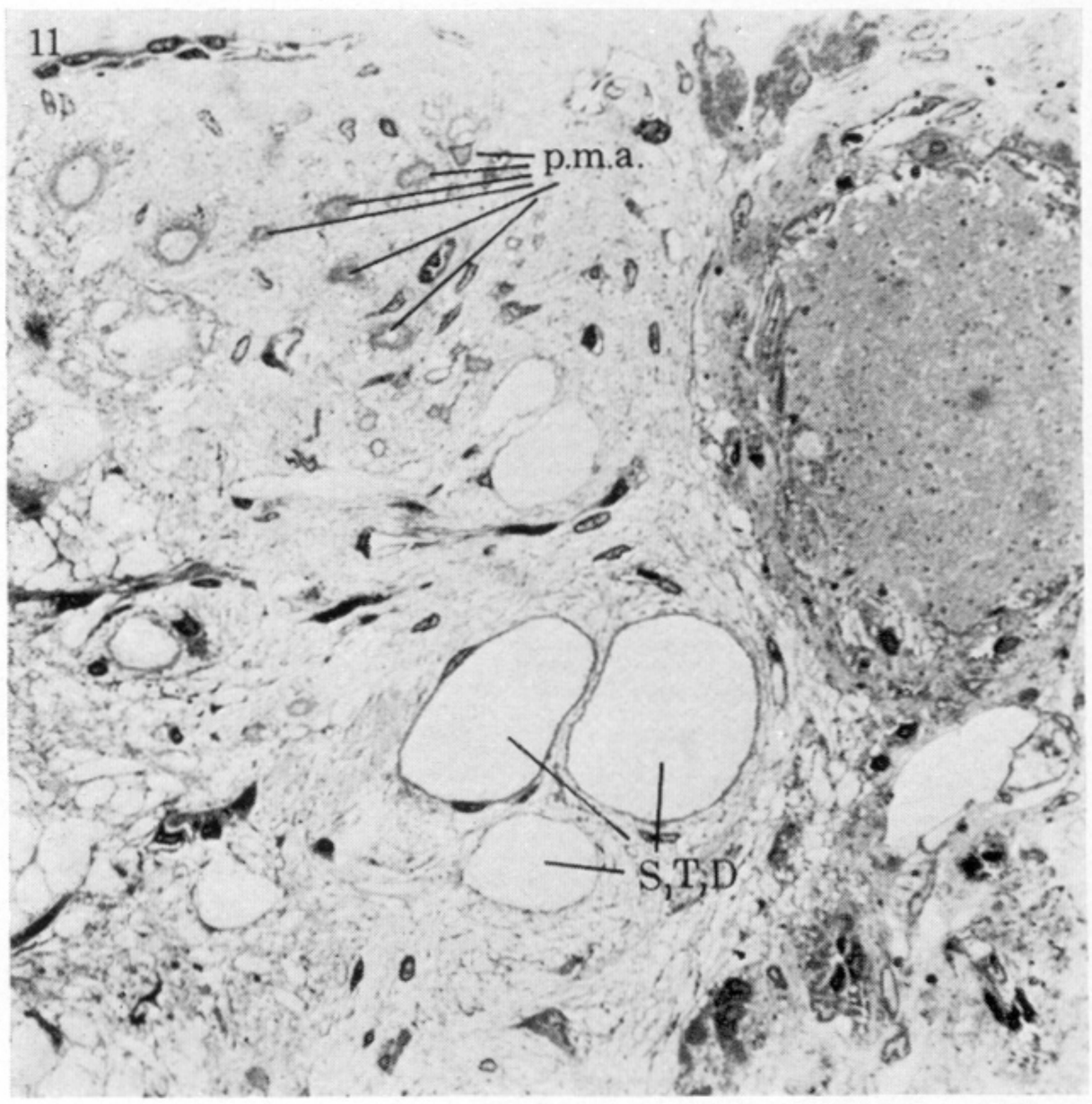

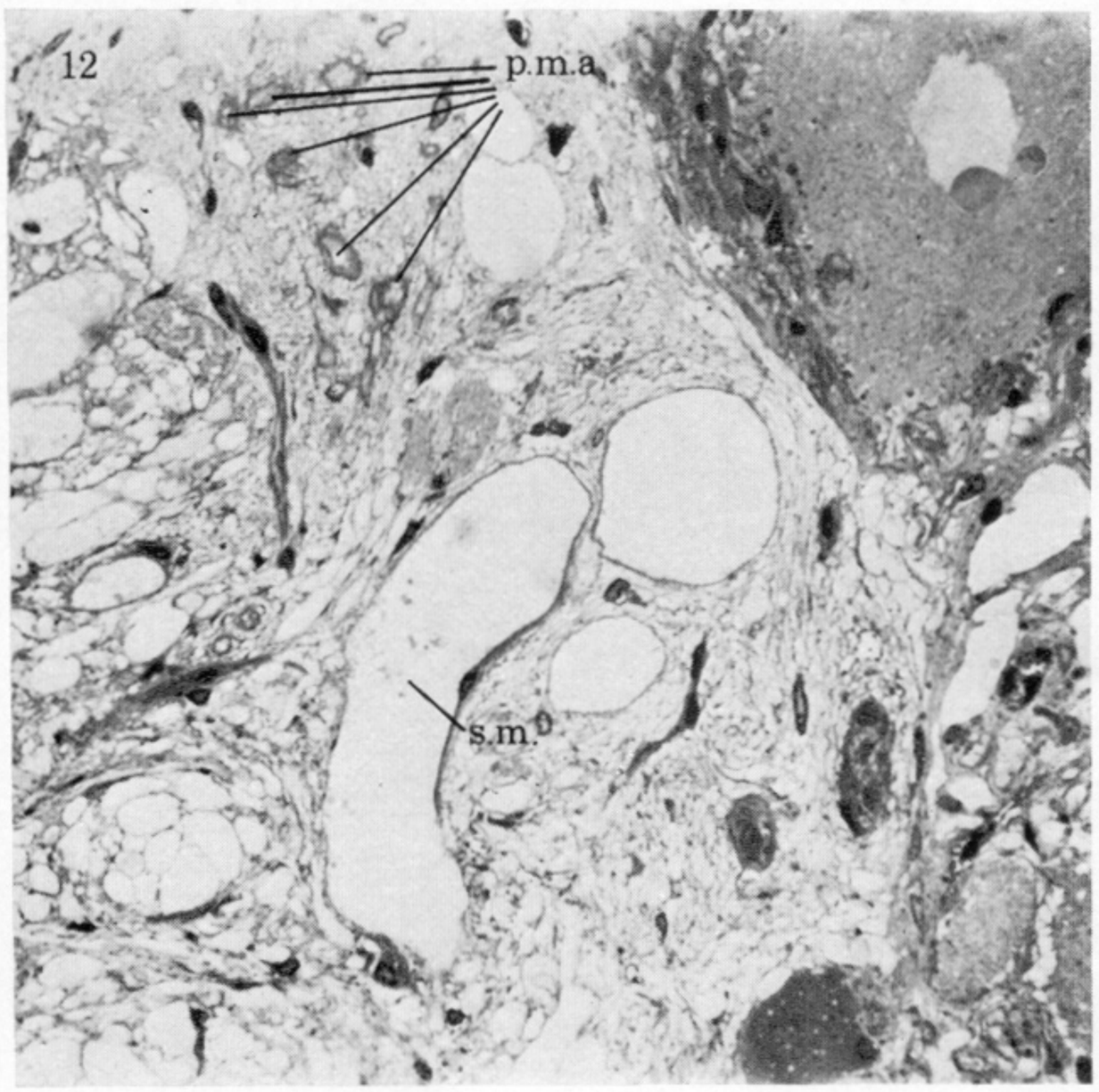

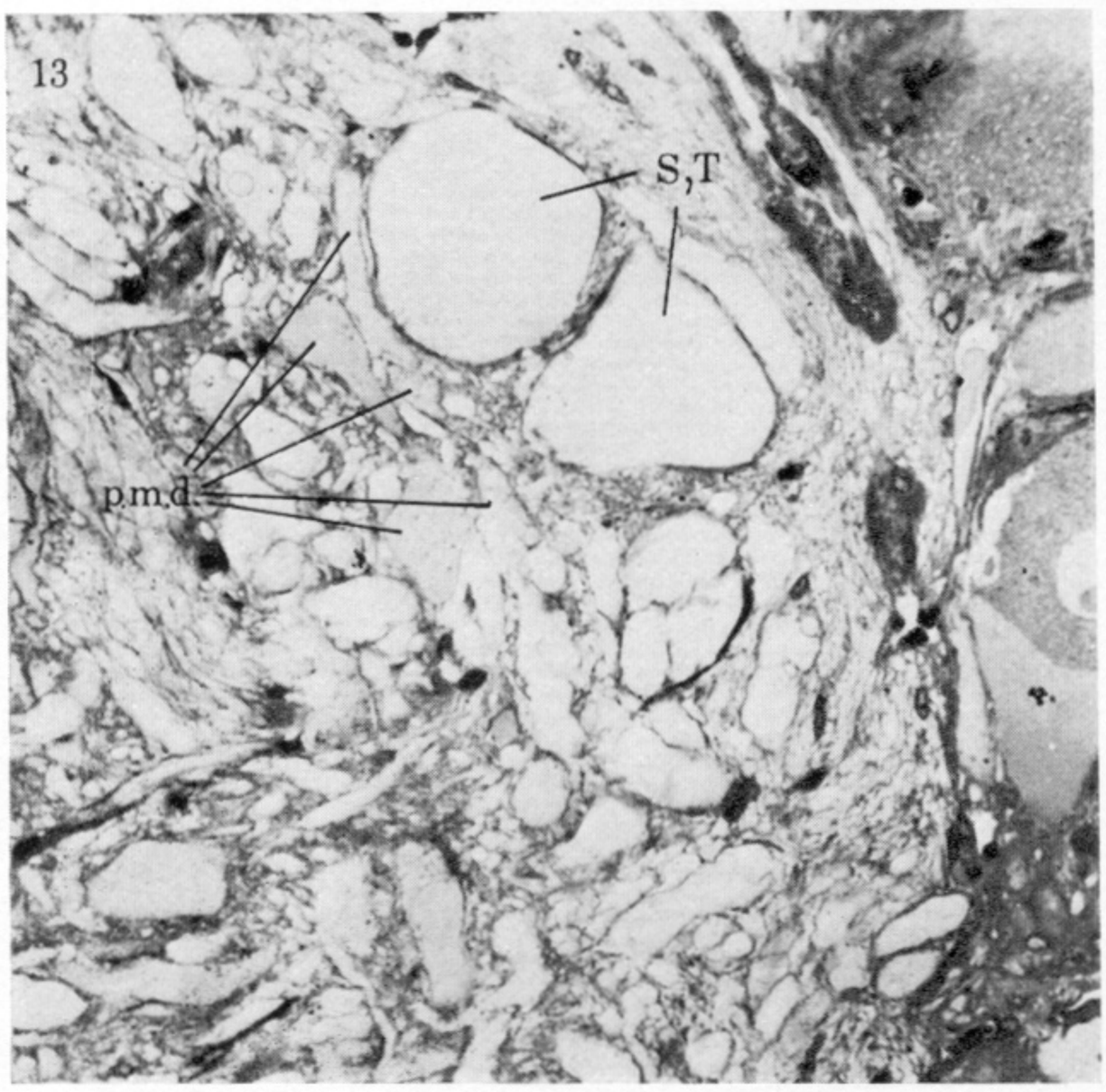

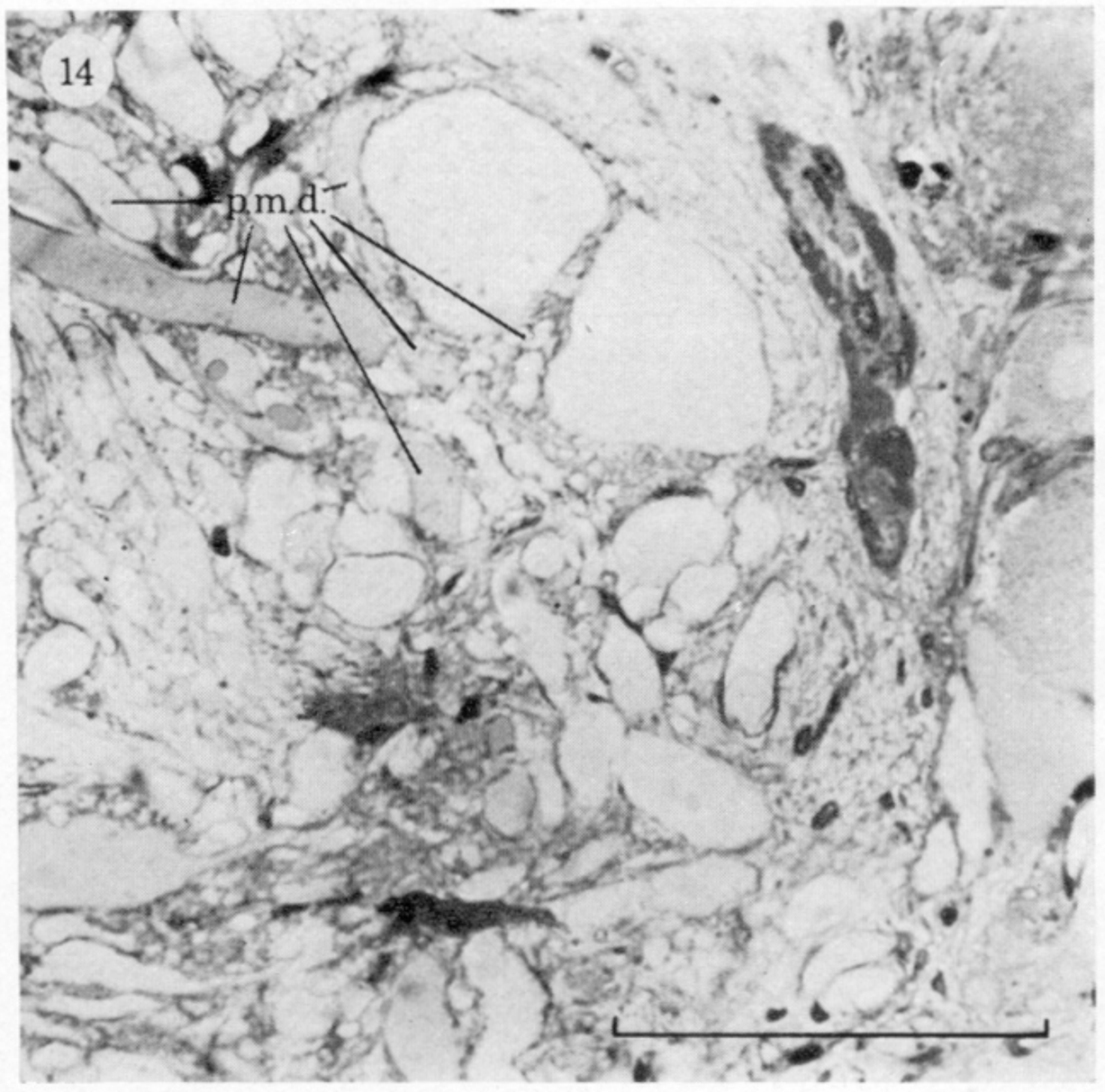

FIGURES 10–14. For description see page 232.

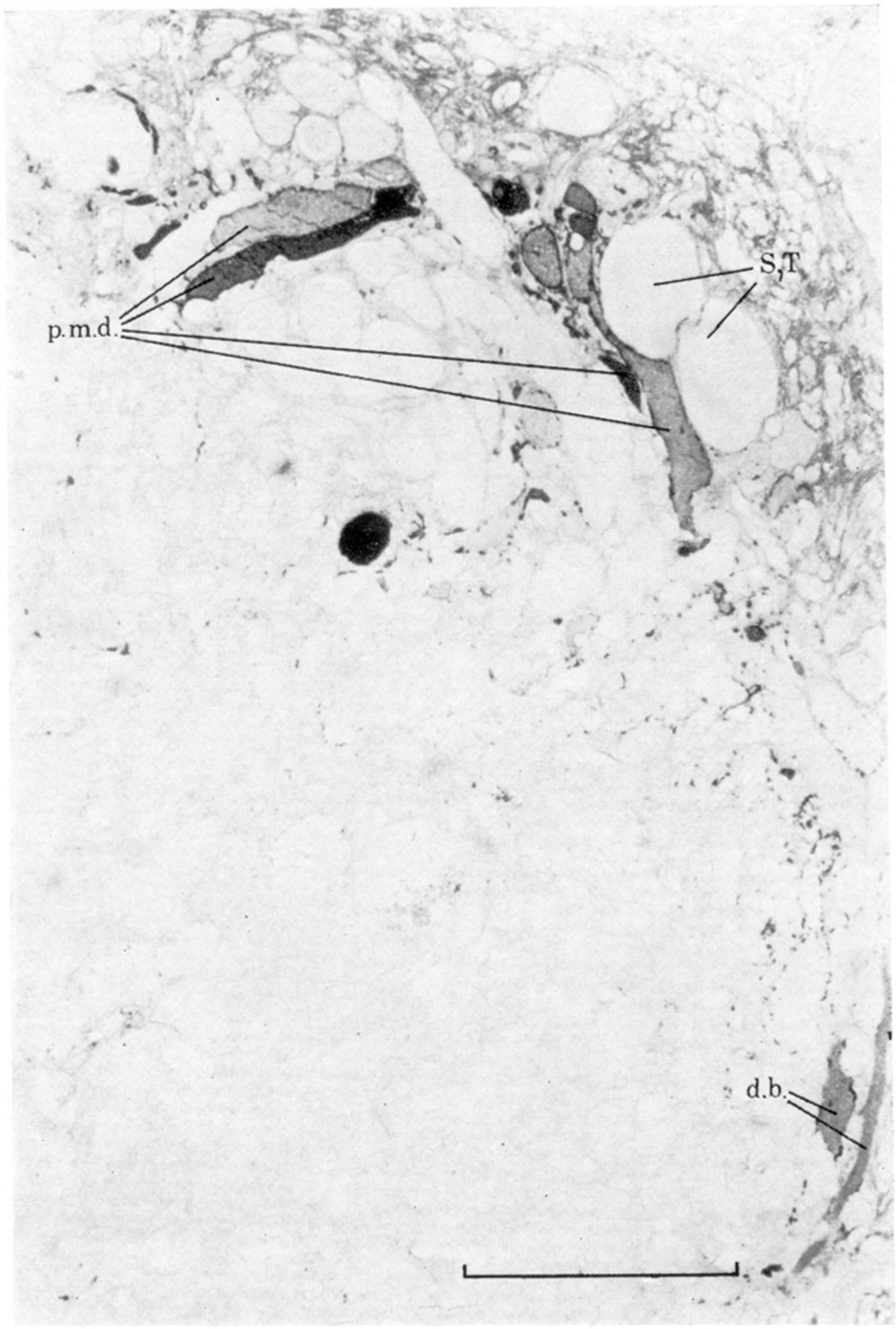

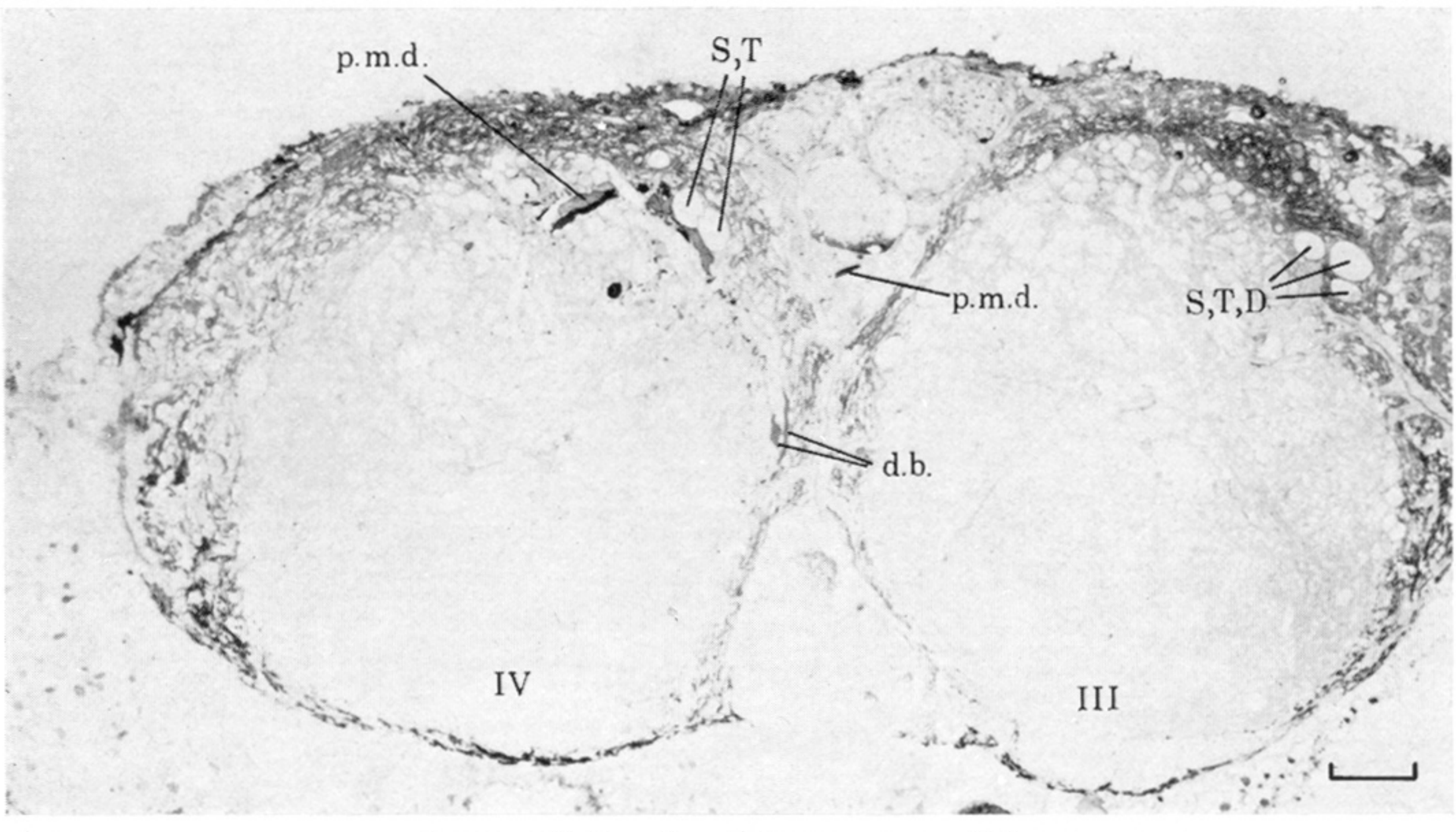

FIGURE 15. For description see page 233.

16

T

v.

v.

S

17

T

s.d.

FIGURES 16 AND 17. For description see opposite.